UC Irvine

UC Irvine Electronic Theses and Dissertations

Title

Generation of Human Microglia from Induced Pluripotent Stem Cells to Study Innate Immunity in Neurological Diseases.

Permalink

https://escholarship.org/uc/item/12b1q5fv

Author

Abud, Edsel Misael

Publication Date

2017

Peer reviewed|Thesis/dissertation

eScholarship.org Powered by the California Digital Library
University of California

UNIVERSITY OF CALIFORNIA,
IRVINE

Generation of Human Microglia from Induced Pluripotent Stem Cells to Study Innate Immunity in Neurological Diseases.

DISSERTATION

submitted in partial satisfaction of the requirements
for the degree of

DOCTOR OF PHILOSOPHY

in Biological Sciences

by
Edsel Misael Abud

Dissertation Committee:
Assistant Professor Mathew Blurton-Jones, Chair
Assistant Research Professor, Wayne W. Poon
Professor Andrea J. Tenner
Associate Professor Kim N. Green
Assistant Professor Mathew A. Inlay

2017

Elements of Chapter 1 and 2 are published in Neuron, Cell Press as Abud et al., 2017. *iPSC-derived human microglia-like cells to study neurological diseases.*

All other materials © 2017 Edsel M. Abud

DEDICATION

This dissertation and labor of love is dedicated to my family: my parents Dr. Nelson and Patricia Abud, my in-laws Don and Cheryl Carrico, my brother Nelson, and sisters Krisnel, Patricia, and Abigail Abud, Trent Waters, Obringer family, whose constant support and encouragement has made this possible. This accomplishment is shared with my partner in life and wife, Kendall Abud, and our loving daughter, Colette Abud. I couldn't imagine life without both of you and your love, which gives me the daily encouragement and added motivation necessary to work in this field. Kendall's continued sacrifices has allowed *our* achievements to be made possible.

TABLE OF CONTENTS

	Page
LIST OF FIGURES AND TABLES	iv
LIST OF ABBREVIATIONS	vi
ACKNOWLEDGMENTS	ix
CURRICULUM VITAE	x
ABSTRACT OF THE DISSERTATION	xiv
INTRODUCTION	1
A. Alzheimer's Disease Neuropathology and the Amyloid Cascade Hypothesis	1
B. Innate Immunity in Alzheimer's Disease	5
C. The Developmental Origin of Microglia	11
D. Studying Microglia Using iPSCs	16
CHAPTER 1: Developing a fully-defined protocol for the generation of human microglia-like cells	23
CHAPTER 2: Examining Alzheimer's Disease genetics using human induced pluripotent stem cell-derived microglia-like cells	68
CONLCUDING REMARKS	93
REFERENCES	99

LIST OF FIGURES AND TABLES

		Page
Figure 1	Rare and common genetic variants contribute to Alzheimer's disease	4
Figure 2	Components of the Innate and Adaptive Immune Systems	7
Figure 3	Microglia arise from yolk sac-derived primitive hematopoietic progenitors	12
Figure 1.1	Schematic of fully-defined iMGL differentiation protocol.	38
Figure 1.2	Genomic stability of iPSCs and iMGLs	39
Figure 1.3	iMGLs differentiation resembles in vivo development	41
Figure 1.4	iMGL transcriptome profile is highly similar to human adult and fetal microglia	42
Figure 1.5	Correlational Matrix of biological samples used in RNA-sequencing and iMGL gene example genes in	45
Table 1.1	Adjusted *p*-values for 12 genes across all groups	47
Figure 1.6	Correlational Matrix of biological samples used in RNA-sequencing and iMGL gene example gene	49
Table 1.2	ELISA cytokine values (pg/ml) from conditioned media of stimulated iMGLs	51
Table 1.3	Gene ontology terms enriched in Adult MG vs Fetal MG and iMGL	53
Table 1.4	Gene ontology terms enriched in Fetal MG vs Adult MG and iMGL	54
Table 1.5	Gene ontology terms enriched in Fetal MG vs Adult MG and iMGL permeability	56
Figure 1.7	iMGLs are physiologically functional and can secrete cytokines, respond to ADP, and phagocytose human synpatosomes.	57
Figure 1.8	iMGLS are positive for microglia surface proteins and perform phagocytosis of *E. coli* particles.	59
Figure 1. 9	iMGLs respond to the neuronal environment in 3D brain organoid	61

co-cultures (BORGS)

Figure 1.10 iMGLs transplanted into the brains of wild-type transplant competent mice are like brain microglia 63

Figure 2.1 Alzheimer Disease risk factor GWAS genes can be investigated using iMGLs and high throughput genomic and functional assays 79

Table 2.1. Related to Figure 2.1. QPCR results of iMGLs stimulated with fAβ or BDTO. 82

Figure 2.2 Microglia AD-GWAS and other CNS-disease related genes can be studied using iMGLs 83

Figure 2.3 TGFβ-1, CX3CL1, CD200 and their impact on key microglial genes are associated with modulating neuronal function and environment 85

Figure 2.4 iPSC-derived microglial cells engraft and phagocytose Aβ like human fetal microglia 87

LIST OF ABBREVIATIONS

Aβ	Amyloid-Beta Peptide
ABCA7	ATP-binding cassette sub family A member 7
ACK	Ammonium-Chloride-Potassium
AD	Alzheimer's disease
ADAM	A Disintegrin and Metalloproteinase Domain-Containing Protein
ALS	Amyotrophic Lateral Sclerosis
ANOVA	Analysis of Variance
APC	Antigen Presenting Cell
APOE	Apolipoprotein E
APP	Amyloid Precursor Protein
Axl	Tyrosine-protein kinase receptor UFO
BACE1	Beta-Secretase 1
BBB	Blood Brain Barrier
BDNF	Brain Derived Neurotrophic Factor
BM-GFP	Green Fluorescent Protein Bone Marrow
CA1	Hippocampal Subfield CA1
CA3	Hippocampal Subfield CA3
CCR	C-C Chemokine Receptor Type
CD	Cluster of Differentiation
CD2AP	CD-associated Protein
CNS	Central Nervous System
CR1	Complement Receptor 1
CRAC-ORAI	Calcium release-activated calcium channel protein 1
CX3CL1	Chemokine (C-X3-C Motif) Receptor 1 Ligand; Fractalkine
CX3CR1	Chemokine (C-X3-C Motif) Receptor 1
DC	Dendritic Cell
DCX	Doublecortin
DCLN	Deep Cervical Lymph Node
DG	Dentate Gyrus
DLB	Dementia with Lewy Bodies
EAE	Experimental Autoimmune Encephalomyelitis
EC	Entorhinal Cortex
FACS	Fluorescent-Activated Cell Sorting
fAD	familial Alzheimer's disease
fAβ	Fibrillar Aβ
GDNF	Glial Derived Neurotrophic Factor
GFAP	Glial Fibrillary Acidic Protein
GFP	Green Fluorescent Protein
Glut1	Glucose Transporter 1
GMP	Good Manufacturing Processes
GPCR	G-protein-coupled receptors
GWAS	Genome Wide Association Study
hNSC	Human Neural Stem Cell

HKLM	Heat-killed Listeria Monocytogenes
HLA-DRB5	HLA class II histocompatibility antigen, DRB5 beta chain
Iba1	Ionophore calcium-binding adapter molecule 1
ICAM-1	Intracellular Adhesion Molecule 1 (aka CD54)
iPSC	induced Pluripotent Stem Cell
IFNγ	Interferon gamma
IL-	Interleukin
Il2rγ	Interleukin-2 Receptor gamma common chain
IgG	Immunoglobulin G
INPP5D	Inositol Polyphosphate-5-Phosphatase
ITAM	Immunoreceptor Tyrosine-based Activation Motifs
KO	Genetic Knockout
LFA-1	Lymphocyte Function-Associated Antigen 1 (aka CD18 & CD11a)
LPS	Lipopolysaccharide
LTP	Long-term potentiation
MCI	Mild Cognitive Impairment
MEF2C	Myocyte Enhancer Factor 2C
MerTk	Proto-oncogene tyrosine-protein kinase MER
MHC-I	Major histocompatibility complex class I
MHC-II	Major histocompatibility complex class II
MMP9	Matrix Metallopeptidase 9
MNS	3,4-methylenedioxy-β-nitrostyrene
mNSC	Mouse Neural Stem Cell
MS4A4A	Membrane-Spanning 4-Domains, Subfamily A, Member 4A
MS4A6A	Membrane-Spanning 4-Domains, Subfamily A, Member 6A
MSD	Meso Scale Discovery
MWM	Morris Water Maze
NFT	Neurofibrillary Tangle
NK Cell	Natural Killer Cell
NF-κB	Nuclear factor kappa-light-chain-enhancer of activated B cell
NSC	Neural Stem Cell
PBS	Phosphate-Buffered Saline
PET	Positron Emission Tomography
PI3K	Phosphatidylinositol 3-Kinase
PICALM	Phosphatidylinositol binding clathrin assembly protein
P2RY12	Purinergic Receptor P2Y, G-Protein Coupled, 12
P2RY13	Purinergic Receptor P2Y, G-Protein Coupled, 13
PTK2B	Protein Tyrosine Kinase 2 Beta
PS-1	Presenilin-1
PS-2	Presenilin-2
PSD-95	Postsynaptic Density Protein 95
qPCR	Quantitative Polymerase Chain Reaction
RAG	Recombination Activating Gene
RIN3	Ras And Rab Interactor 3
ROS	Reactive Oxygen Species
sAD	Sporadic Alzheimer's disease

SCID	Severe Combined Immunodeficiency
SCLN	Superficial Cervical Lymph Node
SORL1	Sortilin-related receptor, L(DLR class) A repeats containing
Syk	Spleen Tyrosine Kinase
TCR	T Cell Receptor
TGF-β	Transforming Growth Factor beta
TGF-βR	Transforming Growth Factor beta receptor
Th1	Type 1 T Helper Cell
Th2	Type 2 T Helper Cell
Th17	Type 17 T Helper Cell
TLR	Toll-like Receptor
TNFα	Tumor Necrosis Factor alpha
Treg	Regulatory T Cell
Trem1	Triggering receptor expressed on myeloid cells 1
Trem2	Triggering receptor expressed on myeloid cells 2
TremL2	Triggering receptor expressed on myeloid cells like 2
WT	Wild-type
YFP	Yellow Fluorescent Protein

ACKNOWLEDGMENTS

I would like to thank my mentor Dr. Mathew Blurton-Jones for all of his encouragement and support through my graduate career. I greatly value Matt's unconditional support to pursue cutting-edge science, involving me in grant writing, including me strategic meetings with collaborators, and trusting that my independent work would provide new insight in to our scientific studies.

I would like to thank my co-mentor Dr. Wayne Poon for all his encouragement and support in my graduate career. I greatly appreciate his sacrifices and investment in me as young scientist and professional. Our scientific discussions were always challenging yet fruitful. I value and appreciate our friendship.

I am extremely grateful for my friends and colleagues that invested in me and my work and played critical and vital roles in the success of my studies. Dr. Ricardo N. Ramirez's scientific discussions and computational biology work on my studies elevated its status to a new level. I look forward to our friendship and continued scientific collaborations. I am internally grateful for Eric S. Martinez and his unwavering dedication to our work. Eric is a friend for life and a fellow colleague, and I look forward to his brilliant success. I thank Cecilia H.H. Nguyen for her dedication and work to my studies, and I thank her for trusting me to be her mentor early in her career and I look forward to her success.

I thank all of my friends in my life for their continued encouragement during my studies by providing an ear to talk to and pulling me away to enjoy life outside of lab. I am thankful for Bassem, Taylor, and Noura Shoucri for their endearing friendship and support in life—our families, ever growing, provide us a relationship to share in our challenges and accomplishments as professionals and parents.

I thank the UC Irvine Medical Scientist Training Program (MSTP) for its support in my career.

I would like to thank the entire Blurton-Jones lab for all that they have helped me with throughout my graduate career.

I also thank our research collaborators for committing their time and resources to my studies.

I would like to thank my committee members Dr. Andrea Tenner, Dr. Kim Green, and Dr. Matthew Inlay for the helpful suggestions and critiques.

This work was supported in parts by NIA RF1AG048099 (MBJ), NIA P50 AG016573 (MBJ), Alzheimer's Association Grant BFG-14-317000 (MBJ) and CIRM RT3-07893 (E.M.A).

CURRICULUM VITAE

Edsel Misael Abud

2007-2011	Research Assistant, Department of Chemistry and Biochemistry, California State University, Long Beach Long Beach, CA Dr. Stephen P. Mezyk
2009-2011	Research Assistant, Division of Pulmonary and Critical Care, The Johns Hopkins University School of Medicine Baltimore, MD Dr. Larissa A. Shimoda
2010-2011	Research Assistant, Department of Chemistry and Biochemistry, California State University, Long Beach Long Beach, CA Dr. Eric J. Sorin and Dr. Stephen P. Mezyk
2011	B.S. Biochemistry and B.A. Chemistry, California State University, Long Beach, Long Beach, CA
2016	M.S., Advancement to Ph.D. Candidacy, in Biological Sciences, University of California, Irvine Dr. Mathew Blurton-Jones
2017	Ph.D. in Biological Sciences, University of California, Irvine Dr. Mathew Blurton-Jones
2019	M.D., School of Medicine, University of California, Irvine

FIELD OF STUDY

Development of methodology for generating human microglia from induced pluripotent stem cells and their transcriptomic and functional validation. The role of the innate immune system in Alzheimer's disease pathogenesis; Human microglia integration in to normal and AD transgenic immune-deficient mouse brains.

HONORS AND AWARDS

2011	Departmental Honors, California State University, Long Beach
2011	Medical Scientist Training Program, M.D.-Ph.D fellowship, School of Medicine, University of California, Irvine

2013	2nd place winner, Affordable Electronic Medical Records App, UC Irvine School of Medicine AppJam, University of California, Irvine
2013-14	CIRM Pre-Doctoral Training Grant (TG2; PI: Drs. Peter J Donovan and Ping H. Wang; annually awarded)
2015-2016	UC Irvine School of Medicine Dean's Service Award, University of California, Irvine
2016	Carl W. Cotman Scholar's Award, UC Irvine MIND, University of California, Irvine

PUBLICATIONS

Original Reports

Abud EM, Ramirez RN, Martinez ES, Healy LM, Nguyen CHH, Newman SA, Yeromin AV, Scarfone VM, Marsh SE, Fimbres C, Caraway CA, Fote GM, Mandany AM, Agrawal A, Kayed R, Glylys KH, Cahalan MD, Cummings BJ, Antel JP, Mortazavi, A, Carson, MJ, Poon WW, Blurton-Jones, M (2017). iPSC-derived human microglia-like cells to study neurological diseases. *Neuron*, in press.

Gonzalez B, **Abud EM**, Abud AM, Poon WW, Gylys, KH (2016). Tau spread, apoE, inflammation, and more: Rapidly evolving basic science in AD. *Neurologic Clinics*, in press.

Chen W, **Abud EM**, Yeung ST, Lakatos A, Nassi T, Wang J, Blum D, Buee, L, Poon, WW, Blurton-Jones, M (2016). Increased tauopathy drives microglia-mediated clearance of beta-amyloid. *Acta Neuropathol Commun* 4:63.

Marsh SE, **Abud EM**, Lakatos A, Karimzadeh A, Yeung ST, Davtyan H, Fote GM, Lau L, Weinger JG, Lane T, Inlay MA, Poon WW, Blurton-Jones M (2016). The adaptive immune system restrains Alzheimer's disease pathogenesis by modulating microglial function. *Proc Natl Acad Sci USA* 113: E1316–25.

Abud EM, Ichiyama, RM, Havton LA, Chang HH (2015). Spinal stimulation of the upper lumbar spinal cord modulates urethral sphincter activity in rats after spinal cord injury. Am. Physiol Renal Physiol 308: F1032–F1040.

Abud EM, Maylor J, Undem C, Punjabi A, Zaiman AL, Myers AC, Sylvester JT, Semenza GL, Shimoda LA (2012) Digoxin inhibits development of hypoxic pulmonary hypertension in mice. *Proc Natl Acad Sci USA* 109: 1239 –1244.

Reports in Progress

Agrawal S, **Abud EM**, Snigdha, S., Agrawal, A. Enhanced Dendritic cell inflammatory and IgM antibody response against amyloid-β in aged subjects (2017). Submitted J Gerontol A Biol Sci Med Sci.

Book Chapters

Abud EM and Blurton-Jones, M (2016). Could stem cells be used to treat or model Alzheimer's disease? *Translational Neuroscience*, pp 203-225, 2016.

Mezyk SP, **Abud EM**, Swancutt KL, McKay, G, Dionysiou DD (2010). Removing Steroids from Contaminated Waters Using Radical Reactions, *ACS Symposium Series 1084 (Contaminants of Emerging Concern in the Environment: Ecological and Human Health Considerations)*, Chapter 9, pp. 213-225.

Conference Abstracts

Chang HH*, **Abud EM***, Havton LA, Epidural stimulation suppresses external urethral sphincter tonic activity in rats with chronic spinal cord injury. *Society for Neuroscience, Nov. 9-13, 2013, San Diego, CA.* Poster Presentation.

Abud EM, Nguyen CHH, Blurton-Jones MM. Using stem cell-derived microglia to study neurological diseases. *UCI Medical Scientist Training Program Symposium*, Jan. 14, 2015, Irvine, CA. Poster Presentation.

Abud EM, Chen BL, Nguyen CHH, Chen W, Davis J, Blurton-Jones MM., Examining the role of CXCR4 in the differential migration of ESC-derived and fetal-derived human neural stem cells. *AD-PD Congress, Mar 18-22, 2015, Nice, France.* Poster Presentation.

Abud, EM, Ramirez, RN, Martinez, ES, Healy, LM, Nguyen, CHH, Scarfone, VM, Marsh, SE, Madany, AM, Fimbres, C, Caraway, CA, Torres, MD, Park, A, Rakez, K., Gylys, KH, Mortazavi, A, Antel, JP, Carson, MJ, Poon, WW, Blurton-Jones, M. Fully-Defined Generation of iPSC-derived Human Microglia to Study Neurological Diseases. *Microglia in the Brain, Keystone, Colorado, USA. June 2016.* Slide Presentation.

Abud, EM, Ramirez, RN, Martinez, ES, Healy, LM, Nguyen, CHH, Scarfone, VM, Marsh, SE, Madany, AM, Fimbres, C, Caraway, CA, Torres, MD, Park, A, Rakez, K., Gylys, KH, Mortazavi, A, Antel, JP, Carson, MJ, Poon, WW, Blurton-Jones, M. Fully-Defined Generation of iPSC-derived Human Microglia to Study Neurological Diseases. *FASEB SRC on Translational Neuroimmunology: From Mechanisms to Therapeutics taking place in Big Sky, MT, USA. July 2016.* Poster Presentation.

Abud, EM, Ramirez, RN, Martinez, ES, Healy, LM, Nguyen, CHH, Scarfone, VM, Marsh, SE, Madany, AM, Fimbres, C, Caraway, CA, Torres, MD, Park, A, Rakez, K., Gylys, KH, Mortazavi, A, Antel, JP, Carson, MJ, Poon, WW, Blurton-Jones, M. Fully-Defined Generation of iPSC-derived Human Microglia to Study Neurological Diseases. *AD-PD Congress, Mar 18-22, 2017, Vienna, Austria.* Slide Presentation.

PRESENTATIONS

October 2013	MSTP Conference, UC Irvine
April 2014	Neuroblitz, UC Irvine

October 2014	MSTP Conference, UC Irvine
February 2015	Neuroblitz, UC Irvine
October 2015	MSTP Conference, UC Irvine
June 2016	Keystone Symposia: Microglia in the Brain
July 2016	Board of Governors Regenerative Medicine Institute, Cedars Sinai
October 2016	MSTP Conference, UC Irvine
March 2017	International Conference on Alzheimer's & Parkinson's; Vienna, Austria

ADMINISTRATIVE SERVICE

2011-2017	Webmaster and MSTP & Life Science Seminar Administrator Medical Scientist Training Program (MSTP), UC Irvine
2012-2013	Electronic Medical Records and Research Co-Chair, Flying Samaritans UC Irvine SOM, UC Irvine
2016-2017	General Secretary Medical Scientist Training Program (MSTP), UC Irvine
2016-2017	Executive Officer Research and Education in Memory Impairments and Neurological Disorders (ReMIND), UC Irvine

TEACHING

2011	Medical Student Tutoring: School of Medicine
2012	Neuroscience Review: School of Medicine
2012	Medical Student Tutoring: School of Medicine
2013	Pathology Review: School of Medic

ABSTRACT OF THE DISSERTATION

Generation of Human Microglia from Induced Pluripotent Stem Cells to Study Innate Immunity in Neurological Diseases.

By

Edsel Misael Abud

Doctor of Philosophy in Biological Sciences

University of California, Irvine, 2017

Assistant Professor Mathew Blurton-Jones, Chair

Microglia play an important role in developmental and homeostatic brain function. They profoundly influence the development and progression of neurological disorders, including Alzheimer's disease (AD). In AD, microglia respond to degenerating neurons, beta-amyloid (Aβ) and tau pathology, and CNS inflammation. AD-etiology involves complex interactions between age, genetic, and environmental risk factors. Recently, GWAS studies in large AD cohorts have identified numerous SNPs present in innate immune genes, many expressed in microglia. These SNPs confer an elevated risk in developing AD, and harboring of these SNPS is considered a risk factor. While the genes themselves are not risk factors, SNPs in these genes may impair the normal function of microglia, such as cytokine production and phagocytosis. Furthermore, many of these genes are involved in the detection or clearance of Aβ, and therefore these SNPs may collectively influence microglia function or influence dysfunction.

Studying human microglia is challenging because of the rarity and difficulty in acquiring cells from human CNS tissue. A methodology for generating human microglia from a renewable source has long remained elusive despite success in generating the other cell-types of the CNS.

This elusiveness existed due to the ontogeny of microglia and their unique transcriptome and functional differences versus other myeloid cells. The goal of my dissertation was to generate human induced pluripotent stem cell (iPSC)-derived microglia (iMGLs) to study their molecular and physiological function in neurological disease. To accomplish this goal, I developed a fully-defined protocol to generate large number of pure (>95%) iMGLs under 40 days.

iMGLs are highly like primary human microglia as assessed via whole-transcriptome and functional analyses. iMGL studies, in *vitro* and *in vivo*, highly suggest that they can be used as surrogates for human p microglia. Using iMGLs, I showed how AD-GWAS related microglial genes were influenced by two hallmark AD proteins—Aβ and Tau. In addition, I showed that iMGLs populate mouse brains and develop microglial-like arborized morphology and respond to Aβ in an AD transgenic mice. Together, this protocol represents an important advance in our ability to study human microglia in the context of development, health, and disease, such as AD.

INTRODUCTION

Alzheimer's disease (AD) is the most common form of age-related dementia and leads to a progressive loss of memory and executive function. People suffering from AD typically first lose declarative memory, then the ability to perform basic everyday functions, and eventually can no longer take care of themselves—robbing them of their independence. The rapid growth in the prevalence of Alzheimer's disease (AD) arguably represents one of the greatest threats to public health in the world. In the USA alone, AD currently affects more than 5 million people and every 68 seconds a new person is diagnosed with AD (Alzheimer's, 2016; Golde et al., 2011). As the world's demographics shifts toward an increasingly aged population, the incidence of AD is predicted to rise exponentially, such that by 2050 a new person will be diagnosed with AD every 33 seconds and 16 million people within the US will be affected. Without effective disease-modifying treatments the costs associated with caring for these patients will likely exceed $1.1 trillion per year in the US alone (Alzheimer's, 2016). The underlying mechanism of neuro-degeneration in AD patients is genetically complex and the identification of genetic variants has been heavily pursued.

A. Alzheimer's Disease Neuropathology and the Amyloid Cascade Hypothesis

Researchers have known since Alois Alzheimer's first report in 1907, that AD patients exhibit widespread brain atrophy and two hallmark lesions (Alzheimer, Stelzmann et al. 1995). Alzheimer described one of these lesions as a "special substance in the cortex" that was refactoring to histological stains. Several decades later, this "special substance" was identified by George Glenner and colleagues as beta-amyloid (Aβ), a small 40-42 amino acid peptide that accumulates as insoluble extracellular amyloid plaques (Glenner and Wong 1984). The second hallmark pathology described by Alzheimer appeared as a "tangle of fibrils indicat[ing] the place where a neuron was previously located". Neurofibrillary tangles (NFTs) were subsequently shown by several groups to be composed of insoluble hyperphosphorylated aggregates of the microtubule-binding protein tau (Grundke-Iqbal, Iqbal et al. 1986, Kosik, Joachim et al. 1986, Pollock, Mirra et al. 1986, Wolozin, Pruchnicki et al. 1986, Wood, Mirra et al. 1986). Both Aβ and tau pathologies have continued since their discovery to be a major focus of AD research and lead therapeutic targets. Yet, compounds that alter the production or degradation of Aβ and the aggregation of tau have thus far failed in late stage clinical trials (Cummings et al., 2014; Doody et al., 2013; Golde

et al., 2011; Siemers et al., 2006). Despite these failures, the 'amyloid cascade hypothesis' remains the prevailing theory regarding the cause and consequences of AD. This hypothesis postulates that overproduction and/or compromised clearance of Aβ is the driving force in AD pathogenesis that in turn leads to downstream insults including tau hyperphosphorylation, neuroinflammation, and synaptic and neuronal loss (Hardy and Selkoe 2002). The amyloid cascade hypothesis is strongly supported by genetic cases of dominantly inherited familial AD (fAD). Although fAD constitutes only 1-2% of all AD, these cases always involve either mutations or triplication of the amyloid precursor protein (APP) gene or mutations in presenilin-1 (PS-1) or presenilin-2 (PS-2). APP, as the name implies, is the precursor protein from which Aβ is proteolytically derived, whereas PS-1 and PS-2 make up the catalytic component of the gamma-secretase complex that releases beta-amyloid from APP. Each of these familial mutations lead to either an overall increase in Aβ production or a shift in the ratio of more aggregation-prone 42 amino acid Aβ versus the 40-amino acid form. In contrast, mutations in tau do not lead to AD but rather cause frontotemporal dementia (Hutton, Lendon et al. 1998). Together, these genetic findings strongly implicate beta-amyloid as the driving factor in AD pathogenesis. As a result, many researchers and the pharmaceutical industry have focused their efforts nearly exclusively on developing therapies aimed at reducing Aβ production or increasing its clearance from the brain. It is only in the last few years following the many failures of Aβ-targeting therapies and the development of new imaging modalities, that the field has begun to realize that Aβ accumulates for some 10-20 years prior to cognitive dysfunction and thus better represents a preventive target rather than a therapeutic one (Jack et al., 2013).

Recently, a worldwide collaborative effort using large patient cohort sizes has enabled genome-wide association studies (GWAS) that have led to the identification of several single nucleotide polymorphisms (SNPs) that modify AD risk (**Figure 1**). These genes, TREM2, CR1, BIN1, CD2AP, EPHA1, CLU, MS4A6A, PICALM, ABCA7, CD33, HLA-DRB5-1, PTK2B, SORL1, RIN3, DSG2, INPP5D, and MEF2C, are largely expressed in innate and adaptive immune cells. The identification of these GWAS genes has revealed that multiple genetic loci contribute to late-onset sporadic AD, which represents the great majority (>98%) of AD cases (Hollingworth et al., 2011; Naj et al., 2011; Seshadri et al., 2010). This is in stark contrast to autosomal dominant forms of AD (mutations in the APP, PS1, or PS2 gene), which account for 1-2% of AD cases.

However, the penetrance for individuals who inherit one of these mutations is 100%. As a result, the great majority of transgenic AD models have utilized overexpression of these mutant forms of APP and/or Presenilins to mimic the development of Aβ pathology. These models have greatly enhanced our understanding of Aβ generation and some of the downstream consequences of Aβ accumulation. However, mouse models cannot model the growing complement of human genes now implicated in AD. Fortunately, the ability to generate induced pluripotent stem cells (iPSCs) from patients has opened an exciting new opportunity to examine the relationships between genetic risk factors and AD-associated phenotypes. The use of iPSCs to model and study AD therefore overcomes a critical barrier to research that will likely greatly advance our understanding of AD.

It is critical to examine and understand the role of newly identified GWAS polymorphisms in disease, and patient-derived iPSCs can likely facilitate this examination. An important point to consider is that SNPs themselves do not necessarily cause disease-associated changes in gene expression. Instead, often SNPs represent altered sequences that are in linkage disequilibrium with a near-by causative mutation or polymorphism(Beecham et al., 2014; Guerreiro and Hardy, 2014). Given the high prevalence of AD risk SNPs in immune-related genes, it is important to study both the normal and disrupted function of these genes in appropriate immune cells, like human microglia. Furthermore, as one recent study has shown that rodent and human immune responses to inflammation are dramatically different (Seok et al., 2013), and studying these genes in human immune cells is likely to be most informative. Microglia are the major inflammatory cell type in the brain and many of the AD-risk SNPs are highly expressed in microglia (e.g. TREM2 and CD33). In addition, mice lack proper orthologs of human genes implicated in as AD risk genes, such as CD33 and CR1. These new GWAS studies have highlighted the notion that impaired or defective response to Aβ, tau, and chronic inflammation by microglia may be responsible for the majority of sporadic AD cases and targeting microglia function in AD may prove to be the foundation for effective AD therapies (Biber, 2017; Colonna and Butovsky, 2017; Gomez-Nicola and Perry, 2015; Mawuenyega et al., 2010). Therefore, a major focus of AD inflammation has recently shifted to understanding how microglia can impact AD pathogenesis (Malik et al., 2015).

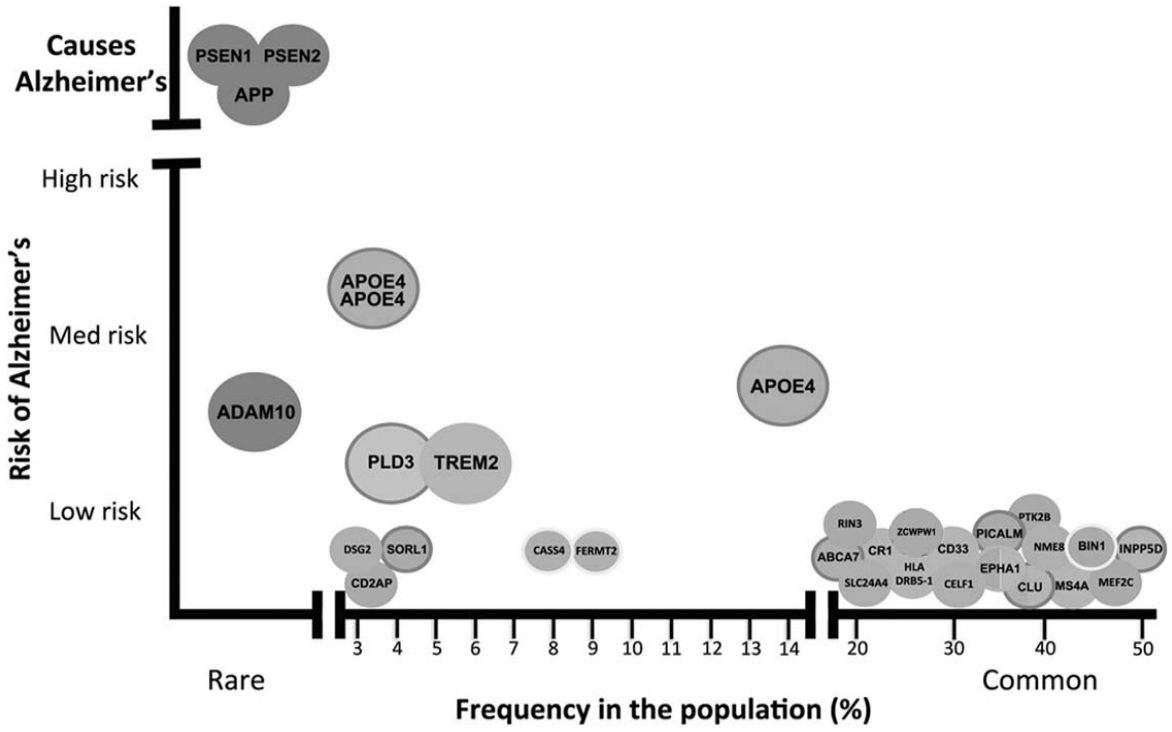

Figure 1: Rare and common genetic variants contribute to Alzheimer disease risk. Genome-wide association studies have identified a number of single nucleotide polymorphisms (SNPs) that increase late-onset AD risk. Both Innate immunity and endocytic risk alleles are common but singly confer a low risk. In contrast, rare variants like TREM2 have confer increased risk. Adapted from Alzheimer's Research UK, 2012; alzheimersresearchuk.org.

To begin investigating the role of microglia in AD, a renewable and consistent source of microglia must be developed. Currently, human microglia can only be obtained from fetal tissue predominately from elective terminations or from adult tissue from neurosurgery. These sources of microglia are inconsistent, variable in age, maturation and disease-phenotype. For example, microgliosis is a recognized component of epilepsy (Turrin and Rivest, 2004) and yet the predominant source of adult tissue for microglial isolation is from patients undergoing resection of epileptic foci. Thus, microglia isolated from such studies are likely to be differentially activated in comparison to either healthy brain microglia or AD patient-derived microglia. One possible solution to this challenge is to harness the advances of induced-pluripotent stem cell (iPSC) technology to generate a consistent and renewable source of human microglia. By studying the responses of these cells to AD-associated pathologies and the effects of AD-associated polymorphisms in human microglia, researchers may be able to greatly expand our understanding of the role of microglia in AD. Therefore, the broad objective of this dissertation is to develop an

approach to produce iPSC–derived microglial cells (iMGLs). I will then examine the effects of AD-associated pathologies on iMGL gene expression and function; showing that microglia play a near causative role in the pathogenesis of Alzheimer's and other CNS diseases.

Next, I will review the current understanding of microglia in AD, focusing on how microglia and other innate immune cells mediate inflammation and phagocytosis in the brain. I will highlight how microglia and other myeloid immune cells develop from different populations and the implications of developmental differences affecting AD pathology. Finally, I will discuss the strategy for generating iPSC microglia to study in AD.

B. Innate immunity and Inflammation in Alzheimer's Disease

In AD, increased levels of inflammatory mediators (e.g. cytokines, complement, etc.) are detected in the brain and CSF of patients (Barnes et al., 2014; Glenner and Wong, 1984; Heppner et al., 2015; Khemka et al., 2014; Veerhuis et al., 2011). These findings indicate a chronic activation of microglial immune pathways. Microglia are the resident innate immune cells of the CNS, and in healthy brains are identified by their highly ramified morphology and small soma (Kettenmann et al., 2011). Microglia are under constant surveillance of their environment and are known to interact with and maintain neuronal synapse in the developing and adult brain (Paolicelli et al., 2011). This neuronal-microglia interaction serves to facilitate CNS homeostasis and balance microglial functional activity. Many microglial functions, such as pruning of synapses, engulfing cells, delivery of brain-derived neurotrophic factors (BDNF), and immune-reactivity to invading pathogens are vital for CNS development and health, (Falsig et al., 2008; Gemma and Bachstetter, 2013; Paolicelli et al., 2011; Parkhurst et al., 2013; Sierra et al., 2010). In turn neuronal surface ligands such as CX3CL1 (fractalkine) and CD200 serve as "ON-OFF" signals for maintaining balanced microglial function through microglia surface receptors CX3CR1 and CD200R, respectively. Disruption of neuron-microglial interactions through neuronal death or activation of microglial surface receptors lead to microglial activation that is characterized by enlargement of the cell body and shortening of processes (amoeboid) (Biber et al., 2007), and this change in morphology is associated with CNS inflammation observed in AD (Karperien et al., 2013). However, microglia activation is not limited to pathways associated with neuronal-interactions.

Aβ can directly activate microglia via cell-surface pattern recognition receptors (PRRs) such as CD36, TLR- 2, -4, and -6, TREM2 and CD33 (Heneka et al., 2014). In broad terms, these PRRs serve to activate normally quiescent microglia in the CNS and increase phagocytosis of beta-amyloid. However, the activation of PRRs has been reported to have both synergistic and opposing consequences, and is further complicated by the fact that peripheral myeloid cells can invade the CNS under inflammation and co-express these surface markers, yet have differing outcomes compared to microglia(Prinz and Priller, 2014; Savage et al., 2015; Varvel et al., 2015).

Recently, a rare variant of triggering receptor expressed on myeloid cells 2 (TREM2; p. R47H) has been associated with a 2-4-fold increased risk in developing LOAD (Late-onset AD)(Guerreiro et al., 2013; Jonsson et al., 2013). In the brain, TREM2 is expressed in microglia (**Figure 2)** and in the periphery TREM2 is detected in macrophages and dendritic cells (Hamerman et al., 2006; Terme et al., 2004). TREM2 signals through its co-adaptor molecule TYRO kinase-binding protein (TYROBP, also known as DAP12), and genetic loss of DAP12 or TREM2 manifests as Nasu–Hakola disease or polycystic lipomembranous osteodysplasia with sclerosing leukoencephalopathy (PLOSL) (Paloneva et al., 2000; Paloneva et al., 2002). As the name suggests, PLOSL is a genetic disease characterized by bone-cysts in the distal bones with white matter dementia (Bianchin et al., 2004). The shared pathology of dementia in PLOSL and AD is of special interest to AD researchers as expression of TREM2 or DAP12 is greatly reduced or absent in PLOSL (Sasaki et al., 2015; Thrash et al., 2009).

TREM2 is detected at increased levels in post-mortem AD-tissue homogenates and is especially pronounced in the AD-vulnerable locations such as the hippocampus (Strobel et al., 2015). Although not completely agreed upon, TREM2 ligands include lipids, LPS, and Aβ (Poliani et al., 2015; Schmid et al., 2002; Wang et al., 2015b). Normal TREM2 function has been implicated in playing a role in increasing phagocytosis of debris, attenuation of TLR activity in dendritic cells, and involved in microglial survival (Ito and Hamerman, 2012; Melchior et al., 2010; Takahashi et al., 2005; Wang et al., 2015b). Furthermore, mutations in TREM2 have been shown to impair its surface expression and reduce phagocytosis *in vitro* (Kleinberger et al., 2014).

However, the role of TREM2 and its expression in myeloid/microglia in the AD brain has quickly become a debated topic. One group of researchers observed TREM2+ cells associated with Aβ plaques in the brains of AD transgenic mice. Flow cytometer analysis of these cells found them to be $CD45^{hi}$, which would traditionally suggest that they are infiltrating macrophages. Moreover, the use of two TREM2KO/AD mouse models has produced conflicting results. The first study looked at amyloid pathology early (~2-4 mo) in TREM2KO/AD mice and found that a lack of infiltrating macrophages ($CD45^{hi}$) was correlated with a reduction in Aβ load (Jay et al., 2015). The same group of authors in an additional study found that small-molecule activation of the nuclear receptors PPARα, PPARδ, PPARγ, LXR, and RXR increased myeloid/microglial phagocytosis of Aβ in AD mouse models. The authors suggested that the mechanism of action lied in nuclear receptor-mediated increase expression of phagocytic MerTK/AXL in infiltrating macrophages ($CD45^{hi}$) positive for TREM2 (Savage et al., 2015). Thus, it appears that data from this first group suggests that infiltrating macrophages predominately express TREM2 in the AD brain, the genetic loss of TREM2 prevents the infiltration of these cells, and TREM2KO is correlated with reduction of beta-amyloid pathology. The finding that reduced pathology in TREM2KO/AD mice was counter to previous reports of TREM2 expression and function in microglia; that is, TREM2 is exclusively expressed in microglia and licenses non-inflammatory type phagocytosis (Kleinberger et al., 2014; Melchior et al., 2010; Takahashi et al., 2005). Thus, the first studies challenged the notion that normal or complete expression of WT TREM2 was protective against AD, as earlier

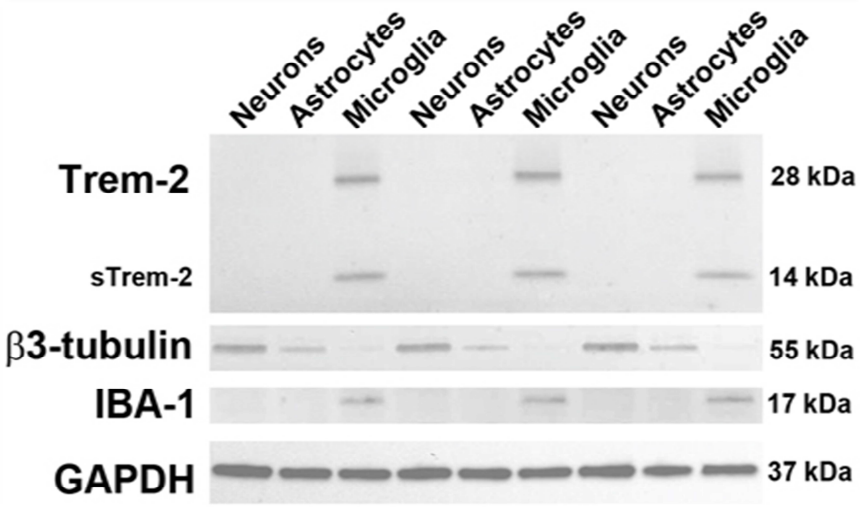

Figure 2: Western Blot analysis of CNS cells demonstrates that TREM2 expression is restricted to microglia**.** Cell protein lysates of human neurons, astrocytes, and microglia were analyzed by western blot. As shown, TREM2 protein is detected in IBA-1 positive microglia but not in neurons (β3-tublilin) or astrocytes (GFAP). The smaller band in the microglial lane likely represents a previously described soluble form of TREM2.

reports suggested that the AD-risk associated SNP of TREM2 R47H resembled a loss-of-function phenotype (Kleinberger et al., 2014; Sasaki et al., 2015; Sirkis et al., 2016; Yeh et al., 2016).

Simultaneously, a second group used a different TREM2KO model crossed with the same AD mice and reported opposite results. Their studies revealed that TREM2 is expressed in microglia by looking at published transcriptome databases and using a CX3CR1-GFPxAPPPS1-S21 mouse to identify microglia. The authors found that Aβ was increased at 8.5 months in TREM2KO/AD and suggested that TREM2 plays an important role in detecting lipids and in the survival of microglia (Wang et al., 2015b). When microglia from WT/AD mice and TREM2KO/AD mice were cultured ex-vivo without M-CSF, the CSF1R ligand required for cell survivability (Elmore et al., 2014), TREM2KO/AD microglia did not survive after 3 days whereas WT/AD mice did survive (Wang et al., 2015b). Thus, this second group's findings suggested that microglia require TREM2 for survival and lipid sensing and suggested these signals also promoted microglia phagocytosis of Aβ. Collectively, the two TREM2KO/AD models provided the field with mixed results and yet, both concluded that TREM2 plays a role in the survival and migration of myeloid cells surrounding AD plaques. Unsurprisingly, previous studies support the notion that myeloid cells increase TREM2 levels under inflammatory conditions and are associated with reduced activation but increased phagocytic activity, further supporting the late TREM2KO model's findings (Melchior et al., 2010; Turnbull et al., 2006). The two TREM2KO/AD studies differed in conclusions in part because amyloid pathology was assessed at two different time points, 4 months and 8.5 months. Recently, these studies were unified by using one TREM2KO/AD mouse model at two time points, 2 and 8 months, to investigate Aβ load. The authors found a disease-dependent progression effect of TREM2 deficiency, showing reduction in plaque volume early in disease but increased plaque volume late in disease (Jay et al., 2017.). The authors also observed reduced myeloid cell numbers, proliferation, and Aβ internalization as disease progressed, suggesting that TREM2 plays a role in critically modulating AD parthenogenesis. Thus, these studies highlight the importance of TREM2 in microglia/macrophages in CNS and suggests that mutations in TREM2 in the context of neurological diseases development, like AD, must be studied in microglia and other peripheral phagocytes. These contrasting studies also highlight the challenges of studying microglial function in mouse models that express supra-physiological levels of APP and PS1 and suggest that studying the normal function of TREM2 and other AD-associated microglial genes in human cells may be

preferable. These experimental results from these mouse models have become even more difficult to interpret given recent evidence that TREM2 itself is cleaved by presenilins to release a disease-associated soluble species (Gispert et al., 2016; Kleinberger et al., 2014; Suarez-Calvet et al., 2016a; Suarez-Calvet et al., 2016b; Wunderlich et al., 2013). Thus, whether presenilins are expressed under a specific neuronal restricted promoter or as a knock-in with normal microglial expression could further influence findings.

Other PRRs in microglia, like CD33, play a role in reducing microglia activation state by reducing their phagocytic capacity. CD33, also known as Siglec-3, is a cell surface marker expressed on myeloid progenitors, monocytes, macrophages, dendritic cells and microglia (Gorczyca et al., 2011). CD33 is expressed only in human cells but is related to Siglec-F in mice, due to the lack of ITIM (immunoreceptor tyrosine-based inhibitory motif) in Siglec-F (Zhang et al., 2007). Sialic acid residues on the surface of cells, like neurons, serve as the endogenous ligand for CD33, and CD33-sialic acid interaction leads to reduction of phagocytic activity but also decreases production of IL-1β (Lajaunias et al., 2005). In addition, sialic acid residues on neurites prevent the tagging of C1q on these neuronal structures and thus, inhibited their subsequent clearance via microglial CR3-mediated phagocytosis (Linnartz et al., 2012). Further confirming these results, the same authors enzymatically added sialic acid to neurites and found that this prevented their removal by macrophages when co-cultured *in vitro* (Linnartz-Gerlach et al., 2016). Thus, CD33 function may be implicated in the directed phagocytosis of apoptotic or necrotic neuronal structures in health or disease. Recently, the CD33 variant rs3865444^{CC} (CC) was identified as an AD risk SNP in recent GWAS studies (Hollingworth et al., 2011). Furthermore, this variant is associated with increased surface expression of CD33 and reduced internalization of Aβ, as detected by immunohistochemistry of human AD brains (Griciuc et al., 2013). Further analysis of the CD33 risk allele in human monocytes discovered two more additional variant genotypes known as rs3865444 ^{CA} (CA) rs3865444 ^{AA} (AA). The CA genotype was correlated with increased CD33 expression but not as high as the CC genotype however, the AA genotype had decreased cell surface expression of CD33 and had increased phagocytic activity. These *in vitro* assays were validated in human post-mortem AD tissue. It is not fully understood how these varying genotypes might confer increased AD risk, but these studies show that the AA phenotype is correlated with increased phagocytosis and reduced PiB amyloid radiotracer binding in humans (Bradshaw et al., 2013). An additional conclusion from these studies is the possibility of screening

peripheral blood mononuclear cells (PBMCs) for biomarkers related to AD-risk alleles like CD33. For example, in collaboration with Dr. Wayne Poon (UC Irvine MIND Institute), the screening of AD patient PBMCs has revealed that CD11c+ blood dendritic cells express the highest values of CD33. Furthermore, CD33 has also been shown to modulate TREM2 expression through CD33 ITIM activity, highlighting the idea that these surface receptor interactions in AD are highly dependent on each other and orchestrate responses with each other (Chan et al., 2015).

Following stimulation of TLRs and CD36 by Aβ, the canonical NF-kB proinflammatory pathway is activated in microglia. This leads to expressed expression of some proinflammatory transcripts including IL-1β, which can increase inflammation and neurotoxicity (El Khoury et al., 2003; Liu et al., 2012; Rapsinski et al., 2015), further exacerbating the degenerative state of neurons. IL-1β signaling through IL1-R also in turn leads to activation of NF-kB and increased cytokine production of CXCL1/2, IL-6, and TNFα (Moynagh, 2005), thus creating a positive feedback cycle of inflammatory activation. Furthermore, IL-1R activity is required for self-renewal of microglia in the brain and suggests one mechanism in which microglial proliferation, over the course of chronic inflammation, is mediated by elevated IL-1β (Bruttger et al., 2015). These cytokines are classical inflammatory molecules and have a role in the recruitment of peripheral leukocytes in to the CNS (Amanzada et al., 2014). While CD36 activity is required for the initial response of TLRs to Aβ, the role of CD36 is predominately an endocytic one; facilitating the crystallization of soluble Aβ in phagolysosomes to promote NLRP3 inflammasome activation. Thus, TLRs serve as the first signal (priming) and CD36 serves as the second signal for NLRP3 inflammasome assembly and subsequent increased IL-1β (Gomez-Nicola and Perry, 2015; Sheedy et al., 2013). It follows that CD36 and TLR activation by Aβ have a synergistic role in increasing IL-1β production. Why would microglia cells increase IL-1β? Is this an attempt to mount an offensive or has the system trapped itself in a vicious loop of inflammation? A recent study has identified IL1-R1 activity as the mechanism behind the proliferation and self-renewal of microglia in the adult brain (Bruttger et al., 2015). Therefore, one potential interpretation could be that IL-1β is being generated to increase microglial numbers in order to clear out beta-amyloid or other perceived pathogens. However, increased IL-1β and microglia has been observed in AD cases and in transgenic AD models, yet Aβ levels remain elevated (Heppner et al., 2015; Nazem et al., 2015; Patel et al., 2005; Rothwell, 2003). Whether microglial IL-1 β levels can be reduced and whether its restriction is beneficial to AD pathology has yet to be fully answered.

Activated microglia in AD, that is microglia that have diverged from homeostatic function, are involved in many functions including ROS generation, cytokine production, phagocytosis and secretion of growth factors (Guillot-Sestier and Town, 2013). As highlighted above, microglial PRRs can be activated to engulf beta-amyloid (i.e. TREM2), increase cytokine production (i.e. IL-1β), or reduce activation state with concurrent reduction in phagocytosis (i.e CD33). Therefore, microglia in AD should be classified as being in a neuroprotective or neurotoxic state but rather be studied as being in a continuum of states that has become imbalanced by the complexities of AD (Guillot-Sestier et al., 2015). This imbalanced phenotype is characterized by mixed functional states where microglia secrete classical inflammatory cytokines, such as IL-1β and IL-6, but also secrete growth factors such as TGFβ-1 and BDNF (Town et al., 2008). The imbalance of inflammatory response has been clearly linked to a more severe AD disease phenotype, suggesting that microglial inflammatory pathways may serve as future therapeutic targets.

C. The Developmental Origin of Microglia

Microglia are the macrophages of the CNS and participate in a variety of functions, such as phagocytosis of debris, apoptic cells as well as facilitating oligo- and neurogenesis during development and in adulthood (De Lucia et al., 2016; Gemma and Bachstetter, 2013; Shigemoto-Mogami et al., 2014; Sierra et al., 2010). Rio Hortega, a student of Santiago Ramon y Cajal, first described microglia as tree-like cells dispersed throughout the brain. Today, Rio Hortega is known as the Father of Microglia and the origin of microglia became immediately debated (reviewed in (Kettenmann et al., 2011). Recent students have determined the ontogeny of microglia to be uniquely different from other myeloid cells and this development is preserved throughout evolution. Elegant linage-tracing studies have shown that microglia develop from yolk sack macrophages (**Figure 3**) as early as embryonic day E7.5 in mice and as early as the third week of gestation in humans (Ginhoux et al., 2010; Kierdorf et al., 2013; Schulz et al., 2012). In one lineage-tracing study, Kiedorf and colleagues, revealed that in the developing embryo, tissue macrophages arise from extra embryonic c-Kit+ CD45- hemangioblast cells that yield CD45+/CX3CR1-/CD115+ progenitors (labeled as A1). A1 cells further differentiate in to CX45+/CX3CR1+/CD115+ (A2) microglia progenitors that invade the brain utilizing matrix metalloproteinase (MMPs) 8 and 9 at day 10.5 days post conception (Kierdorf et al., 2013). Once in the brain, microglia further invade the deeper structures of the brain and begin to tile in volume.

After further development and maturation, microglia are distinguished by their small soma and ramified processes expressing surface microglia/macrophage markers, like ionized calcium binding adapter molecule (Iba1), CD115 (CSF-1R), fractalkine receptor (Cx3cr1), CD68, CD45, CD11b, TMEM119, and P2ry12 (Ito et al., 1998; Karperien et al., 2013) (Andjelkovic et al., 1998; Bennett et al., 2016; Butovsky et al., 2014; Haynes et al., 2006; Pont-Lezica et al., 2011; Rezaie and Male, 1999). Once in the brain, microglia are distinguishable from other CNS macrophages, like perivascular or meningeal macrophages by their transcriptomic profile and function (reviewed in(Prinz and Priller, 2014).

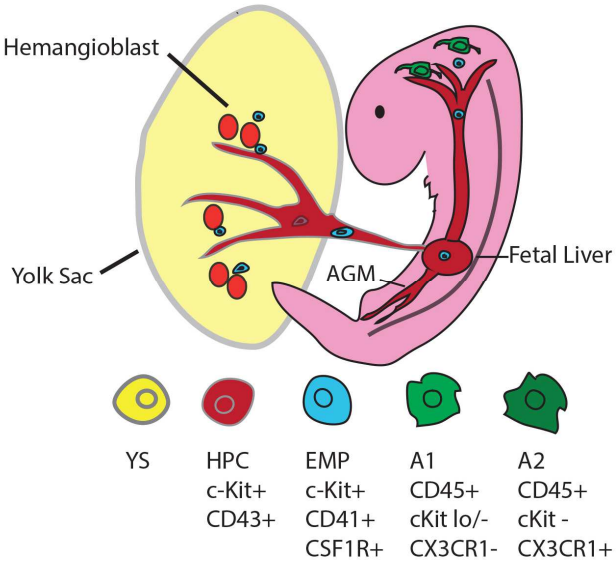

Figure 3: Microglia arise from yolk sac-derived primitive hematopoietic progenitors. Lineage tracing studies in mice have identified the earliest hematopoietic precursors capable of giving rise to tissue-resident macrophages, like microglia in the CNS, to come from the yolk-sac (YS). YS cells yield c-Kit^{+}/CD43^{+} to hematopoietic progenitors (HPC) that also give rise to erythromyeloid progenitors (EMPs) that are c-Kit^{+}/CD41^{+}/CSF1R^{+}. EMPs yield primitive red blood cells (not depicted) and early macrophages that are CX3CR1^{+}/CD45^{+}, eventually giving rise to microglia in the brain.

Molecular Programs Involved in Microglial Genesis.

Many of the microglial surface markers play important roles in the cellular programs that guide microglial development, maturation, and function. Several of these microglial proteins, such as CSF1R, are also vital for their self-renewal and homeostasis within the brain (Elmore et al., 2015; Elmore et al., 2014; Wang et al., 2012). These molecular programs involve the temporal and spatial expression of transcription factors, cytokine receptors, and cytokines themselves. The transcription factor runt-related transcription factor-1 (RUNX1) was found to be richly expressed in the yolk sac and has been shown to be necessary for the development of early myeloid cells, specifically microglia, when utilizing a RUNX1-cre reporter mouse model (Ginhoux et al., 2010; Samokhvalov et al., 2007). Further establishing the importance of RUNX1 in yolk sac

hematopoiesis, and microglia development, knockout of RUNX1 in mice fail to undergo hematopoiesis and are embryonically lethal (Liakhovitskaia et al., 2010). Studies using RUNX1 knockout mice also revealed that the myeloid transcription factor Sfpi1/PU.1 is a direct downstream target of RUNX1 because mice lacking RUNX1 did not express PU.1(Huang et al., 2008). PU.1 transcriptional activity is also detected in early hematopoiesis and is involved in directing the differentiation of myeloid and lymphoid cells in hematopoietic progenitors/stem cells (Arinobu et al., 2007; DeKoter et al., 2002; Nutt et al., 2005; Zhang et al., 1996). Like RUNX1, knockout of PU.1 exhibits reduced myeloid and lymphoid cells, and PU.1 -/- mice die soon after birth (McKercher et al., 1996; Scott et al., 1994; Zhang et al., 1996). mRNA expression analysis using RT-qPCR from sorted erythromyeloid, A1, A2, and embryonic microglial cells revealed that Spi1/PU.1 and interferon regulator factor 8 (IRF8) expression was continuously expressed during the development of microglia, and Iba1+ embryonic microglia cells were absent in embryonic PU.1-/- mice (Kierdorf et al., 2013). However, Iba1+ embryonic microglia were present in IRF8 -/-, albeit at statistically lower numbers compared to IRF8 +/+ mice, suggesting a dispensable role for IRF8 in the establishment of microglia. Therefore, the transcription factors RUNX1 and PU.1 are necessary for establishing early hematopoietic progenitors that give rise to microglia, and thus are required for microglia development**.**

PU.1 is also needed to promote the expression of CSF-1R, a receptor tyrosine kinase that is required for the development and maintenance of myeloid cells (Aikawa et al., 2010). Mice deficient of CSF1R lack large numbers of myeloid cells and microglia are virtually absent in the CNS (Ransohoff and Cardona, 2010; Saijo and Glass, 2011). Furthermore, recent innovative studies using pharmacological inhibition or genetic ablation of CSF1R have revealed that microglia still depend on CSF1R signaling for survival in the adult brain (Bruttger et al., 2015; Elmore et al., 2015; Elmore et al., 2014). These same studies also revealed the capacity of microglia to self-renew in the adult brain and showed that these cells may rise from potentially previously unidentified CNS-resident progenitors. Interestingly, genetic ablation of CSF1 (M-CSF) affects monocyte/macrophage subpopulations but has a very small impact on microglial numbers, suggesting an additional ligand involved in CSF1R signaling in microglia (Nandi et al., 2012; Wang et al., 2012; Yoshida et al., 1990). In fact, CSF1R has been shown to have two ligands with overlapping but distinct functions, Colony stimulating factor 1 (CSF1; also known as M-CSF) and interleukin 34 (IL-34).

Both M-CSF and IL-34 are involved in the commitment, proliferation, and maintenance of microglia, monocytes, macrophages and dendritic cells (Droin and Solary, 2010; Luo et al., 2013). The differences in the development of these distinct myeloid populations largely depend on the temporal and spatial expression of M-CSF and IL-34 (Nandi et al., 2012). Using an IL-34-LacZ reporter mouse model, it was found that IL-34 is made by neurons in the CNS and keratinocytes in the dermis, and IL-34, but not M-CSF, is important for development and maintenance of microglia and Langerhans cells (LCs). Microglia numbers in LacZ knock-in Il-34 deficient mice were severely reduced in the neocortical areas of the brain but cerebellum levels were indistinguishable from wild-type controls (Wang et al., 2012). In the same study, LacZ activity was detected in the cortex and in the hippocampus but not in the meninges or cerebellum, thus suggesting that IL-34 expression may be predominately expressed in neocortical areas of the brain. The spatial distribution of IL-34 and M-CSF can therefore influence the gene expression profiles of microglia populations in across brain-regions. Recently, Butovsky and colleagues (Butovsky et al., 2014) established a unique microglia signature that is dependent on TGFβ-1 signaling. In additional to the role TGFβ-1, transcriptome profile variance analysis of region-specific microglia revealed that cerebellar, olfactory, and retinal microglia cluster together but are separate from neocortical/hippocampal microglia. One interpretation of this data is that while both M-CSF and IL-34 cytokines are important for microglial survival varying neuroanatomical expression of these CSF1R ligands also influence their unique genetic profiles. With the advancement of new techniques and technologies, previously observed diversity of microglia in the brain is currently being studied (Hanisch, 2013). Whole-transcriptome profiling of murine microglia from varying regions have now shown that young adult microglia from the hippocampi and cerebellar remain in more immune surveillance state and subsequently these differences are diminished during aging (Grabert et al., 2016).

Microglial ontogeny studies have been informative for how microglia develop; yet once in the brain they are very difficult to separate from peripheral myeloid cells. Isolated microglia can be distinguished in the brain using flow cytometer analysis of its CD11b/CD45 expression, which is lower compared to blood-borne myeloid cells (Ford et al., 1995). However, microglial CD45 and CD11b expression levels can increase due to pro-inflammatory activation such as stimulation with LPS, but their levels are thought to never increase to those of peripheral myeloid cells (Carson et al., 1998). Therefore, microglia can be isolated according to their $CD11b^{int}/CD45^{lo\text{-}int}$ profile

and investigated for unique molecular signatures. As mentioned above, recent mRNA expression analysis of isolated microglia, blood, and tissue mononuclear cells *ex-vivo* have established a microglial-signature (Butovsky et al., 2014; Hickman et al., 2013). Direct RNA-sequencing of murine microglia and macrophages identified 626 greatly enriched microglial transcripts including *Hexb, P2y12, P2y13, Gpr34, Cx3cr1*, *Tgfbr1*, and *Trem2* (Hickman et al., 2013). In humans, *P2y12, Gp34, MerTK, C1qa, Pros1,* and *Gas6* were all highly expressed via RT-PCR in human fetal and adult microglia compared to blood monocytes (Butovsky et al., 2014). Immunohistochemical and proteomic analyses identified P2ry12 as a unique cell surface marker of quiescent and alternatively active microglia, and TGFβ-1 maintained the expression of P2ry12 in primary cultured microglia (Butovsky et al., 2014; De Simone et al., 2010; Haynes et al., 2006; Moore et al., 2015). Gene-pathway analysis identified TGFβ-1 as a hub gene influencing the expression of many microglial genes and TGFβ-1 knock-out/IL-2-promoter-TGFβ-1 mice lack microglia in the brain, yet peripheral myeloid cells were intact (Butovsky et al., 2014). Therefore, TGFβ-1 signaling is necessary for microglia development, and maintenance of quiescent microglia phenotype (Butovsky et al., 2014; De Simone et al., 2010; Goldmann et al., 2013). As microglia continue to be implicated as modulators of many CNS diseases, like AD, it is important to understand what molecular programs not only influence microglial physiology, but to be able to distinguish microglia from other CNS myeloid cells including myeloid cells derived bone-marrow precursors. These CNS and periphery derived cells have also been implicated to be playing a role in health and disease and in some cases have been used as microglial-substitutes *in vitro* or have been adopted as potential disease-modifying phagocytic cells in place of chronically 'activated' microglia (reviewed in(Biber et al., 2016; Ransohoff and Cardona, 2010)).

Bone-marrow derived myeloid cells that contribute to the pathological progression of neurological diseases, such as AD, do so in several ways. In the proper brain parenchyma itself, peripheral myeloid cells have been detected in AD and EAE models by immunohistochemistry or using flow cytometer analysis (Hohsfield and Humpel, 2015; Stalder et al., 2005; Varvel et al., 2015). Similar same studies have used biochemical assays to show that these myeloid cells in the CNS differently secrete higher levels of pro-inflammatory cytokines IL-1β, IL-12, IL-6, and IL-23 compared to microglia (Remington et al., 2007; Wlodarczyk et al., 2014; Yamasaki et al., 2014). Thus, peripheral cells are suggested to exacerbate CNS pathology. Because these infiltrating cells down regulate cell surface markers upon entering the CNS and can adopt similar morphological

and functional similar to microglia in the brain, it is important to understand what separates these two populations, especially when studying the function of microglial genes identified as AD risk genes (Yamasaki et al. 2014.) The discussion of the origin of mononuclear phagocytes provides some explanation for why resident CNS microglia and invading myeloid cells may differentially respond to disease and pathology and greatly highlight the need for generating microglia that is faithful to microglia ontogeny.

D. Studying Microglia Using iPSCs.

Despite the widely-accepted importance of microglia in human neurological disease, methods to generate microglia from pluripotent human stem cells were yet to be reported at the beginning of my dissertation studies. Only until recently, late 2016 and early 2017, two technical reports been reported on generating human microglial-like cells from pluripotent stem cells. While these studies will be discussed later, both studies provided data on the generation protocol, functional, and genomic validation of their microglial-like cells (Muffat et al., 2016; Pandya et al., 2017). Moreover, both papers developed protocols that were either dependent on unguided embryoid body differentiation or reliant on co-cultures, limiting the yield and purity of cells. Both studies attempted to make microglia from stem cells and the characterization of their hematopoietic precursor was limited or used protocols that were more suited for bone-marrow-like differentiation. As highlighted above, microglia rise from yolk sac hematopoietic progenitors early in development and are a separate population from embryonically derived peripheral myeloid cells (Hoeffel et al., 2015). It is therefore critical to develop new tools and technology that will allow researchers to study the role of human microglial in neurological disease and test novel compounds to modulate microglial function in AD. This deficiency may arise in part from the difficulty in distinguishing microglia from similar peripheral-derived macrophages. To begin generating microglia from iPSCs, the correct primitive hematopoietic progenitor that reflects *in vivo* microglial hematopoietic cells must therefore be used. Thus, my dissertation required careful study of hematopoietic development and applying this knowledge to generating a hematopoietic precursor from iPSCs that would give rise to microglia cells.

Hematopoiesis in vitro as a Source of Microglial Precursors

Many labs have worked out the generation of human hematopoietic progenitor/stem cells, and their embryonic development has been recaptured *in vitro* (Sturgeon et al., 2013). Embryonic hematopoiesis first starts in the blood-islands of yolk sac cells in a process called primitive hematopoiesis (de Jong and Zon, 2005; Jagannathan-Bogdan and Zon, 2013). As highlighted above, primitive hematopoiesis gives rise to early yolk sac microglia-progenitors. This early program also gives rise to large primitive erythrocytes as detected by the production early globulins (Kennedy et al., 2007). These HPCs are further identified by their enriched expression of CD235a, which is controlled by increasing ActivinA/Nodal pathways and concurrently inhibiting WNT/β-catenin signaling. Corollary to this pathway is the establishment of definitive hematopoiesis, which closely resembles late yolk sack, AGM, fetal liver, and adult bone-marrow hematopoiesis and requires reduced ActivinA/nodal and elevated WNT/β-catenin signaling (Sturgeon et al., 2014). Definitive hematopoiesis is the term used to describe c-Myb dependent generation of hematopoietic stem cells (HSCs) that seed the fetal liver and bone marrow in development and give rise to lymphoid tissue(Kennedy et al., 2012). Interestingly, RUNX1 has been identified as a transcriptional program required for definitive hematopoiesis and for microglial development. However, RUNX1 splice variants A and B are differentially expressed under the downstream promoter P2, and are responsible for primitive hematopoiesis (Ran et al., 2013), whereas the presence of an upstream promoter leads to RUNX1C expression (Samokhvalov et al., 2007). Recent differentiation of RUNX1C-GFP embryonic stem cells to hematopoietic cells has revealed that definitive hematopoiesis can be characterized by the presence of RUNX1C, concurrent expression of definitive transcription factor c-Myb, and the capacity to give rise to lymphoid progenitors (Ditadi et al., 2015; Hoeffel et al., 2015). Therefore, it is appropriate to use primitive but not definitive HPCs to being the development of a microglia differentiation protocol. Fortunately, many stromal-cell and stromal-free protocols can generate early primitive HPCs from hPSCs, albeit with varying efficiency and challenges (Choi et al., 2011; Kennedy et al., 2007; Salvagiotto et al., 2011; Sturgeon et al., 2013; Uenishi et al., 2014; Vodyanik et al., 2005). Therefore, primitive hematopoietic progenitors, as developed from Flk-1^{+}, CD235a^{+} cells can potentially give rise to microglia in a dish. However, current published "microglial-like" cell models do not take advantage of these hematopoietic differentiation programs. Instead, they utilize adult bone marrow cells (Leone et al., 2006), or in the case of murine microglial-cells, isolate CD45+/Iba1+ myeloid cells generated as a side product in Embryoid-Body (EB) neural

differentiation (Beutner et al., 2010; Roy, 2012). Because of these challenges, very few attempts have been made to improve on a previously published protocol generating microglia from mouse embryonic stem cells or others have adapted monocyte-derived macrophages as model systems of microglia *in vitro*. These model systems have fallen short in their attempts of generating a better microglial-like cell.

Current Microglial Models

Current models of microglial cells have been predominately differentiated from murine pluripotent-stem cells (Beutner et al., 2013; Beutner et al., 2010; Napoli et al., 2009), human bone marrow cells, or human blood monocytes (Leone et al., 2006; Noto et al., 2014; Ohgidani et al., 2014). These cells express similar characteristics of primary microglia in morphology *in vitro* and are positive for shared microglia/macrophage markers, like CX3CR1, Iba1, and TREM2. Each one of these model systems have fallen short in providing the appropriate platform for studying microglial function *in vitro*.

Prior to the start of my dissertation studies and 2016, the most extensive work for generating microglia had been performed using mouse embryonically derive stem cells (ESCs) (Beutner et al., 2013; Beutner et al., 2010). These ESC-derived murine microglia (ESdMs) are generated from EBs undergoing neuronal differentiation and as a consequence of adding recombinant GM-CSF, microglial-like cells arise after 60 days (Beutner et al., 2010). These cells migrate to CX3CL1 and express common microglial/macrophage markers CD11b, CSF1R, and Iba1. An interesting although surprising phenotype of these cells is that they can be passaged for more than 20 cycles and maintain high phagocytic activity (Napoli et al., 2009). This is in stark contrast to primary fetal or adult microglia cultures that do not proliferate past 40 days of culture and develop a quiescent phenotype *in vitro* (Caldeira et al., 2014). Furthermore, recent gene-expression PCA analysis of these cells revealed that they cluster with immortalized microglial line BV2 and the macrophage line RAW 264.7 than primary cultured or ex vivo microglia (Butovsky et al., 2014). Thus, the use of this approach for generating microglia-like cells appears to generate an immortalized macrophage cell that expresses some microglial makers, perhaps due to soluble and non-soluble cues from adjacent developing neuronal cells. ESdMs have not been adapted by the field perhaps because mouse primary microglia are more readily and routinely isolated from

fresh tissue, the similarities of easily cultured BV2s, or avoiding the pitfalls associated with transcriptomic divergence highlighted in Butovsky and colleagues' studies.

In the differentiation of human microglial-like cells from monocytes and bone marrow cells, CD45 expression is lower compared to macrophage levels by flow cytometry (Leone et al., 2006; Noto et al., 2014). However, these cells are derived from adult hematopoietic cell and may actually phenotypically resemble CNS infiltrating myeloid cells more than microglial and would therefore exhibit differing functions in CNS-disease (Ransohoff, 2011). In EAE for example, infiltrating monocytes exacerbate inflammation yet, do not contribute to the microglial pool, clearly outlining different roles of microglia and monocytes in EAE disease progression (Ajami et al., 2011). Therefore, studying monocyte-derived microglial-like cells and their function in the context of disease may provide differing results compared to microglia. Moreover, manipulation of CNS-related diseases Again, other studies have shown that monocyte derived cells *in vitro* or *in vivo* can exhibit some qualities of microglia, such as phagocytosis and cytokine secretion, but fail to recapture bona-fide microglia function, like P2ry12-mediated reactivity, ramified morphology, and controlled synaptic pruning (Stalder et al., 2005; Town et al., 2008).

As mentioned earlier, two studies have recently reported generating human microglia-like cells from pluripotent stem cells (Muffat et al., 2016; Pandya et al., 2017). The first protocol generated microglial-like cells from hESCs and iPSCs, called pMGs (Muffat et al., 2016). pMGs are generated from EBs using a chemically defined medium and exposing the cells to different levels of M-CSF and IL-34 over 60 day. The major questions left unanswered by the authors are related to the reproducibility and yield of their microglial protocol. The use of EBs yields a mixture of "compact phase-bright neutralized spheroids" and "cystic" EBs (YS-EBs). These EBs represent two different germ lineages; mesoderm lineage cells and developing neuroectodermal cells, which are simultaneously present within their culture system. As such, these other cell types likely serve as an endogenous source of all mentioned molecules. For example, neurons and glia can produce M-CSF, IL-34, CD200, CX3CL1, and TGFβ. Furthermore, their methodology of enriching for single cell precursors using adhesion to non-specific modified TC plastic (Primaria) also suggests that contaminating cells, such as adherent neuroectoderm-derived cells like astrocytes, can be the source of all cytokines required for myeloid/microglia generation. Additionally, the selection by adhesion step involves continuously exposing adherent cells to mixed EBs over the course of a

month, thus increasing the likelihood of exposing their adherent myeloid cells to differentiating CNS and mesoderm conditioned media. Notably, they do not add TGFβ-1 to their media, despite evidence suggesting that TGFβ-1 can influence both the generation of microglia and establishment of a microglial signature *in vivo* and *in vitro* (Butovsky et al., 2014). Finally, there is a limited amount of quantitative novel functional assays, again raising questions on the efficiency of the protocol. pMGs do integrate with 3D neuronal co-cultures and a representative image and video recording shows extension projection by pMGs, thus showing the beginnings of ramified processes. The authors generated pMGs from MECP2 mutant lines and observed that these cells were smaller in size compared to WT MECP2 lines. While preliminary, this early study shows that iPSC-derived cells can be used to begin address the impact gene mutations have on microglia function. Muffat and colleagues' protocol attempted to recapitulate microglia ontogeny and development by focusing on using yolk sac-like EBs to generate their microglial cells and while questions remain, perhaps due to brevity of a technical report, the progress highlighted that human microglial-like cells could be generated *in vitro.* Furthermore, their use of serum-free defined media allowed for the generation of allogenic neurons and astrocytes.

Like the Muffat et al study, they were concerns with the efficiency and reproducibility of their protocol the second report. While Muffat et al used chemically defined cultures, this differentiation protocol is reliant on co-culture with primary cells (Pandya et al., 2017). Pandya and colleagues generates hematopoietic progenitors using mouse OP9 stromal co-cultures or a chemically defined protocol to produce a myeloid cell they label as iPS-MG and consider microglia-like. Both stromal-derived and feeder-free hematopoietic precursors are not fully characterized and are propagated using G-CSF, GM-CSF, and FLT3L---cytokines that are known to produce common myeloid progenitors (CMPs) derived from more definitive hematopoiesis occurring in the bone-marrow (Choi et al., 2011; Ditadi et al., 2015; Kennedy et al., 2012; Redecke et al., 2013; Sturgeon et al., 2014; Vodyanik et al., 2005). These precursors were then plated with human astrocytes in serum-based media supplemented with only M-CSF. While the hematopoietic protocol could be replaced with their defined media, the authors did not provide an astrocyte-free differentiation step.

The characterization of iPS-MGs was performed with few experiments that were limited qualitative functional assays using immunofluorescence as primary read out. For example, iPS-

MGs are isolated from astrocyte-co culture using FACS and CD39 expression, which has been recently reported to be present in microglia (Butovsky et al., 2012). They find that ~8% of their iPS-MG in astrocyte co-culture are CD39 positive. After isolation, iPS-MGs were large amoeboid cells in culture, internalized pHrodo-red conjugated E. *coli* particles, and produced ROS species in response to E. *coli* as assessed by immunofluorescence imaging. The authors also used microarray to assess iPS-MG RNA-expression and compared their profile to that of macrophages, dendritic cells, iPSCs, and commercially-sourced fetal microglia. The authors co-transplanted mouse iPS-MGs with glioblastoma cells lines in the brains of immune deficient mice and found that mouse CX3CR1-GFP iPS-MGs migrated to glioblastoma lines. Immunofluorescence analysis of transplanted mouse iPS-MGs showed amoeboid-like morphology of engrafted cells in the brain. Interestingly, injection of mouse neonatal or iPS-MG and subcutaneous injection of dendritic cells dramatically increased the survivability of glioblastoma-harboring mice. As the transplant studies focused only in regions where glioblastoma cells were present, there remains a question of whether human or mouse iPS-MGs populate immune deficient mouse brains and exhibit microglial-like ramified morphology. The response of iPS-MGs to CNS-like environment can be further studied by imaging analysis of mouse or human 2D or 3D culture studies. The 2D studies are highly feasibly as their protocol already requires co-culture with astrocytes. Mouse 3D culture studies are feasible studies as mouse CNS tissue is readily isolated and cultured. Their use of the mouse CX3CR1-GFP iPS-MG would allow for discerning iPS-MG versus endogenous microglia in mouse 3D cultures. Furthermore, the use of RNA-seq data would allow comparative meta-analysis across all microglia-differentiation protocols.

Both studies have limitations in the production iPS-derived microglia and validation of their cells by functional and transcriptomic analyses. The low yield amount of microglia cells generated from both protocols limited the ability to quantitatively assess microglia using multiple functional assays. Therefore, the need for the generation of large numbers of human microglia from a renewable source cannot be understated. To effectively study microglia function in health and disease, a large number of iPSC-derived microglia that resemble as close as possible to actually microglia is necessary. As seen further in my dissertation document, my iPS-microglia differentiation protocol produces a robust amount of primitive human hematopoietic progenitors as well as large numbers of microglia. Microglia dysfunction in AD will be best studied in human cells that serve as both a model of disease and a technology for developing innate immune AD

therapies. To this end, my recent publication (Abud, et al, 2017, Neuron in press) and dissertation studies have culminated in a fully-defined microglial differentiation protocol from iPSCs. My two-step protocol does not require co-culture with cells, including at the iPSC stage, where some labs still use mitotically-inactivated mouse embryonic fibroblasts (MEFs) as a source of FGF2, and can be scaled to meet end-user needs. Both iHPCs and iMGLs are highly like their *in vivo* counterparts as validated by whole-transcriptome analysis using RNA-sequence and functional validation using diverse quantitative functional assays including, comparative phagocytosis assays, migration assays, calcium-imaging studies, as well as population of mouse brains via transplantation studies. To begin addressing the role of microglia in AD, I apply similar gene expression and quantitative functional assays to show that microglia can profoundly influence the AD pathogenesis.

CHAPTER ONE

DEVELOPING A FULLY-DEFINED PROTOCOL FOR THE GENERATION OF HUMAN MICROGLIA-LIKE CELLS

INTRODUCTION

Microglia are the innate immune cells of the CNS and play important roles in synaptic plasticity, neurogenesis, homeostatic functions and immune activity. Elegant lineage tracing studies have shown that microglia originate from yolk sac erythromyeloid progenitors (EMP) generated during primitive hematopoiesis (Ginhoux et al., 2010; Kierdorf et al., 2013; Schulz et al., 2012). EMPs further develop to early primitive macrophages that migrate into the developing neural tube, and become microglial progenitors (Kierdorf et al., 2013; Prinz and Priller, 2014). Microglia progenitors then mature and develop ramified processes used to survey their environment, facilitate CNS development, modulate synaptic plasticity, and respond to CNS injury and pathology. Recently, murine studies identified key cytokines, cell receptors, and transcription factors required for microglia development and survival *in vivo*. These factors include IL-34 and TGFβ-1 (Butovsky et al., 2014; Greter et al., 2012; Wang et al., 2012; Yamasaki et al., 2014). Thus, the generation of microglia from iPSCs appears to be dependent on mimicking developmental biological cues under controlled conditions *in vitro.* There has been of great interest in the field to derive human microglia from a renewable source, such as induced pluripotent stem cells.

The generation of human microglia from iPSCs would provide a considerable benefit to the field of neuroimmunology by providing a renewable source of primary human microglia to study microglia physiology as related to CNS hemostatic development and establishment and/or progression of disease. We hypothesized that iPSCs could be differentiated to human microglia *in vitro* by providing cues that mimic the environment present in the developing embryo. As microglia are derived from primitive hematopoietic precursors, generation of a robust and reproducible two-step protocol would be required—first, primitive hematopoietic precursor generation followed by microglia generation from these precursors. Addressing this critical need, we report the effective and robust generation of human iPSC microglial-like cells (iMGLs) that

resemble fetal and adult microglia and demonstrate their capacity to be utilized as primary microglia surrogates.

MATERIALS AND METHODS

Contact for Reagent and Resource Sharing

Further information and requests for resources and reagents should be directed to and will be fulfilled by the Lead Contact, Mathew Blurton-Jones, Ph.D. (mblurton@uci.edu).

Experimental Model and Subject Details

Chemical Reagents

All cell culture flasks, reagents, supplements, cytokines, and general reagents were purchased from Thermo Fisher Scientific, unless otherwise noted

Cell Culture

Maintenance and Culture of Human Pluripotent Stem Cells (hPSCs)

All stem cell work was performed with approval from UC Irvine Human Stem Cell Research Oversight (hSCRO) and IBC committees. The use of human fibroblast and PBMC samples for iPSC reprogramming and differentiation was approved by the University of California, Irvine Institutional Review Board (IRB Protocol #2013-9561) and informed consent was obtained from all subjects. Human iPSC cell lines ADRC 2 (Male), 4 (Male), 5 (Female), 12 (Male), 14 (Male), 20 (Female), 22 (Female), 76 (Male), 85 (Female), and 86 (Female) were generated by the UCI Alzheimer's Disease Research Center (ADRC) Induced Pluripotent Stem Cell Core using non-integrating Sendai virus (Cytotune) and are available to other researchers via http://stemcells.mind.uci.edu/. iPSCs were confirmed to be sterile and karyotypically normal via G-banding (WiCell.org). Pluripotency of all lines was confirmed via (http://pluritest.org) and further confirmed using the Human Pluripotent Stem Cell Functional Identification Kit (R&D Systems), per manufacturer's instructions.

iPSCs were maintained in 6-well plates (Corning) in feeder-free conditions using growth factor-reduced Matrigel (MTG, BD Bioscience) in complete TeSR-E8 medium (StemCell Technologies)

in a humidified incubator (5% CO_2, 37ºC). iPSCs were fed fresh media daily and passaged every 7-8 days.

Differentiation of iPSCs to Hematopoietic Progenitor Cells (iHPCs)

Human iPSC-derived hematopoietic progenitors were generated using defined conditions with several modifications to previously published protocols (Kennedy et al., 2007; Sturgeon et al., 2014).

iHPC Differentiation Base Medium Formulation: IMDM (50%), F12 (50%), insulin (0.02 mg/ml), holo-transferrin (0.011 mg/ml), sodium selenite (13.4 μg/ml), ethanolamine (4 μg/ml)(can use ITSG-X, 2% v/v, Thermo Fisher Scientific), L-ascorbic acid 2-Phosphate magnesium (64 μg/ml; Sigma), monothioglycerol (400 μM), PVA (10 ng/ml; Sigma), Glutamax (1X), chemically-defined lipid concentrate (1X), non-essential amino acids (NEAA; 1X), Penicillin/Streptomycin (P/S;1%). Use 0.22 μm filter.

Day (-1): iPSCs were washed with room temperature 1X DPBS (minus Ca^{2+} and Mg^{2+}) once. Wash was aspirated to waste and TrypLE Select (1X; 37ºC; 1 ml per 6-well) and placed in incubator (5% CO_2, 37ºC). After 3-5 minutes, cell plate was placed in cell culture hood and the side of the plate was lightly tapped to dislodge loosely adherent iPSCs for 30 seconds. After lightly tapping the plate, 1 ml of room temperature 1X DPBS (minus Ca^{2+} and Mg^{2+}) was added to each 6 well plate. Cells were collected in to a 15-ml conical tube (Corning) using a 10-ml Stripette® (Corning). Cells were centrifuged at 200 x *g* for 5 minutes at room temperature. After centrifugation, supernatant was aspirated to waste and cells were suspended in E8 medium + Y-27632 ROCK Inhibitor (RI,10 μM; R&D Systems), and gently triturated to generate a single-cell suspension, counted, and cell density adjusted to seed at 5 x 10^5 cells/cm^2 in tissue-culture treated 6-well plates. Final volume was adjusted to 1.5 ml of E8+ RI. Cells were cultured for 24 hours under normoxic conditions (20% O_2, 37ºC).

Day (0): Cells were gently collected in to 50 ml conical tube (Corning) using 10-ml Stripette® and centrifuged at 300 x *g* for 6 minutes at room temperature (all media changes will require this step using these parameters.). Media was aspirated to waste, and media was changed to basal medium complete with FGF2 (50 ng/ml), BMP4 (50 ng/ml), Activin-A (12.5 ng/ml), RI (1 μm) and LiCl

(2mM) at 2 ml per well in a 6-well plate, Cells were then placed in humidified tri-gas incubator under hypoxic cell culture conditions ($5\%O_2$, $5\%CO_2$, 37ºC).

Day (2): Cells were quickly and gently collected in to 50 ml conical using 10 ml Stripette® and centrifuged. Supernatant was aspirated to waste and media was changed to pre-equilibrated (at $5\%O_2$, $5\%CO_2$, 37ºC for 1 hour) base media supplemented with FGF2 (50 ng/ml) and VEGF (50 ng/ml) and placed back in hypoxia incubator.

Day (4): Media was changed to 2 ml per well with basal media containing FGF2 (50 ng/ml), VEGF (50 ng/ml), TPO (50 ng/ml), SCF (10 ng/ml), IL-6 (50 ng/ml), and IL-3 (10 ng/ml) and placed at normoxia incubator.

Days (6 and 8): Cells were supplemented with 1ml per well of Day 4 medium.

Day (10): Cells were collected and prepped for FACS (see Method Details) and $CD43^+$ cells were isolated by FACS for iMGL differentiation. Additionally, iPSC-derived HPCs (Cellular Dynamics International) were identified as a commercial source of $CD43^+$ progenitors.

Differentiation of iHPCs to iMGLs

iMGL Differentiation Base Medium: Differentiation media consists a base media: phenol-free DMEM/F12 (1:1), insulin (0.2 mg/ml), holo-transferrin (0.011 mg/ml), sodium selenite (13.4 μg/ml) (can use ITS-G, 2%v/v,Thermo Fisher Scientific), B27 (2% v/v), N2 (0.5%, v/v), monothioglycerol (200 μM), Glutamax (1X), NEAA (1X), and additional insulin (5 μg/ml; Sigma). Use 0.22 μm filter.

Day (0; or day 10 from iPSC): Isolated $CD43^+$ iHPCs were washed using iMGL base differentiation medium and centrifuged at 300 x *g* for 6 minutes at room temperature. After centrifugation, supernatant was aspirated to waste and iHPCs were gently suspended in complete differentiation medium: M-CSF (25 ng/ml), IL-34 (100 ng/ml; Peprotech), and TGF□-1 (50 ng/ml; Militenyi) added fresh each time. Cell density was adjusted to seed at density of 1-2 $x10^5$ cells in 2 ml of complete medium per well in growth factor-reduced Matrigel-coated 6-well plates.

Every two days: Complete differentiation media was supplemented with 1 ml per well.

Day (12; or day 22 from iPSC): Early iMGLs were collected (300x *g* for 6 mins at room temperature) and a 50% media change was performed.

Every two days: Complete differentiation media was supplemented with 1 ml per well.

After 25 days of microglial differentiation (35 days from iPSC), iMGLs were cultured in complete differentiation media supplemented with CD200 (100 ng/ml, Novoprotein) and CX3CL1 (100 ng/ml; Peprotech) for an additional three days before use in studies.

3D Brain-Organoid Cell Culture

Human 3D brain organoids were generated as previously described with some modifications (Lancaster et al., 2013) with modifications. iPSCs were cultured and maintained on Vitronectin XF (Stem Cell Technologies) in 6-well tissue culture treated plates (BD Falcon) and maintained with TeSR-E8 media (Stem Cell Technologies) daily, at 37°C with 5% CO_2. At approximately 80% confluency, iPSCs were detached from the Vitronectin XF substrate using the standard ReLeSR protocol (Stem Cell Technologies) and centrifuged, pelleted, and suspended in embryoid body (EB) media, which consists of KO DMEM/F12 (Invitrogen), KOSR (20% v/v), Glutamax (1X), NEAA (1X), 2-Mercaptoethanol (0.1mM), bFGF (4 μg/ml), and HSA (0.1% v/v) and ROCK inhibitor (50 μM), to form EBs. Approximately $1x10^4$ cells were plated per well of a standard V-bottom 96-well plate coated with Lipidure (1% v/v; AMSBio) to avoid having the EBs attach to the 96-well plate. After 4 days in EB media with bFGF (4 ng/ml) and ROCK inhibitor (50 μM), both the bFGF and ROCK inhibitor were discontinued leaving the brain organoids in basic EB media for an additional 3 days (7 days total). After the EB media phase, the EB media is replaced with neural epithelium (NE) media which consists of DMEM/F12, N2 supplement (0.1% v/v), Glutamax (1X), MEM-NEAA (0.1X), Heparin solution (0.2mg/ml; Sigma), and filtered using 0.22 μm PES filter (EMD Milipore). The brain organoids were transferred to an ultra-low attachment 24-well plate (Corning) using cut P200 pipette tips, with 1-2 EBs per well in 1 ml NE media. The EBs were neuralized in the NE media for five days, after which they were transferred into Matrigel (Corning) using a mold created from siliconized parafilm and a sterile empty P200 box. The brain organoids were kept in a 6-cm suspension petri dish with differentiation media consisting of KO DMEM/F12 (50%), Neurobasal medium (50%), N2 supplement (0.1% v/v), B27 without vitamin A supplement (0.1% v/v), Insulin solution (0.1% v/v; Sigma), 2-Mercaptoethanol

(0.1mM), Glutamax (1X v/v), MEM-NEAA (1X), and Penicillin/Streptomycin (0.1% v/v). After five days of being exposed to differentiation media containing B27 without vitamin A, the differentiation media was replaced by a formulation that is identical except for the replacement of B27 without vitamin A to B27 with vitamin A; at this time point, the brain organoids are also transferred to a 125 ml spinning flask bioreactor (Corning) siliconized with Sigmacote (Sigma), where they were fed differentiation media with vitamin A weekly for 8 weeks. After 12 weeks, Borgs were utilized for iMGL co-culture studies.

Rat Cortical and Hippocampal Neuron Isolation

All procedures were performed under an IUCAC approved protocol. Primary cortical and hippocampal neuron cultures were derived from embryonic rat (E18) as previously described (Loo et al., 1993). Briefly, dissected tissue was dissociated with trypsin, triturated, and plated on 6-well plates coated with poly-L-lysine coated in NB medium (serum-free Neurobasal supplemented with 1% B27). Cells were plated at a density of 5×10^6 cells/ml and maintained in culture until used for assays.

PBMCs and Monocytes Isolation from Human Blood

Human blood samples were collected from healthy donors through the UCI ICTS Blood Donor Program with approved IRB. Human peripheral blood mononuclear cells (PBMCs) were isolated from healthy donors using Ficoll-paque (GE Healthcare) gradient separation. In brief, blood was layered on top of Ficoll-Paque and centrifuged in swinging bucket rotator without brake (400x *g*, 40 minutes, 18°C). After centrifugation, plasma and upper layers were removed and PBMCs isolated from the interphase. Cells were then washed once with ice-cold PBS and used immediately. CD14 and CD16 monocytes were isolated via negative selection from PBMCs using the EasySep™ Monocyte Enrichment Kit (Stemcell Technologies) per manufacturer's instructions. Isolated cells were washed three times with PBS and sorted by FACS for either RNA-sequence analysis or used for further macrophage differentiation.

Monocyte-derived Macrophages

Isolated monocytes were plated onto tissue culture treated 6-wells at 2 $x10^6$ cells/ml in RPMI-1640 media at 37°C 5%CO_2 incubator. After two hours, media was aspirated to waste and

adherent monocytes washed three times with DPBS and replaced with complete media composed of RPMI-1640, FBS (10% v/v), Penicillin/streptomycin (1% v/v), Glutamax (1X). To generate MD-Mφ, M-CSF (25 ng/ml) was added to wells and cells differentiated for 5 days.

RNA-seq library construction

Cells were harvested and washed three times with DPBS and stored in RNAlater, RNA preservation solution. RNA was extracted from all cell types using RNeasy Mini Kit (Qiagen) following manufacturer's guidelines. RNA integrity (RIN) was measured for all samples using the Bioanalzyer Agilent 2100 series. All sequencing libraries analyzed were generated from RNA samples measuring a RIN score ≥ 9. The Illumina TruSeq mRNA stranded protocol was used to obtain poly-A mRNA from all samples. 200 ng of isolated mRNA was used to construct RNA-seq libraries. Libraries were quantified and normalized using the Library Quantification Kit from Kapa Biosystems and sequenced as paired-end 100 bp reads on the Illumina HiSeq 2500 platform.

Confocal Microscopy and Bright-field Imaging

Immunofluorescent sections were visualized and images captured using an Olympus FX1200 confocal microscope. To avoid non-specific bleed-through, each laser line was excited and detected independently. All images shown represent either a single confocal *z*-slice or *z*-stack. Bright-field images of cell cultures were captured on an Evos XL Cell Imaging microscope. Image analysis was performed using Olympus.

FACS and Flow Cytometer Analysis

iHPCs were collected using cold (4ºC) sterile filtered and degassed FACS buffer (1X DPBS, 2% BSA, and 0.05mM EDTA) spiked with human SCF (5 ng/ml). Cells were then filtered through 70 μm mesh to remove large clumps, washed with spiked FACS buffer (300 x *g* for 5 min 18ºC), then stained (1:200) using spiked FACS buffer on ice for 1 hour in the dark using the following antibodies: anti CD34-FITC clone 561, anti CD41-PE clone HiP8, anti CD43-APC clone CD43-10G7, anti CD45-APC/Cy7 clone HI30 (Tonbo), anti CD235a-PE/Cy7 clone HI264, and ZombieViolet™ live/dead stain, all from Biolegend unless noted. After staining, iHPCs were washed once with spiked FACS buffer and suspended using spiked FACS buffer (500-700 μl) and sorted utilizing the BD FACSARIA Fusion (BD Biosceinces). Sorted cells were collected in cold

basal iHPC differentiation medium spiked with SCF (10 ng/ml). Collected CD43+ iHPCs were thenplated for iMGL differentiation as mentioned above. iMGLs were suspended in FACS buffer and incubated with human Fc block (BD Bioscience) for 15 min at 4^{o}C. For detection of microglial surface markers, cells were stained with anti CD11b-FITC clone ICRF44, anti CD45-APC/Cy7 clone HI30 (Tonbo), anti CX3CR1-APC clone 2A9-1, anti CD115-PE clone 9-4D, and anti CD117-PerCP-Cy5.5 clone 104D2, ZombieViolet^{TM} live/dead stain, all from Biolegend (San Diego, CA). Cells were sorted on a FACS Aria II, FACS Aria Fusion (BD Biosciences) and data analyzed with FlowJo software (FlowJo).

Cytospin and May-Grunwald Giemsa Stain

Cells (1x10^{5}) were suspended in FACS buffer (100 µl) and added to Shandon glass slides (Biomedical Polymers) and assembled in a cytology funnel apparatus. Assembled slides containing cells were loaded in a cytospin instrument and centrifuged (500 rpm, 5 min). Slides were allowed to air-dry for two minutes and immediately stained in May-Grunwald stain (100%; Sigma) for 5 min. Next, slides were washed in PBS for 1.5 min and immediately placed in Giemsa stain (4%; Sigma) for 20 min at room temperature. Slides were washed in double-distilled water 6 times and allowed to air-dry for 10 min. Slides were preserved using glass coverslips and permount (Sigma).

RNA Isolation

Cells were stored in RNAlater stabilizing reagent and RNA was isolated using Qiagen RNeasy Mini Kit (Valencia, CA) following manufacturer's guidelines.

iMGL Co-culture with Rat Neurons

Rat hippocampal or cortical neurons were cultured for 21 days with 50% media change every 3-4 days. iMGLs were cultured with neurons at a 1:5 ratio (1 x10^{6} iMGL to 5 x 10^{6} neurons) in 50% iMGL and 50% NB medium. After 3 days, iMGLs were collected for RNA isolation.

iMGL Transplantation in MITRG Mice Brains

All animal procedures were performed in accordance with NIH and University of California guidelines approved IAUC protocols (IAUC #2011-3004). MITRG mice were

purchased from Jax (The Jackson Laboratory, #017711) and have been previously characterized (Rongvaux et al., 2014). MITRG mice allow for xenotransplantation and is designed to support human myeloid engraftment. iMGLs were harvested at day 38 and suspended in injection buffer: 1X HBSS with M-CSF (10 ng/ml), IL-34 (50 ng/ml), and TGFβ-1 (25 ng/ml). iMGLs were delivered using stereotactic surgery as previously described (Blurton-Jones, et al, 2009) using the following coordinates; AP: -0.6, ML: ± 2.0, DV: -1.65. Brains were collected from mice at day 60 post-transplantation per established protocols (Blurton-Jones, et al, 2009). After transplantation mice were killed and brains collected using previously established protocol. Briefly, mice were anesthetized using sodium-barbiturate and perfused through the left-ventricle with cold 1X HBSS for 4 min. Perfused mice were decapitated and brain extracted and dropped-fixed in PFA (4% w/v) for 48 hours at 4ºC. Brains were then washed 3 times with PBS and sunk in sucrose (30% w/v) solution for 48 hours before coronal sectioning (40 μm) using a microtome (Leica). Free-floating sections were stored in PBS sodium azide (0.05%) solution at 4ºC until IHC was performed.

Immunocytochemistry and Immunohistochemistry

For ICC, cells were washed three times with DPBS (1X) and fixed with cold PFA (4% w/v) for 20 min at room temperature followed by three washes with PBS (1X). Cells were blocked with blocking solution (1X PBS, 5% goat or donkey serum, 0.2% Triton X-100) for 1 h at room temperature. ICC primary antibodies were added at respective dilutions (see below) in blocking solution and placed at 4ºC overnight. The next day, cells were washed 3 times with PBS for 5 min and stained with Alexa Fluor® conjugated secondary antibodies at 1:400 for 1 h at room temperature in the dark. After secondary staining, cells were washed 3 times with PBS and coverslipped with DAPI-counterstain mounting media (Fluoromount, southern Biotech). For BORG IHC, tissue was collected and dropped-fixed in PFA (4% w/v) for 30 min at room temperature and then washed three times with PBS. BORGs were then placed in sucrose solution (30% w/v) overnight before being embedded in O.C.T (Tissue-Tek). Embedded tissue was sectioned at 20 μm using a cryostat and mounted slides were stored at -20ºC until staining. For BORG staining, mounted tissue was removed from storage and warmed by placing at room temperature for 30 min. Tissue were rehydrated and washed with room temperature PBS (1X) 3 times for 5 min. Heat-mediated antigen retrieval was performed by using Citrate Buffer (10mM Citrate, 0.05% Tween 20, pH=6.0) at 97ºC for 20 min and then allowed to cool to room

temperature. After antigen retrieval, slides were washed three times with PBS. Slides were then washed once in PBS-A solution (1X PBS with 0.1% Triton X-100) for 15 min. Tissue was blocked using PBS-B solution (PBS-A, 0.2% BSA, and 1.5% goat or donkey serum) for 1 h at room temperature. After block, primary antibodies were added to PBS-B solution (250-350 µl/ slide) at appropriate dilutions (see below) and incubated overnight at room temperature. The next day, slides were washed with PBS-A solution 3 times for 5 min each. Tissue were blocked for 1 h using PBS-B solution at room temperature. After block, slides were incubated with Alexa Fluor® conjugated secondary antibodies (all at 1:500) and Hoechst stain (1X) in PBS-B (for 250-300 µl/slide) for 2 h at room temperature in the dark. After secondary staining, slides were washed 5 times with PBS for 5 min. Slides were cover slipped using fluoromount (Southern Biotech). For mouse brain IHC, brains were collected, fixed, and processed as mentioned above. Free-floating sections were blocked in blocking solution (1X PBS, 0.2% Triton X-100, and 10% goat serum) for 1 h at room temperature with gentle shaking. For human TMEM119 staining, heat mediated antigen retrieval was performed prior to blocking, as performed previously (Bennett et al., 2016). Free-floating tissue antigen retrieval was performed by placing floating sections in a 1.5 ml micro centrifuge tube containing 1 ml of Citrate Buffer solution and placing in a pre-heated temperature block set at 100ºC. Tissue was heated for 10 min at 100ºC then removed and allowed to come to room temperature for 20 min before washing with PBS 3 times for 5 min and then proceeding with blocking step. Primary antibodies were added to staining solution (1X PBS, 0.2% Triton X-100, and 1% goat serum) at appropriate dilutions (see below) and incubated overnight at 4ºC with slight shaking. The next day, sections were washed 3 times with PBS and stained with Alexa Fluor® conjugated secondary antibodies at 1:400 for 1 h at room temperature with slight shaking in the dark. After secondary staining, sections were washed in PBS 3 times for 5 min and mounted on glass slides. After mounting, slides were cover slipped with DAPI-counterstain mounting media (Fluoromount, southern Biotech). Primary antibodies:

mouse anti-β3Tubulin (1:500; Biolegend, 801201)

mouse anti-human Cytoplasm (SC121,1:100; Takara Bio Inc., Y40410),

mouse anti-human Nuclei (ku80, 1:100; Abcam, ab79220)

chicken anti-GFAP (1:500; Abcam, ab4674)

rabbit anti-Iba1 (1:500; Wako; 019-19741)

goat anti-Iba1 (1:100; Abcam ab5076) * recommend use with Alexa Fluor 488 or 555 secondary antibody only.

mouse anti-ITGB5 (1:500; Abcam, ab177004)

mouse anti-MMP-9 (1:500; EMD Millipore, AB19016)

mouse anti-human Mertk (1:500; Biolegend, 367602)

rabbit anti-P2ry12 (1:125; Sigma; HPA014518)

rabbit anti-Pros (1:500; Abcam, ab97387)

rabbit anti-PU.1 (1:500; Cell Signaling Technology, 2266S)

rabbit anti-human Tmem119 (1:100; Abcam, ab185333)

goat anti-human Trem2 (1:100; R&D Systems, AF1828)

rabbit anti-Tgfbr1 (1:500; Abcam, ab31013).

rabbit anti-Cx3cr1 (1:1000; Bio-Rad/AbD Serotec, AHP1589)

ADP migration and calcium imaging assays

Trans-well migration assays to ADP was performed as previously described (De Simone et al., 2010; Moore et al., 2015). iMGLs ($5.5x10^4$ cells/well) were cultured in serum-free basal media without cytokines pre-exposed to DMSO or PSB0739 (50 μM, Tocris) for 1hr at 37ºC in 5% CO_2 cell culture incubator. Cells were then washed three times with basal medium and plated in trans-well migration chambers (5 μm polycarbonate inserts in 24 wells; Corning) containing Adenosine 5'-phosphate (ADP, 100 μM; Sigma) in the bottom chamber in 37ºC in 5% CO_2. After 4 hours, cells were washed three times with PBS (1x) and fixed in PFA (4%) for 15 minutes at room temperature. Cells were stained with Hoechst stain for 10 mins to visualize nuclei of cells. A blinded observer counted total cells per slide and then scrubbed cells off top surface using a cotton-swab, washed with PBS, and recounted to record migrated cells. Migration was reported as migrated over total cells per well. Fluorescent images of cells were captured using Olympus IX71 inverted microscope.

For calcium imaging, iMGLs were plated on poly-L-lysine-coated coverslips and 1 hour later were incubated with Fura-2-AM (Molecular Probes) calcium dye diluted in Ringer solution

containing (in mM): NaCl 140, KCl 4.5, $CaCl_2$ 2, $MgCl_2$ 1, HEPES 10, glucose 10, sucrose 5, pH=7.4. After 1-hour incubation, the dye was washed out 3 times using Ringer solution and treated for 1 hour with either P2ry12 inhibitor PSB0739 (50 μM, Tocris) or Vehicle (DMSO) and used for experiments. Baseline Ca^{2+} signal (I_{340}/I_{380}) were measured for more than 100 s and then ADP (10 μM) was introduced under steady flow after baseline measurement. Ca^{2+} recordings were performed on Zeiss (Axiovert 35)-based imaging setup and data acquisition was conducted with Metafluor software (Molecular Devices). Data analysis was performed using Metafluor, Origin Pro, and Prism 6.0.

Phagocytosis Assays

iMGLs and MD-Mφ, were incubated with mouse anti CD16/32 Fc-receptor block (2 mg/ml; BD Biosciences) for 15 minutes at 4ºC. Cells were then stained with anti CD45-APC clone HI30 (Tonbo Biosciences; San Diego, CA) at 1:200 in flow cytometer buffer. Samples were then analyzed using Amnis Imagestreamer®^{x} Mark II Imaging Flow Cytometer (Millipore). pHrodo-red *E.coli* and human synaptosome phagocytosis was analyzed using the IDEAS software onboard Internalization Wizard algorithm. Additive free Anti-CD11b antibody (Biolegend, #301312) was used for CD11b blockade.

Human synaptosomes

The synaptosome preparation protocol was adapted from (Gylys et al., 2000). Human tissue samples were obtained at autopsy and minced, slowly frozen in 0.32 M sucrose with 10% DMSO and stored at −80 °C. To obtain a crude synaptosome fraction, tissue was thawed in a 37 °C water bath and homogenized in 10 mm Tris buffer (pH 7.4) with proteinase inhibitors (Roche) and phosphatase inhibitors (Sigma-Aldrich) using a glass/Teflon homogenizer (clearance 0.1–0.15 mm). The homogenate was centrifuged at 1000 *g* at 4 °C for 10 min, the supernatant was removed and centrifuged again at 10 000 *g* at 4 °C for 20 min. Resulting pellets were suspended in sucrose/Tris solution and stored at −80 °C. Synaptosomes were conjugated to pHrodo-red per the manufacturer's protocol.

Mesoscale Multiplex Cytokine and Chemokine Assay

iMGL culture media was replaced with basal media for 2 hours prior to stimulation with IFNγ (20 ng/ml), IL1β (20 ng/ml), and LPS (100 ng/ml) for 24 hours, after which cells were collected for RNA and conditioned media assessed for cytokine secretion. To simultaneously assess multiple cytokine and chemokine analytes from iMGL conditioned media, conditioned media from each treatment group was processed and analyzed using the V-PLEX human cytokine 30-plex kit (Mesoscale) per the manufacturer's protocol.

RNA-sequence analysis

RNA-seq reads were mapped to the hg38 reference genome using STAR (Dobin et al., 2013) aligner and mapped to Gencode version 24 gene annotations using RSEM(Li and Dewey, 2011). Genes with expression (< 1 FPKM) across all samples were filtered from all subsequent analysis. Differential gene expression analysis was performed on TMM normalized counts with EdgeR (Robinson et al., 2010). Multiple biological replicates were used for all comparative analysis. A p-value ≤ 0.001 and a 2-fold change in expression were used in determining significant differentially expressed genes for respective comparisons. PCA analysis was performed using the R package "rgl" and plotted using "plot3d". Clustering was performed using R "hclust2" and visualized using Java Tree View 3.0 (http://bonsai.hgc.jp/~mdehoon/software/cluster/software.htm). Differential gene analysis between groups was performed using the R package "limma" and significant genes (adjusted p < 0.01) were used for Gene ontology and pathway analysis. Gene ontology and pathway analysis was performed using Enrichr data base (http://amp.pharm.mssm.edu/Enrichr/) (Chen et al., 2013; Kuleshov et al., 2016).

Statistical Analysis

Statistical analysis was performed using Graphpad Prism 7 software. Comparisons involving more than two groups utilized one-way ANOVA followed by Tukey's *post hoc* test and corrected p-values for multiple comparisons were reported. Comparison's with more than two groups and comparing to a control or vehicle group utilized one-way ANOVA followed by Dunnett's *post hoc* test with corrected p-values for multiple comparisons reported. Two-Way ANOVA were followed by Sidak's multiple-comparison *post-hoc* test Comparisons of two groups

utilized two-tailed Students t-test. All differences were considered significantly different when $p<0.05$. Statistical analysis for RNA-sequencing is detailed above and all further statistical analysis details are reported in the figure legends.

Data and Software Availability

Raw and normalized RNA-sequence data can be obtained at NCBI. The GEO Accession Super Series ID number for the data reported in this paper is GEO: GSE89189.

RESULTS

Human microglia-like cells are generated from iPSCs.

A two-step fully-defined protocol was developed to efficiently generate microglia-like cells (iMGLs) from iPSCs in just over five weeks (**Figure 1.1**). This approach was used to successfully produce iMGLs from 10 independent iPSC lines (**Figure 1.2**). A critical prerequisite is the robust differentiation of iPSCs to hematopoietic progenitors (iHPCs). While many protocols exist for the generation of HPCs, many of them are reliant on co-culture with mouse stromal cells (e.g. OP9s) or utilize a cell-free system that utilizes commitment factors such as GM-CSF and FLT3L, which are essential factors involved in definitive hematopoiesis producing bone-marrow myeloid cells (Hoeffel et al., 2015; Schulz et al., 2012; Vodyanik et al., 2005). Therefore, we generated a fully-defined primitive hematopoietic differentiation protocol. This approach recapitulates microglia ontogeny as iHPCs represent early primitive hematopoietic cells derived from the yolk sac that give rise to microglia during development (Ginhoux et al., 2010; Kierdorf et al., 2013). Our protocol (depicted in **Figure 1.1**) yields primitive iHPCs that are $CD43^+/CD235a^+/CD41^+$ after 10 days (Kennedy et al., 2007; Sturgeon et al., 2014). FACS sorting for $CD43^+$ cells reveal that our approach produces iHPCs with a >90% purity (**Figure 1.1B**). The resulting iHPCs resembled a commercial source (Cellular Dynamics International) and represent the hematopoietic progenitor used to generate iMGLs. Next, $CD43^+$ iHPCs were grown in serum-free differentiation medium (formulated in house) containing CSF-1, IL-34, and TGFβ1. By day 14, cells expressed the myeloid-associated transcription factor PU.1 and the microglia-enriched protein TREM2 (**Figure 1.1A iii**) demonstrating an early commitment toward microglial fate.

Because this protocol yields large amounts of iMGLs, microglia development was studied *in vitro* as cells could be characterized every 4 days by flow cytometry.

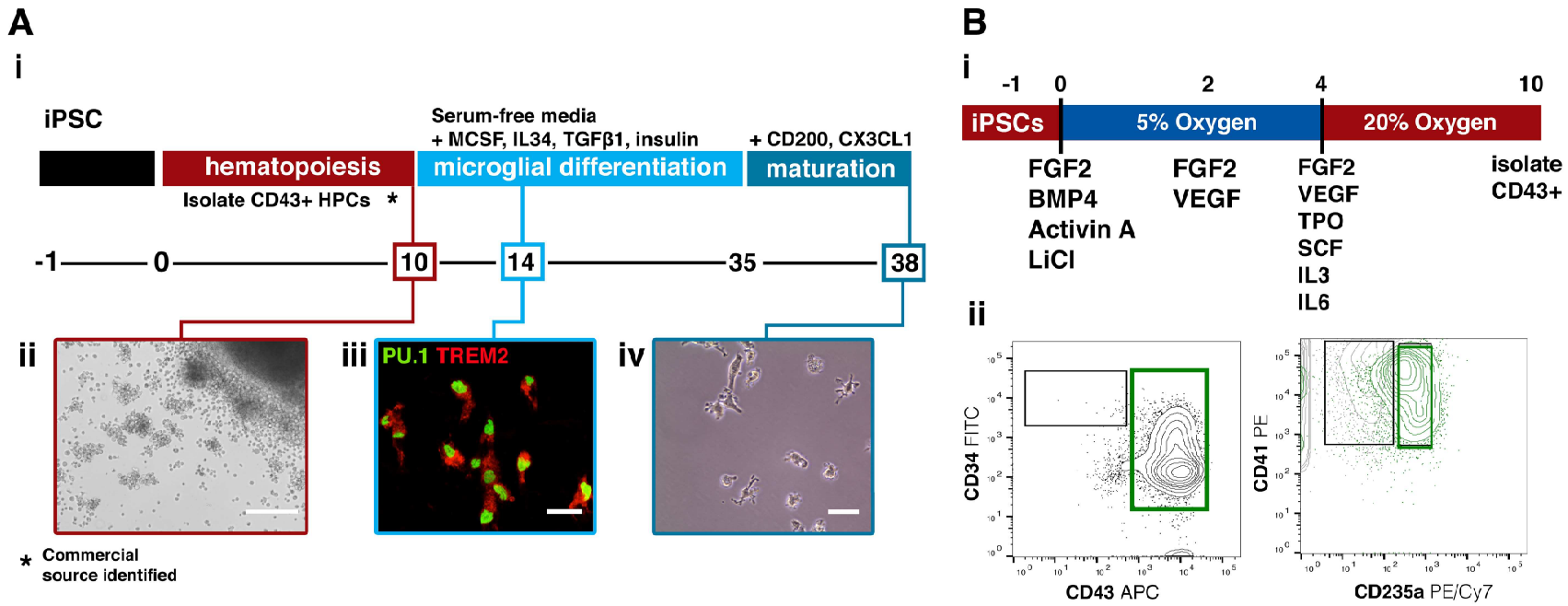

Figure 1.1: Schematic of fully-defined iMGL differentiation protocol. (**Ai**) Human iPSCs are differentiated to $CD43^+$ iHPCs for 10 days and then cultured in serum-free microglia differentiation media containing human recombinant MCSF, IL-34, and TGFβ-1. Differentiation is carried out for an additional 25 days after which iMGLs are exposed to human recombinant CD200 and CX3CL1 for 3 days. (**ii**) Representative image of iHPCs in cell culture at day 10. Scale bar = 100 µm. (**iii**) By day 14, iMGLs express PU.1 (green) and TREM2 (red). Scale bar = 50 µm. (**iv**) Representative phase contrast image of iMGL at day 38. (**B**) Schematic of differentiation of iPSCs to iHPCs. (**i**) Single-cell iPSCs are differentiated in a chemically defined media supplemented with hematopoietic differentiation factors and using 5% O_2 (4 days) and 20% O_2 (6 days). (**ii**) After 10 days, $CD43^+$ iHPCs are $CD235a^+/CD41a^+$.

Day 14 early iMGLs were c-kit^{-}/CD45^{+} (**Figure 1.3**), suggesting commitment towards a

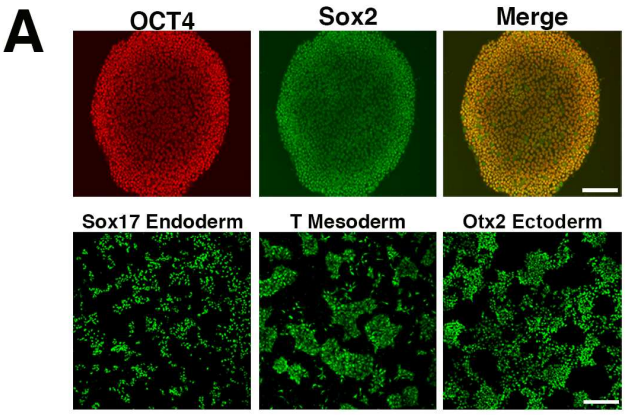

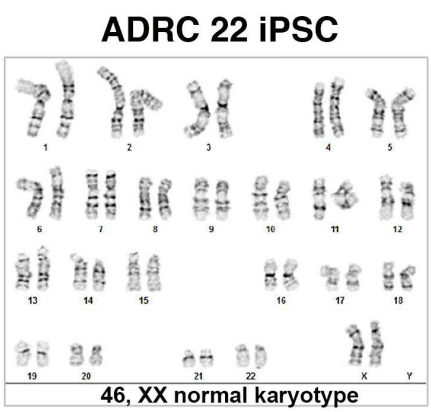

C

iPSC ID	Source	iPSC Karyotype	Sex	Pluritest Score	Pluritest (pass vs. fail)	Novelty Score	Novelty (pass vs. fail)
ADRC iPS 2	Fibroblast	46 XY normal	Male	19.29	Pass	1.511	Pass
ADRC iPS 4	Fibroblast	46 XY normal	Male	23.09	Pass	1.449	Pass
ADRC iPS 5	Fibroblast	46 XX normal	Female	21.85	Pass	1.409	Pass
ADRC iPS 12	PBMC	46 XY normal	Male	26.45	Pass	1.519	Pass
ADRC iPS 14	Fibroblast	46 XY normal	Male	26.85	Pass	1.418	Pass
ADRC iPS 20	Fibroblast	46 XX normal	Female	27.19	Pass	1.376	Pass
ADRC iPS 22	Fibroblast	46 XX normal	Female	22.82	Pass	1.404	Pass
ADRC iPS 76	PBMC	46 XY normal	Male	21.37	Pass	1.433	Pass
ADRC iPS 85	Fibroblast	46 XY normal	Male	33.73	Pass	1.325	Pass
ADRC iPS 86	Fibroblast	46 XX normal	Female	32.70	Pass	1.276	Pass

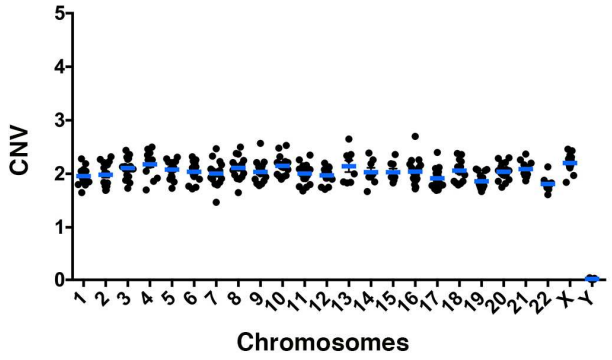

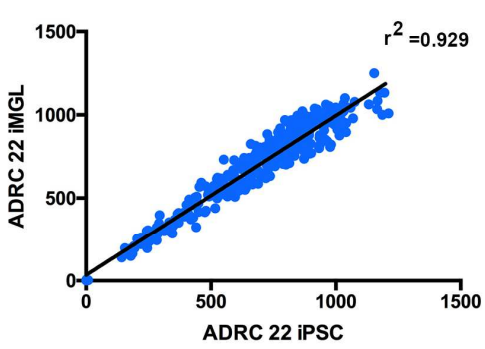

E

ID	Karyotype	Sex	Aneuploidy
iPSC			
ADRC iPS 5	46 XX normal	Female	No
ADRC iPS 14	46 XY normal	Male	No
ADRC iPS 22	46 XX normal	Female	No
ADRC iPS 76	46 XY normal	Male	No
ADRC iPS 76 Replicate	46 XY normal	Male	No
CDI iHPC	46 XY normal	Male	No
iMGL			
ADRC iMGL 5	46 XX normal	Female	No
ADRC iMGL 14	46 XY normal	Male	No
ADRC iMGL 22	46 XX normal	Female	No
ADRC iMGL 76	46 XY normal	Male	No
ADRC iMGL 76 Replicate	46 XY normal	Male	No
CDI iMGL	46 XY normal	Male	No

myeloid lineage. Additionally, cells can be further subdivided into CD45^{+}/CX3CR1^{-} (A1) and

Figure 1.2: Genomic stability of iPSCs and iMGLs**.** (**A**) Top: Representative fluorescent images of iPSCs expressing the pluripotent markers OCT4 (red) and SOX2 (green). Scale bar =300 μm. Bottom: Functional validation of pluripotency in iPSCs. Representative fluorescent images of iPSCs differentiated to endoderm, mesoderm and ectoderm and stained for Sox17, T (Brachyury), and Otx2 respectively to validate differentiation potential. Scale bar =200 μm. (**B-C**) Karyotype and Pluritest scores indicate all iPS lines generated using Sendai virus and used in this study were karyotypically normal and pluripotent. The Pluritest is a microarray-based assessment of pluripotency based on iPS whole transcriptome analysis referenced to a library of functionally validated iPSCs (Muller, F.J. et al. 2011). (**D-E**) Maintenance of genomic stability over the course of iMGL differentiation using pluripotent iPS or commercial hematopoietic progenitors. CNV assessment of differentiated iMGLs reveals genomic stability is maintained over the course of differentiation. (**D**) Representative Nanostring nCounterKaryotype results demonstrate that microglia derived from ADRC iPS line 22 do not inherit extrachromosomal DNA over the course of differentiation. (**E**) Quantification of the 338 probe sets across all 24 chromosomes do not reveal any chromosomal abnormalities (n=6). (**F**) Representative analysis of iMGL derived from its iPSC show strong CNV correlation (r^2=0.929) showing sensitivity of assay and genomic stability of derived iMGLs.

$CD45^+/CX3CR1^+$ (A2) populations; similar to developing microglial progenitors identified *in vivo* (Kierdorf et al., 2013). CD45 expression was consistently monitored in developing iMGLs and compared to monocyte-derived macrophages (MD-Mφ). While CD45 expression increased with maturation, levels never reached that of macrophages (**Figure 1.3D**), consistent with murine development (Kierdorf et al., 2013). A small population of iMGLs (~10%) also expressed intermediate CD11b levels by day 14 that also increased as cells matured, but again never reached macrophage levels (**Figure 1.3E, F**). By day 38, iMGLs resemble human microglia, but not monocytes nor macrophages by cytospin/Giemsa staining (**Figure 1.3G**) and express many other microglial-enriched proteins including Mertk, Itgb5, Cx3cr1, Tgfbr1, and Pros1 protein (**Figure 1.4**). Like murine microglia development *in vivo*, iMGLs developing *in vitro* express PU.1, TREM2, and $CD11b^{int}/CD45^{low}$ (**Figure 1.3, D-F**). As iMGLs mature *in vitro,* they also become more ramified, similar to microglia *in vivo* (**Figure 1.3F**). Furthermore, purinergic receptor P2ry12 and Trem2 co-expression was enriched in iMGLs when compared to monocytes and quantification reveals our protocol yielded iMGLs of high purity (>97.2%, n=5) (**Figures 1.3G and Figure 1.4 A, B**). Genomic integrity was also maintained over the course of differentiation. Assessing copy number variants across all chromosomes demonstrated that extra chromosomal fragments were not acquired by iMGLs when compared to their respective iPSCs (n=6, **Figure 1.2D,E**). A comparison of a representative differentiation across the entire probeset (n=383, nCounter®

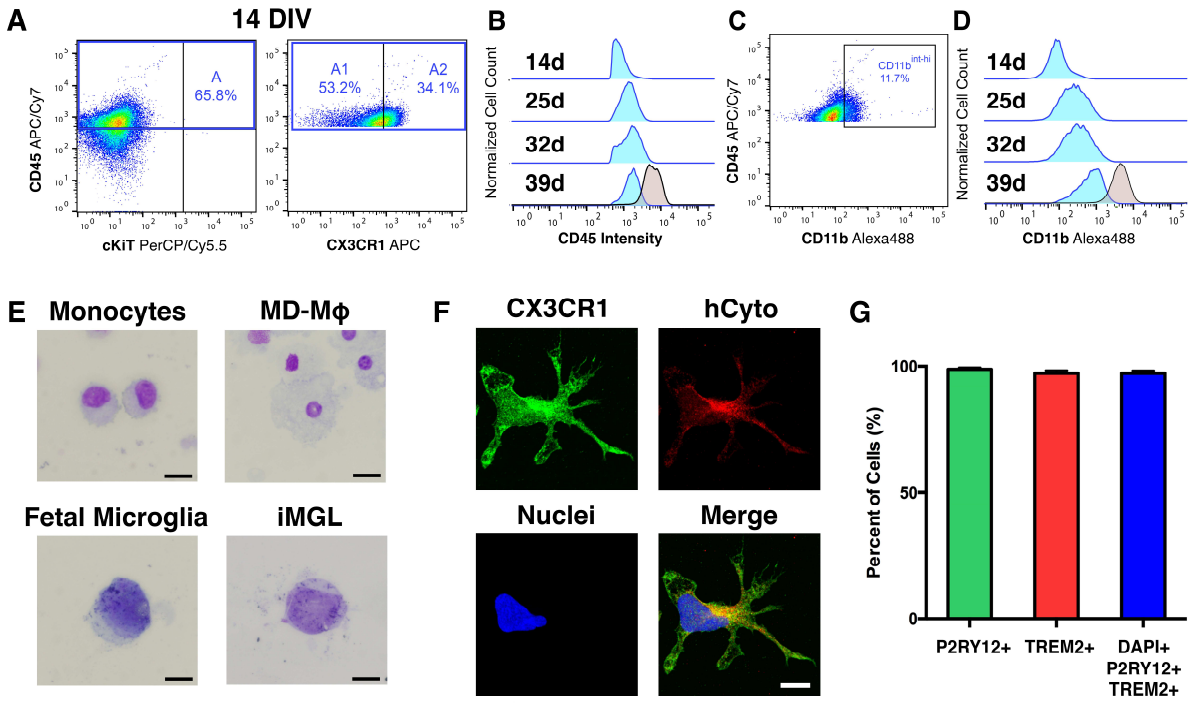

Figure 1.3: iMGLs differentiation resembles in vivo development. (**A**) iMGLs develop from $CD45^{+}/CX3CR1^{-}$ (A1) and $CD45^{+}/CX3CR1^{+}$ (A2) progenitors. (**B**) CD45 fluorescence intensity shows that iMGLs (blue) maintain their $CD45^{lo\text{-}int}$ profile when compared to monocyte-derived macrophages (MD-Mφ). (**C**) iMGL progenitors are $CD11b^{lo}$ and increase their CD11b expression as they mature. At 14 DIV, a small population (~11%) cells with $CD11b^{int\text{-}hi}$ are detected. (**D**) CD11b fluorescence intensity demonstrates that CD11b expression increases as iMGLs age, resembling murine microglial progenitors identified by Kierdorf, et al 2013. (**E**) Mary-Grunwald Giemsa stain of monocytes, MD-Mφ, fetal microglia, and iMGLs. Both fetal microglia and iMGL exhibit a high nucleus to cytoplasm morphology compared to monocytes and MD-Mφ. Scale bars = 16 µm. (**F**) iMGLs also exhibit extended processes and express CX3CR1 (green) together with the human cytoplasmic marker (hCyto, SC121; red). (**G**) Differentiation yields >97.2% purity as assessed by co-localization of microglial-enriched protein P2RY12 (green), microglial-enriched TREM2 (red) and nuclei (blue (n=5 representative lines).

Human Karyotype Panel) revealed a high correlation between the iPSC and iMGL genomes (r^2 > 0.92, **Figure 1.2F**). Importantly, this protocol typically yielded 30-40 million iMGLs from one million iPSCs, suggesting that our approach can be readily scaled-up for high content screening.

iMGLs resemble human fetal and adult microglia

Next, the iMGL transcriptome was profiled in comparison to human primary fetal microglia (Fetal MG) and adult microglia (Adult MG). $CD14^{+}/CD16^{-}$ monocytes (CD14 M),

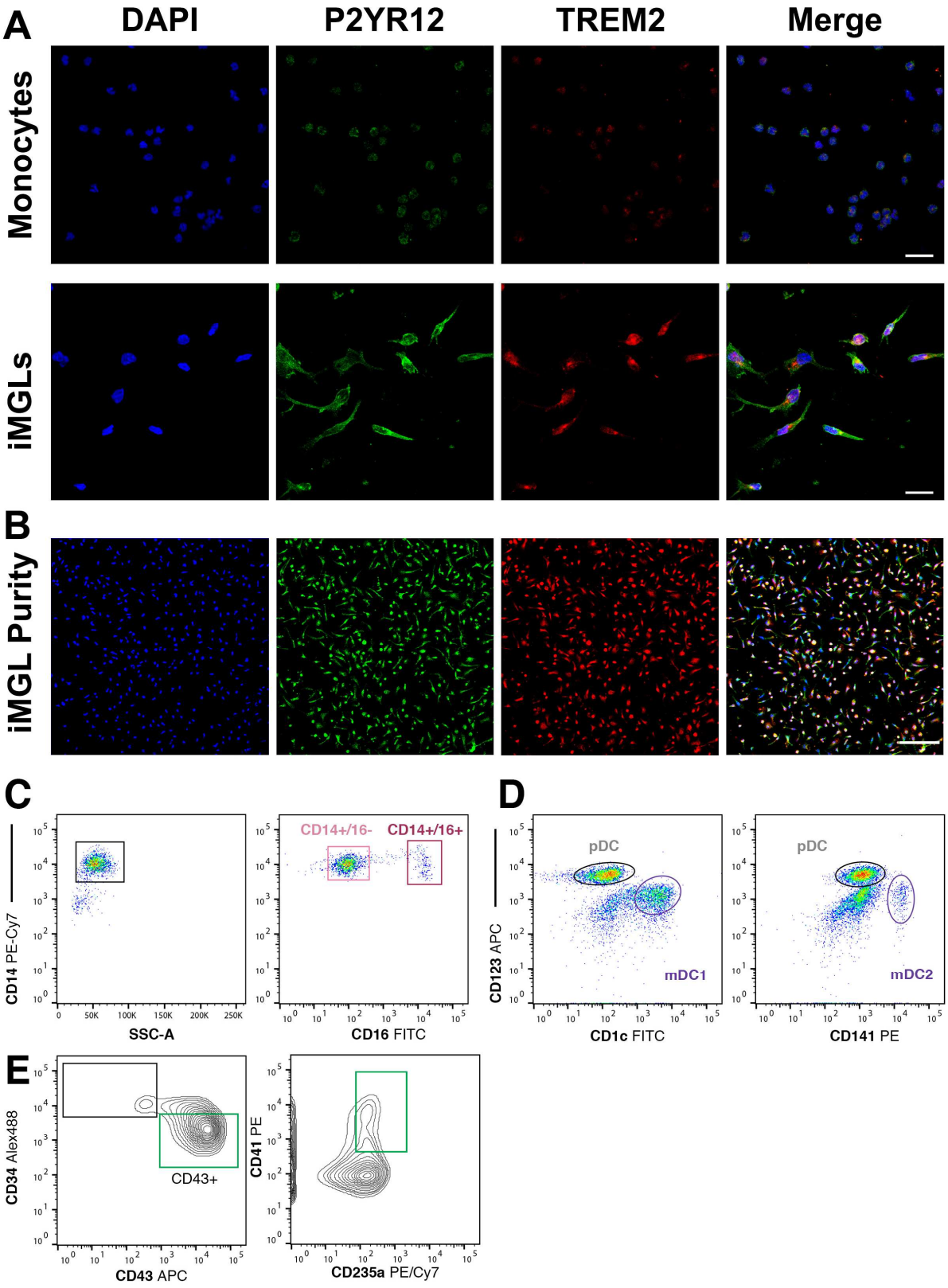

$CD14^+/CD16^+$ inflammatory monocytes (CD16 M), myeloid dendritic cells (Blood DCs), iHPCs, and iPSCs were also examined to compare iMGLs to stem cells and other myeloid molecular

Figure 1.4: Assessment of iMGL purity by P2RY12/TREM2 co-localization and flow cytometry characterization of monocytes, dendritic cells and commercial iHPCs**.** (**A**) Specificity assessment of rabbit anti-human P2ry12 (HPA014518, also recently validated by (Mildner et al., 2017), and goat anti-human Trem2 (R&D, AF1828) in human monocytes and iMGLs. scale bar = 20 μm (**B**) Representative immunofluorescent images (from 5 representative lines) of iMGL purity by P2ry12/Trem2/DAPI co-localization. scale bar = 100μm (**C**) Human $CD14^+/CD16^-$ monocytes and $CD14^+/CD16^+$ inflammatory monocytes, CD14M and CD16M respectively, were isolated from young healthy human blood (18-39 y.o.) by FACS. Cells were first gated on viability (not shown), then CD14 to avoid contaminating leukocytes, and finally sorted according to CD16 expression and collected for RNA. (**D**) Human myeloid dendritic cells (Blood DCs) were isolated from young healthy human blood (18-39 y.o.) using untouched myeloid DC enrichment kit followed by FACS. To avoid plasmacytoid DC contamination, DCs were stained for CD123, and myeloid DC subtypes CD1c, and C141 were collected for RNA. (**E**) A commercial iPSC-HPC source ($CD43^+/235a^+/CD41^+$) cells were identified and used to compare to in-house HPC differentiation and further iMGL differentiation.

signatures. Correlational analysis and Principal Component Analysis (PCA) revealed striking similarity of iMGLs (blue) to Fetal MG (orange) and Adult MG (green) (**Figures 1.5 and 1.6**). Furthermore, the first principal component PC1 (21.3 % variance, **Figure 1.5A** arrows) defines the differentiation time-series from iPSC through iHPC to our iMGL cells while PC2 and PC3 define the dendritic and monocyte trajectories, respectively. Biclustering analysis using 300 microglial, macrophage, and other immune related genes adapted from previous studies (Butovsky et al., 2014; Hickman et al., 2013; Zhang et al., 2014) identified similarities between groups and highlighted common gene clusters, but also uncovered differences between all groups. Again, this analysis showed that iMGLs cluster with microglia, but are distinct from other myeloid cells, iHPCs and iPSCs (**Figure 1.5B**).

Importantly, iMGLs, Fetal MG, and Adult MG express canonical microglial genes such as P2RY12, GPR34, C1Q, CABLES1, BHLHE41, TREM2, ITAM PROS1, APOE, SLCO2B1, SLC7A8, PPARD, and CRYBB1 (**Figure 1.5C and Table 1).** When compared to monocytes, iMGLs express the myeloid genes, RUNX1, PU.1, and CSF1R (**Figure 1.6C**), but do not express monocyte-specific transcription factors, IRF1, KLF4, NR4A1 (Abdollahi et al., 1991; Hanna et al., 2011; Lavin et al., 2014) (**Figure 1.6D**). Differential analysis between iMGLs, CD14 M, and CD16 M (**Figure 1.6F**) further emphasized that iMGLs predominantly express microglial genes (greater than two-fold change and $p<0.001$) including CX3CR1, TGFBR1, RGS10, and GAS6, but not monocyte and macrophage genes KLF2, TREM1, MPO, ITGAL, and ADGRE5. At the

protein level, iMGLs, like primary microglia, are $CD45^{lo}$ compared to $CD45^{hi}$ MD-Mφ, and express the microglia surface proteins Cx3cr1, Tgfbr1, P2ry12 and Pros1 (**Figures 1.8A-C**). Collectively, unbiased whole-transcriptome analysis and protein expression of key microglial markers strongly establishes iMGLs as a cell model that highly resembles primary human microglia that can be used to study microglia physiology and function in human health and disease.

Whole transcriptome differential analysis revealed increased expression of 1957 genes and 1071 genes in iMGLs when compared to Fetal MG or Adult MG, respectively. We also observed decreased expression of 1916 genes compared to fetal MG and 1263 genes compared to Adult MG. Enrichment analysis between iMGLs and primary microglia show that iMGLs are enriched for pathways involving cell cycle processes, migration, microtubule cytoskeletal organization, and inflammatory response, but do not differ in core myeloid GO terms (**Tables 1.3-1.5**). These terms reflect expected processes in which iMGLs are cued to respond to the environment and possess a capacity for renewal and maturation that have previously been reported in cultured microglia (Butovsky et al., 2014). Differential analysis between Fetal MG and Adult MG identified pathways related to responses to environment like migration and phagocytosis regulation, but not key myeloid genes in Fetal MG. Adult MG enrichment includes ECM organization, nervous system regulation, cell adhesion, and negative regulation of cell proliferation.

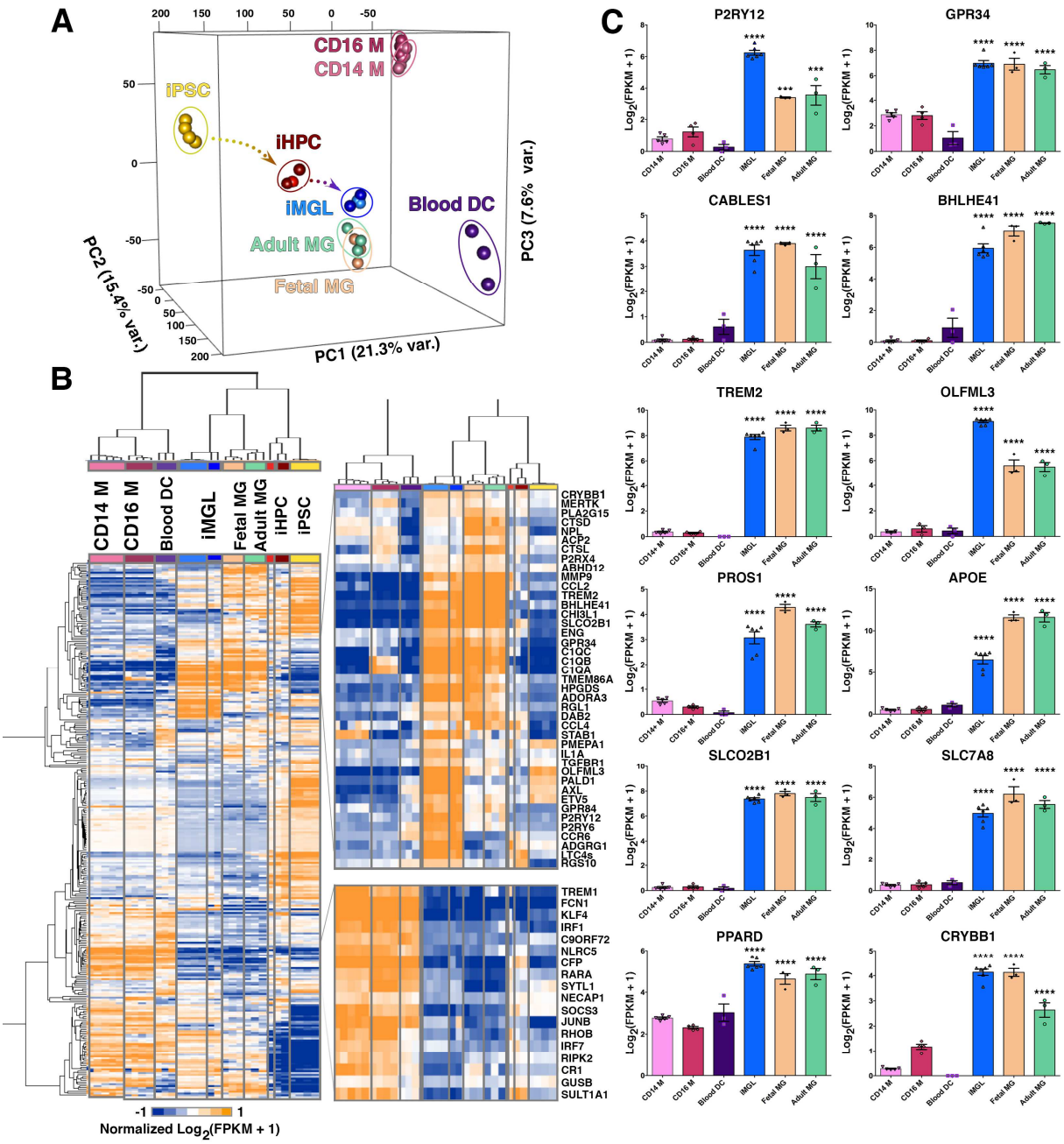
A
CD16 M
CD14 M
iPSC
iHPC
iMGL
Blood DC
Adult MG
Fetal MG
PC1 (21.3% var.)
PC2 (15.4% var.)
PC3 (7.6% var.)
B
CD14 M
CD16 M
Blood DC
iMGL
Fetal MG
Adult MG
iHPC
iPSC
CRYBB1
MERTK
PLA2G15
CTSD
NPL
ACP2
CTSL
P2RX4
ABHD12
MMP9
CCL2
TREM2
BHLHE41
CHI3L1
SLCO2B1
ENG
GPR34
C1QC
C1QB
C1QA
TMEM86A
HPGDS
ADORA3
RGL1
DAB2
CCL4
STAB1
PMEPA1
IL1A
TGFBR1
OLFML3
PALD1
AXL
ETV5
GPR84
P2RY12
P2RY6
CCR6
ADGRG1
LTC4S
RGS10
TREM1
FCN1
KLF4
IRF1
C9ORF72
NLRC5
CFP
RARA
SYTL1
NECAP1
SOCS3
JUNB
RHOB
IRF7
RIPK2
CR1
GUSB
SULT1A1
-1
1
Normalized Log2(FPKM + 1)
C
P2RY12
GPR34
CABLES1
BHLHE41
TREM2
OLFML3
PROS1
APOE
SLCO2B1
SLC7A8
PPARD
CRYBB1
Log2(FPKM + 1)

Figure 1.5: iMGL transcriptome profile is highly similar to human adult and fetal microglia. (**A**) 3D Principal Component Analysis (PCA) of iMGLs (blue), human adult microglia (Adult MG; green), human fetal microglia (Fetal MG; beige), $CD14^{+}/CD16^{-}$ monocytes (CD14 M; pink), $CD14^{+}/16^{+}$ monocytes (CD16 M; maroon), blood dendritic cells (Blood DC; purple), iHPCs (red), and iPSCs (yellow) (FPKM ≥ 1, n=23,580 genes). PCA analysis reveals that iMGL cluster with Adult and Fetal MG and not with other myeloid cells. PC1 (21.3% variance) reflects the time-series of iPSC differentiation to iHPC (yellow arrow) and then to iMGLs (blue arrow). PC2 (15.4% variance) reflects the trajectory to Blood DCs. PC3 (7.6% variance) reflects the trajectory to monocytes (**B**) Heatmap and biclustering (Euclidean-distance) on 300 microglia, myeloid, and other immune related genes (Butovsky et al., 2014; Hickman et al., 2013; Zhang et al., 2014). A pseudo-count was used for FPKM values (FPKM +1), log_2-transformed and each gene was normalized in their respective row (n=300). Representative profiles are shown for genes up and down regulated in both human microglia (fetal/adult) and iMGLs. (**C**) Bar graphs of microglial-specific or –enriched genes measured in iMGL, Fetal and Adult MG, Blood DC, CD14 M, and CD16 M as [Log_2 (FPKM +1)] presented as mean ± SEM. Data was analyzed using one-way ANOVA followed by Tukey's corrected multiple comparison *post hoc* test. Statistical annotation represents greatest p-value for iMGL, Fetal MG, and Adult MG to other myeloid cells. CD14 M (n=5, CD16 M (n=4), Blood DC (n=3), iMGL (n=6), Fetal MG (n=3), and Adult MG (n=3). *$p<0.05$, **$p<0.01$, ***$p<0.001$, ****$p<0.0001$. Complete statistical comparisons are provided in **Table 1.1**

Table 1.1: Adjusted *p*-values for 12 genes across all groups.

	GENES					
COMPARISONS	**P2RY12**	**GPR34**	**CABLES1**	**BHLHE41**	**TREM2**	**OLFML3**
CD14+ M VS. CD16+ M	0.7965	> 0.9999	> 0.9999	> 0.9999	0.9987	0.9871
CD14+ M VS. BLOOD DC	0.7531	0.0063	0.5606	> 0.9999	0.6405	> 0.9999
CD14+ M VS. IMGL	< 0.0001	< 0.0001	< 0.0001	0.0064	< 0.0001	< 0.0001
CD14+ M VS. FETAL MG	< 0.0001	< 0.0001	< 0.0001	< 0.0001	< 0.0001	< 0.0001
CD14+ M VS. ADULT MG	< 0.0001	< 0.0001	< 0.0001	< 0.0001	< 0.0001	< 0.0001
CD16+ M VS. BLOOD DC	0.2047	0.0129	0.6603	> 0.9999	0.8586	0.9976
CD16+ M VS. IMGL	< 0.0001	< 0.0001	< 0.0001	0.0111	< 0.0001	< 0.0001
CD16+ M VS. FETAL MG	0.0004	< 0.0001	< 0.0001	< 0.0001	< 0.0001	< 0.0001
CD16+ M VS. ADULT MG	0.0002	< 0.0001	< 0.0001	< 0.0001	< 0.0001	< 0.0001
BLOOD DC VS. IMGL	< 0.0001	< 0.0001	< 0.0001	0.0256	< 0.0001	< 0.0001
BLOOD DC VS. FETAL MG	< 0.0001	< 0.0001	< 0.0001	0.0001	< 0.0001	< 0.0001
BLOOD DC VS. ADULT MG	< 0.0001	< 0.0001	< 0.0001	< 0.0001	< 0.0001	< 0.0001
IMGL VS. FETAL MG	< 0.0001	> 0.9999	0.9483	0.0256	0.0633	< 0.0001
IMGL VS. ADULT MG	< 0.0001	0.8258	0.3015	0.0001	0.0633	< 0.0001
FETAL MG VS. ADULT MG	0.9987	0.9431	0.1407	0.2995	> 0.9999	0.9998
COMPARISONS	**PROS1**	**APOE**	**SLCO2B1**	**SLC7A8**	**PPARD**	**CRYBB1**
CD14+ M VS. CD16+ M	0.8814	> 0.9999	0.9999	> 0.9999	0.4125	0.0011
CD14+ M VS. BLOOD DC	0.4077	0.9103	0.9994	0.9965	0.9185	0.6963
CD14+ M VS. IMGL	< 0.0001	< 0.0001	< 0.0001	< 0.0001	< 0.0001	< 0.0001
CD14+ M VS. FETAL MG	< 0.0001	< 0.0001	< 0.0001	< 0.0001	< 0.0001	< 0.0001
CD14+ M VS. ADULT MG	< 0.0001	< 0.0001	< 0.0001	< 0.0001	< 0.0001	< 0.0001
CD16+ M VS. BLOOD DC	0.9391	0.9455	0.9941	0.9987	0.138	0.0002
CD16+ M VS. IMGL	< 0.0001	< 0.0001	< 0.0001	< 0.0001	< 0.0001	< 0.0001
CD16+ M VS. FETAL MG	< 0.0001	< 0.0001	< 0.0001	< 0.0001	< 0.0001	< 0.0001
CD16+ M VS. ADULT MG	< 0.0001	< 0.0001	< 0.0001	< 0.0001	< 0.0001	< 0.0001
BLOOD DC VS. IMGL	< 0.0001	< 0.0001	< 0.0001	< 0.0001	< 0.0001	< 0.0001
BLOOD DC VS. FETAL MG	< 0.0001	< 0.0001	< 0.0001	< 0.0001	0.0004	< 0.0001

BLOOD DC VS. ADULT MG	< 0.0001	< 0.0001	< 0.0001	< 0.0001	< 0.0001	< 0.0001
IMGL VS. FETAL MG	0.0008	< 0.0001	0.2803	0.0127	0.091	> 0.9999
IMGL VS. ADULT MG	0.2533	< 0.0001	0.9909	0.4987	0.403	< 0.0001
FETAL MG VS. ADULT MG	0.1787	> 0.9999	0.7213	0.4966	0.9658	< 0.0001

Table 1. 1. Adjusted *p*-values for 12 genes across all groups. one-way ANOVA followed by Tukey's *post-hoc* test. * p<0.05, **p<0.001, ***p<0.0001.

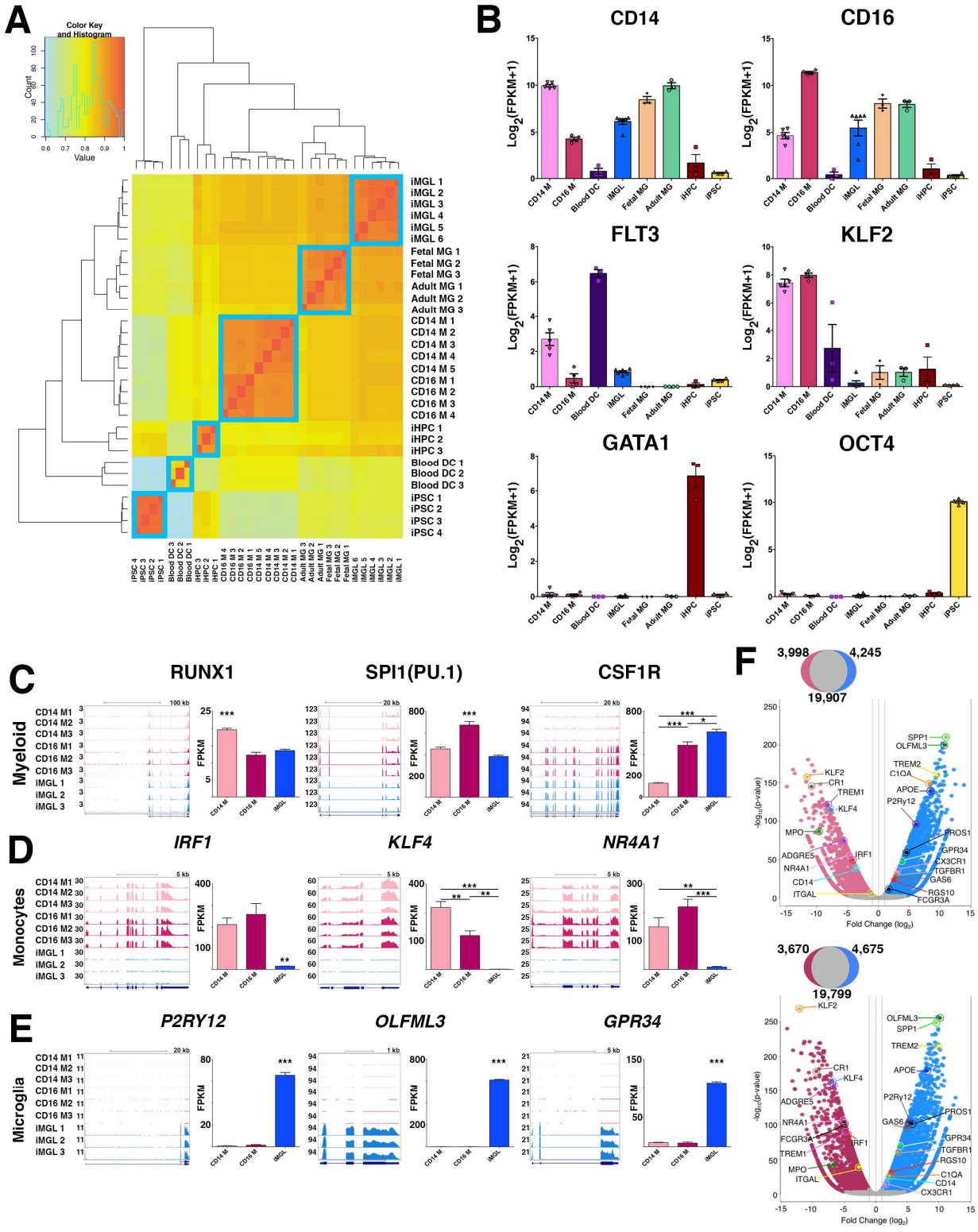
A
Color Key and Histogram
Count
Value
iMGL 1
iMGL 2
iMGL 3
iMGL 4
iMGL 5
iMGL 6
Fetal MG 1
Fetal MG 2
Fetal MG 3
Adult MG 1
Adult MG 2
Adult MG 3
CD14 M 1
CD14 M 2
CD14 M 3
CD14 M 4
CD14 M 5
CD16 M 1
CD16 M 2
CD16 M 3
CD16 M 4
iHPC 1
iHPC 2
iHPC 3
Blood DC 1
Blood DC 2
Blood DC 3
iPSC 1
iPSC 2
iPSC 3
iPSC 4
B
CD14
CD16
FLT3
KLF2
GATA1
OCT4
Log2(FPKM+1)
CD14 M
CD16 M
Blood DC
iMGL
Fetal MG
Adult MG
iHPC
iPSC
C
RUNX1
SPI1(PU.1)
CSF1R
Myeloid
FPKM
D
IRF1
KLF4
NR4A1
Monocytes
E
P2RY12
OLFML3
GPR34
Microglia
F
3,998
4,245
19,907
3,670
4,675
19,799
-log10(p-value)
Fold Change (log2)
SPP1
OLFML3
TREM2
C1QA
APOE
P2Ry12
KLF2
CR1
TREM1
KLF4
MPO
PROS1
ADGRE5
IRF1
GPR34
CX3CR1
NR4A1
TGFBR1
CD14
GAS6
ITGAL
RGS10
FCGR3A
C1QA

.

Figure 1.6: Correlational Matrix of biological samples used in RNA-sequencing and iMGL gene example genes. (**A**) Spearmen correlational matrix of biological samples used in RNA-sequencing highlights strong intra-group correlation. iMGLs correlate well with Fetal and Adult MGs suggesting strong gene expression similarity between samples. (**B**) Histograms of key genes found across different samples. CD14 and FCGR3A (also known as CD16) expressed in all myeloid cells including microglia, although enriched in CD14 M and CD16 M, respectively. As expected, FLT3 is highly expressed in Blood DCs and not in other cells and is barely detected in all three microglia groups. The monocyte/macrophage-specific transcription factor KLF2 was enriched in only CD14 M and CD16 M. Whereas GATA1 and OCT4 were only detected in iHPCs and iPSCs, respectively. (**C-F**) RNA-sequencing expression profile of iMGL reveals they are unique from $CD14M^-$ and CD16M and highly express microglial genes. (**C-E**) RNA-seq coverage maps and gene FPKM values in CD14 M, CD16 M, and iMGL for (**C**) for the myeloid genes RUNX1, PU.1, and CSF1R (**D**) monocyte-enriched genes IRF1, KLF4, and NR4A1 and (**E**) microglial-enriched genes P2RY12, OLFML3, and GPR34 in iMGL. For all RNA coverage maps, the y-axis represents Reads Per Million (RPM) scaled accordingly for all samples. Histogram comparisons using FPKM values for all genes are shown as the mean± s.e.m. Biological replicates for CD14 M (n=5), CD16 (n=4), and iMGL (n=6) are included for comparison by one-way ANOVA followed by Turkey's multiple-comparison post-hoc test. **p<0.001, ***p<0.0001. (F) Representative volcano plots of differentially expressed genes (p-value < 0.001, two-fold change) in iMGL (blue), CD14 M (light pink), and non-significant (grey). Key genes are both colored and labeled uniquely. Fold change (log_2) and $-log_{10}$(p-value) indicate the x and y-axis respectively. Grey dashed vertical lines indicate a two-fold change in gene expression. Venn diagrams indicate total number of differentially expressed genes for each condition.

Functional validation of iMGLs

Next, iMGLs were validated as surrogates of microglia using both functional and physiological assays. To this end, cytokine/chemokine secretion by iMGLs was measured following stimulation by Lipopolysaccharide (LPS), IL-1β or IFNγ. IL-1β and IFNγ are two cytokines that are elevated in AD patients and mouse models (Abbas et al., 2002; Blum-Degen et al., 1995; Patel et al., 2005; Wang et al., 2015a) (**Figure 1.7C**). Basally, iMGLs secrete 10 of the examined cytokines at low but detectable levels (**Table 1.2**). However, in response to IFNγ or IL-1β, iMGLs secrete 8 different chemokines including TNFα, CCL2, CCL4, and CXCL10. As expected, iMGLs robustly responded to LPS with induction of all measured cytokines except for CCL3 (**Table 1.2** for values). Collectively, iMGLs differentially release cytokines/chemokines based on their cell-surface receptor stimuli, a finding that closely aligns with the responses observed in acutely isolated primary microglia (Rustenhoven et al., 2016).

iMGLs express the microglial-enriched purinergic receptor P2ry12, which sense extracellular nucleotides from degenerating neurons, and is critical for microglial homeostatic function (De Simone et al., 2010; Moore et al., 2015) (**Figure 1.4A, B**). In response to ADP, iMGLs chemotax toward ADP and produce detectable calcium transients (**Figure 1.7D, E**), that were both negated by a P2ry12-specific inhibitor, PSB0739. These physiological findings further underscore that iMGLs respond appropriately to stimuli and express functional surface receptors, such as P2ry12, enabling quantitative analyses of microglial physiology.

Microglia, like astrocytes, play a critical role in synaptic pruning (Aguzzi et al., 2013; Paolicelli et al., 2011; Stephan et al., 2012). Because *in vitro* synaptosome phagocytosis assays are an established surrogate to study pruning, the ability of iMGLs to phagocytose human synaptosomes (hS) was quantitatively assessed. In comparison to MD-Mφ, iMGL phagocytosis of pHrodo-labeled hS was less robust (**Figure 1.7F, G**). However, iMGLs preferentially internalized hS when compared to *E. coli* particles and normalized to MD-Mφ (**Figure 1.8D, E**) supporting the notion that iMGLs and microglia are more polarized toward homeostatic functions than MD-Mφ.

Table 1.2: ELISA cytokine values (pg/ml) from conditioned media of stimulated iMGLs.

	Treatments[1]							
	Vehicle		IFNγ		IL-1β		LPS	
Cytokines	**mean ± SE**	**p-value**	**mean ± SE**	**p-value**	**mean ± SE**	**p-value**	**mean ± SE**	**p-value**
TNFα	2.56 ± 0.16	NA	58.82 ± 8.80	0.0008	29.74 ± 0.65	0.0471	116.49 ± 9.77	< 0.0001
IL6	0.00 ± 0.00	NA	12.22 ± 1.44	0.5649	13.92 ± 0.41	0.4736	274.39 ± 15.25	< 0.0001
IL8	339.21 ± 11.29	NA	3549.05 ± 181.22	< 0.0001	3,004.54 ± 47.58	< 0.0001	4,347.96 ± 75.61	< 0.0001
IL10	0.00 ± 0.00	NA	4.59 ± 2.35	0.1599	4.42 ± 1.33	0.1779	31.31 ± 1.52	< 0.0001
IL1α	1.59 ± 0.07	NA	1.48 ± 0.25	0.9999	4.89 ± 1.45	0.2535	30.55 ± 2.19	< 0.0001
CCL2	96.59 ± 6.27	NA	993.26 ± 55.76	0.0052	275.98 ± 19.54	0.7069	5,695.46 ± 275.72	< 0.0001
CCL3	104.91 ± 7.70	NA	295.39 ± 19.72	0.0043	556.24 ± 54.01	< 0.0001	0.00 ± 0.00	0.0807
CCL4	3,140.81 ± 165.84	NA	4,514.72 ± 10.01	< 0.0001	4,492.26 ± 51.35	< 0.0001	4,594.57 ± 33.96	< 0.0001
CXCL10	9.62 ± 1.48	NA	0.00 ± 0.00	0.1762	69.49 ± 4.73	< 0.0001	73.72 ± 4.53	< 0.0001
CCL17	4.70 ± 0.83	NA	25.82 ± 1.98	0.0168	21.75 ± 1.94	0.0464	92.96 ± 7.70	< 0.0001

Table 1.2. Elisa cytokine values (pg/ml) from conditioned media of iMGLs stimulated by IFNγ, Il-1β, and LPS for Figure 3B. Values and statistics are reported in mean ± standard error. n=3 per group. One-Way ANOVA followed by Dunnett's *post-hoc* test. Adjusted *p*-values for multiple comparisons are reported. * $p<0.05$, ** $p<0.001$, *** $p<0.0001$.

Table 1.3: Top GO pathways enriched in Adult MG compared to Fetal MG and iMGLs.

Adult MG vs Fetal MG				Adult MG vs iMGL			
Description	**GO ID**	**LogP (-)**	**Log (q-value)**	**Description**	**GO ID**	**LogP (-)**	**Log(q-value)**
Extracellular matrix organization	0030198	38.10	-34.18	Regulation of cell migration	0030334	13.23	-9.58
Circulatory system development	0072359	36.87	-33.23	Regulation of cell adhesion	0030155	11.46	-8.12
Single organism cell adhesion	0098602	32.24	-29.04	Actin filament-based process	0030029	11.03	-7.78
Regulation of nervous system development	0051960	28.56	-25.55	Regulation of anatomical structure morphogenesis	0022603	10.95	-7.74
Regulation of cellular component movement	0051270	26.49	-23.54	Cell junction organization	0034330	10.29	-7.12
Adaptive immune response	0002250	25.87	-22.96	Enzyme linked receptor protein signaling pathway	0007167	9.73	-6.76
Response to cytokine	0034097	20.02	-17.49	Circulatory system development	0072359	8.59	-5.79
Epithelial cell proliferation	0050673	19.25	-16.74	Single-organism catabolic process	0044712	8.13	-5.42
Central nervous system development	0007417	19.12	-16.63	Oxidation-reduction process	0055114	7.78	-5.11
Negative regulation of cell proliferation	0008285	18.82	-16.34	Plasma membrane organization	0007009	7.35	-4.76
Tissue morphogenesis	0048729	18.50	-16.06	Cellular response to oxygen-containing compound	1901701	7.31	-4.73
Muscle structure development	0061061	17.98	-15.56	Negative regulation of cell proliferation	0008285	7.28	-4.72
Single organism cell adhesion	0050808	17.86	-15.48	Positive regulation of phosphorylation	0042327	7.14	-4.63
Regulation of nervous system development	0042063	17.26	-14.91	Renal system development	0072001	6.77	4.30
Regulation of Growth	0040008	16.62	-14.32				

Table 1.3. Gene ontology terms enriched in Adult MG vs Fetal MG and iMGL.

Table 1.4: Top GO pathways enriched in Fetal MG compared to Adult MG and iMGL.

Fetal vs Adult MG				Fetal MG vs iMGL			
Description	**GO ID**	**LogP (-)**	**Log (q-value)**	**Description**	**GO ID**	**LogP (-)**	**Log(q-value)**
Leukocyte chemotaxis	0030595	6.92	-3.07	Single-organism catabolic process	0044712	10.41	-6.64
Response to acidic pH	0010447	4.07	-1.33	Regulation of cell migration	0030334	9.90	-6.26
Inorganic ion homeostasis	0098771	4.04	-1.31	Iron ion transport	0006826	8.68	-5.52
Regulation of cell migration	0030334	3.80	-1.18	Divalent metal ion transport	0070838	8.44	-5.34
Circulatory system process	0003013	3.72	-1.13	Carbohydrate metabolic process	0005975	7.39	-4.59
Melanosome organization	0032438	3.70	-1.13	Small GTPase mediated signal transduction	0007264	6.69	-3.99
Anion transport	0006820	3.54	-1.01	Angiogenesis	0001525	6.64	-3.97
Macrophage migration	1905517	3.47	-0.95	Positive regulation of transport	0051050	6.15	-3.59
Transmembrane receptor protein tyrosine kinase signaling pathway	0007169	3.23	-0.81	Positive regulation of intracellular signal transduction	1902533	6.12	-3.57
Negative regulation of receptor activity	2000272	3.14	-0.76	Aminoglycan metabolic process	0006022	6.03	-3.50
Positive regulation of phagocytosis, engulfment	0060100	3.13	-0.76	Cell projection assembly	0030031	5.81	-3.31
Sterol import	0035376	3.13	-0.76	Cell-substrate adhesion	0031589	5.68	-3.21
Behavior	0007610	3.11	-0.75				
Positive regulation of transport	0051050	3.02	-0.70				
Vesicle organization	0016050	2.96	-0.65				

Table 1.4. Gene ontology terms enriched in Fetal MG vs Adult MG and iMGL.

As iMGLs and primary microglia express both C1q and CR3 (CD11b/CD18 dimer), iMGLs were used to assess whether synaptic pruning in human microglia primarily involves this pathway as seen in mice (Chung et al., 2013). Using an additive-free CD11b antibody, iMGL phagocytosis of hS was significantly reduced (-40.0%, ***p<0.0001)(**Figure 1.7H, I).** In contrast, an inhibitor of Mertk (UNC569), also implicated in synaptic pruning, only marginally decreased iMGL hS phagocytosis (-12.6%, *p<0.05)(**Figure 1.7H, I**). Similar to studies in murine KO models, our data indicates that MERTK plays a minor role in human microglia-mediated synaptic pruning (Chung et al., 2013), whereas C1q/CR3 is integral for microglia-mediated synaptic pruning in humans.

iMGL maturation and homeostasis is modulated by a CNS environment

Next, we examined whether iMGL maturation can be achieved with direct contact with the CNS environment. Therefore, iMGLs were cultured with rat-hippocampal neurons (21 DIV) to assess how iMGLs respond to neuronal surface cues (**Figure 1.9A**). Rat-hippocampal neurons were used because they readily form synapses in culture and can be generated with limited variability. iMGLs were subsequently separated from neurons by FACS with human specific CD45 and CD11b antibodies and profiled at the transcriptome level (**Figure 1.9B)**. Differential gene expression analysis revealed that neuronal co-culturing upregulated 156 and downregulated 244 iMGL genes (**Figure 1.9C,D**). FFAR2 and COL26A1 are two genes differentially expressed in iMGLs cultured with only defined factors and indicate a developmentally primed microglia profile.

Table 1.5: Top GO pathways enriched in iMGL compared to Fetal MG and Adult MG.

iMGL vs Fetal MG				iMGL vs Adult MG			
Description	**GO ID**	**LogP (-)**	**Log (q-value)**	**Description**	**GO ID**	**LogP (-)**	**Log(q-value)**
Single organism cell adhesion	0098602	30.48	-26.23	Mitotic cell cycle process	1903047	28.46	-24.22
Mitotic cell cycle process	1903047	21.34	-17.87	Regulation of cell cycle	0051726	19.26	-15.94
Immune system development	0002520	18.56	-15.55	DNA replication	0006260	17.22	-14.09
Regulation of cellular component movement	0051270	16.11	-13.32	Chromatin organization	0006325	11.44	-8.64
Mitotic cell cycle phase transition	0044772	15.94	-13.18	Regulation of nuclear division	0051783	11.25	-8.47
Leukocyte migration	0050900	15.19	-12.49	Immune system development	0002520	10.90	-8.15
Taxis	0042330	14.76	-12.12	DNA-dependent DNA replication	0006261	10.22	-7.51
Positive regulation of cell differentiation	0045597	14.76	-12.12	Negative regulation of transcription from RNA polymerase II promoter	0000122	10.20	-7.50
Inflammatory response	0006954	14.64	-12.03	Microtubule cytoskeleton organization	0000226	9.96	-7.27
Anatomical structure formation involved in morphogenesis	0048646	13.83	-11.27	Leukocyte activation	0045321	9.57	-6.94
Positive regulation of cell proliferation	0008284	13.82	-11.26	Regulation of small GTPase mediated signal transduction	0051056	9.16	-6.56
Positive regulation of intracellular signal transduction	1902533	12.20	-9.73	Cell cycle G2/M phase transition	0044839	9.01	-6.44
Positive regulation of hydrolase activity	0051345	11.80	-9.35	Signal transduction by p53 class mediator	0072331	8.47	-5.99
Negative regulation of multicellular organismal process	0051241	11.67	-9.23	Regulation of transcription involved in G1/S transition of mitotic cell cycle	0000083	8.34	-5.88
Negative regulation of cell proliferation	0008285	11.62	-9.18	Cellular response to oxygen-containing compound	1901701	8.15	-5.73

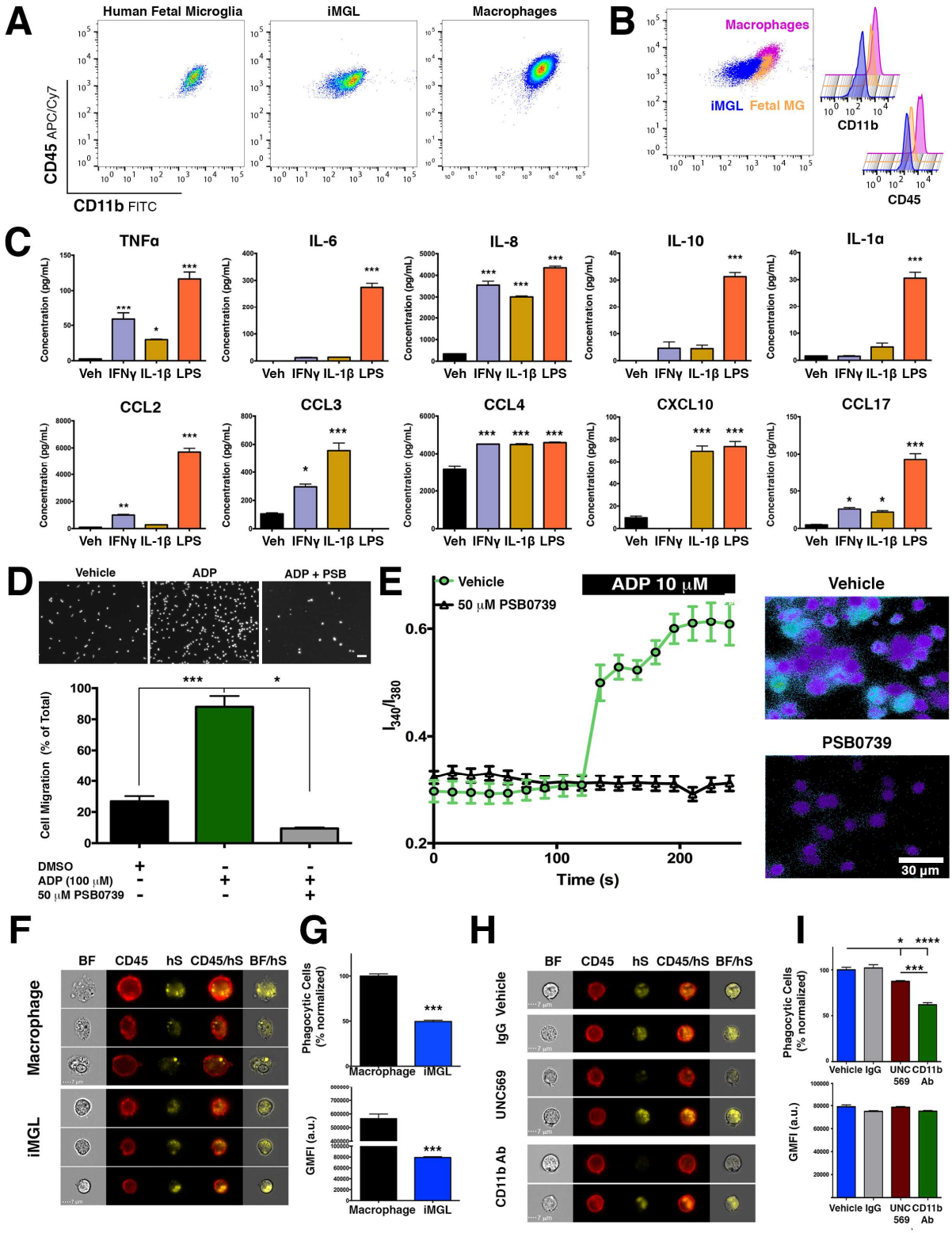
A
Human Fetal Microglia
iMGL
Macrophages
CD45 APC/Cy7
CD11b FITC
B
Macrophages
iMGL Fetal MG
CD11b
CD45
C
TNFα
IL-6
IL-8
IL-10
IL-1α
CCL2
CCL3
CCL4
CXCL10
CCL17
Concentration (pg/mL)
Veh IFNγ IL-1β LPS
D
Vehicle
ADP
ADP + PSB
Cell Migration (% of Total)
DMSO
ADP (100 μM)
50 μM PSB0739
E
Vehicle
50 μM PSB0739
ADP 10 μM
I340/I380
Time (s)
Vehicle
PSB0739
30 μm
F
BF
CD45
hS
CD45/hS
BF/hS
Macrophage
iMGL
G
Phagocytic Cells (% normalized)
GMFI (a.u.)
Macrophage
iMGL
H
BF
CD45
hS
CD45/hS
BF/hS
IgG Vehicle
UNC569
CD11b Ab
I
Phagocytic Cells (% normalized)
GMFI (a.u.)
Vehicle
IgG
UNC 569
CD11b Ab

Figure 1.7: iMGLs are physiologically functional and can secrete cytokines, respond to ADP, and phagocytose human synpatosomes**. (A-B)** By flow cytometry analysis, iMGL (blue) are $CD45^{lo\text{-}int}$ similar to fetal MG (orange) but different from $CD45^{hi}$ MD-Mφ (fuchsia). (**B**) Histogram of CD11b intensity (left) reveals that Fetal MG express slightly more CD11b than iMGL but less than MD-Mφ. (**C**) iMGLs secrete cytokines and chemokines when stimulated for 24 hours with either IFNγ (20 ng/ml), IL-1β (20 ng/ml), or LPS (100 ng/ml) by ELISA multiplex. (**D**) ADP (100 μM) induces iMGL migration in a trans-well chamber (5 μm). Pre-exposure to the P2ry12 antagonist, PSB0739 (50 μM, 1 hr) completely abrogates ADP-induced iMGL migration (***p<0.0001). (**E**) ADP induces calcium flux in iMGLs via P2ry12 receptors. (*Left*) Exposure to ADP leads to elevated calcium influx (I_{340}/I_{380} ratio) in vehicle group (green trace) but not in PSB0739-treated group (black trace). (*Right*) Representative images of ADP-induced calcium flux at 240 s in vehicle (top) and PSB0739 (bottom). (**F**) iMGLs phagocytose human brain-derived synaptosomes (hS). Representative images captured on Amnis Imagestream display phagocytosis of hS by MD-Mφ and iMGLs. (**G**) Quantification of phagocytosis shows that iMGLs internalize hS at 50% of macrophage capacity (p<0.0001). **(H**) Representative images of iMGL phagocytosis of hS in the presence of either a Mertk inhibitor UNC569 (top) or anti-CD11b antibody (bottom). (**I**; top) iMGL phagocytosis of hS phagocytosis is reduced byby approximately 12% (burgundy bar, p<0.05) by blocking Mertk, but 40% (p<0.0001, green bar) by inhibiting CR3 via CD11b blockade. (**I**; bottom) Sub-analysis of iMGLs exhibiting a phagocytic event reveals similar average amounts of internalization across treatment groups (p=0.1165). All histograms reported as mean ± SEM. Cytokine and migration assays one-way ANOVA, followed by Dunnett's multiple-comparison *post-hoc* test, ***p<0.0001, **p<0.001, *p<0.05; Cytokine assay: n=3 wells/group. Migration Assay: n=5 fields /condition. Calcium assay: vehicle (n=37 cells), PSB0739-treated (n=17 cells), I_{340}/I_{380} represented as mean ± SEM at each time point. Phagocytosis assay: MD-Mφ vs iMGL: Unpaired t-test, **p<0.001, n=3 wells/group. MERTK and CR3 assay, one-way ANOVA, followed by Tukey's multiple-comparison *post-hoc* test, ***p<0.0001; n= 6 for vehicle, n=3 wells/group.

In contrast, co-culturing microglia with neurons increased expression of Siglec11 and 12, human-specific sialic-acid binding proteins that interact with the neuronal glycocalyx, function in neuroprotection, and suppress pro-inflammatory signaling, and thus maintain a microglia homeostatic state (Linnartz-Gerlach et al., 2014; Wang and Neumann, 2010). Additionally, we saw increased expression of microglial genes CABLES1, TRIM14, MITF, MMP2, and SLC2A5.

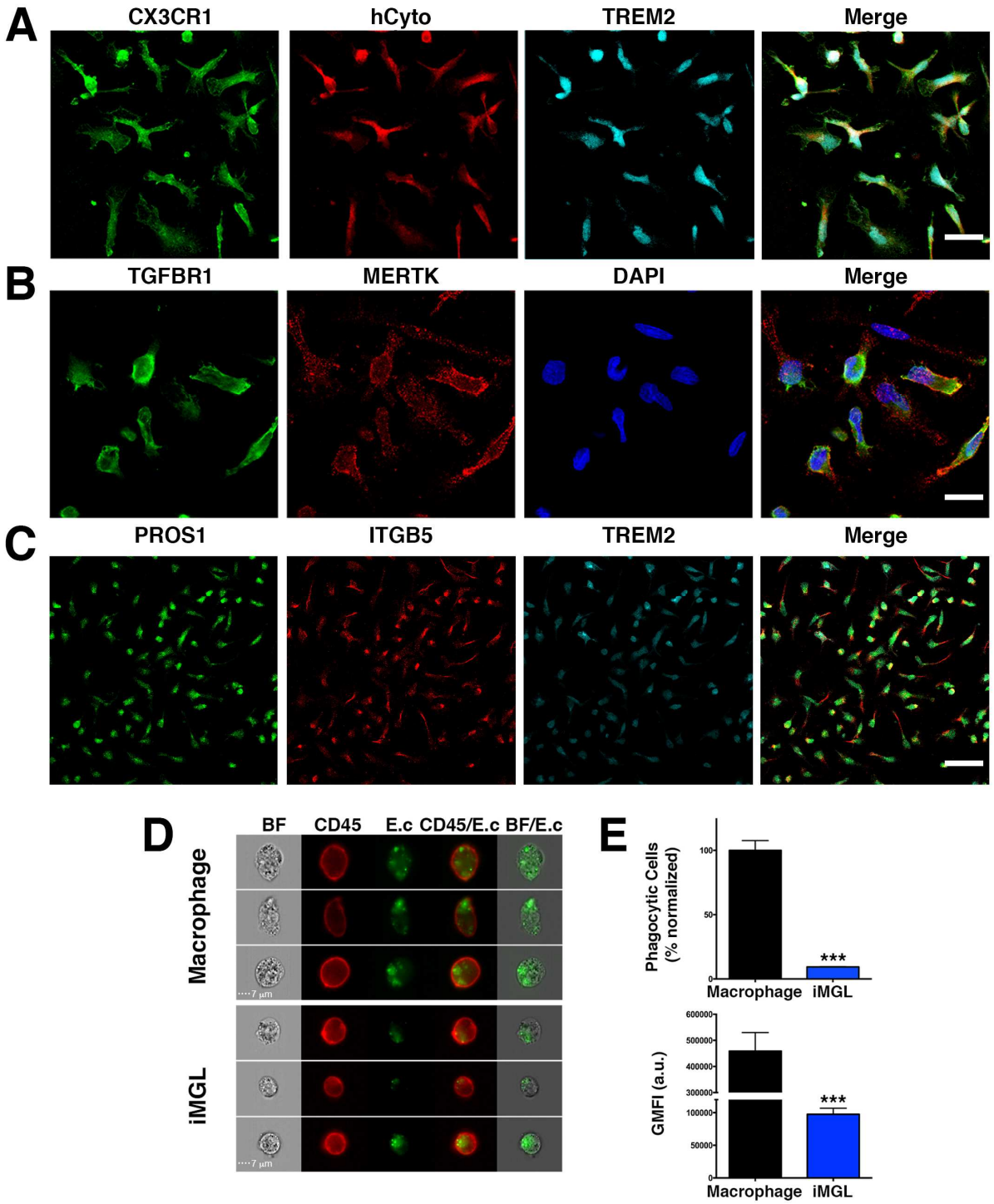

Overall, these results implicate both soluble and surface CNS cues as factors in microglia maturation (Biber et al., 2007)(**Figure 1.9E**,**F**).

A fundamental characteristic of microglia is the surveillance of the CNS environment with their highly-ramified processes. To investigate how iMGLs might interact within a human brain

Figure 1.8: iMGLS are positive for microglia surface proteins and perform phagocytosis of *E. coli* particles. Representative immunofluorescent images of iMGL expressing microglial markers (**A**) CX3CR1 (green), hCyto (human cytoplasm marker, SC121; red), TREM2 (cyan). scale bar = 20 μm (**B**) Co-localization of TGFBR1(green), MERTK (red), nuclei (DAPI, blue) scale bar = 20 μm. (**C**) PROS1 (green), ITGB5 (red), TREM2 (cyan). scale bar = 100 μm (**D-E**) Assessment of phagocytosis of pHrodo-labeled *E. coli* (E.c; green) (**D-E**) in human monocyte-derived macrophages (black) and iMGLs (blue). (**D**) Representative bright field and immunofluorescent images captured by Amnis Imagestream flow cytometer visualizing phagocytosis of E.c within macrophages (top) and iMGL (bottom). (**E**) Quantification of percent phagocytic cells (top) reveals that iMGLs (blue) phagocytose E.c almost 10-fold less frequently than macrophages (black) as expected. (**B:** bottom) The amount of E.c internalized (by GMFI) within phagocytic cells further illustrates the greater phagocytic capacity of macrophages compared to iMGLs. Student's t-test,*** $p<0.001$, n=3/group.

environment, iMGLs were cultured with hiPSC 3D brain-organoids (BORGs). BORGs include neurons, astrocytes, and oligodendrocytes that self-organize into a cortical-like network, but lack microglia (**Figure 1.9**). To test if iMGLs invade BORGs similarly to how microglia enter the developing neural tube (Chan et al., 2007; Rezaie and Male, 1999), iMGLs were added to BORG cultures. By day three, iMGLs had embedded into the BORGS and were not detected in the media, suggesting rapid iMGL chemotaxis toward CNS cues (**Figure 1.9A-C**). By day 7, iMGLs (green) also tiled and extended varying degrees of ramified processes within the 3D organoid environment (**Figure 1.9D-F**). To determine whether iMGLs respond to neuronal injury, BORGS were pierced with a 25-gauge needle**.** After injury, iMGLs clustered near the injury site and adopted a more amoeboid morphology, resembling "activated" microglia found in injured or diseased brains (Kettenmann et al., 2011) (**Figure 1.9G-I)**. Collectively, these data demonstrate that iMGLs can integrate within an *in vitro* 3D CNS environment, mature, ramify, and respond to injury similar to brain microglia.

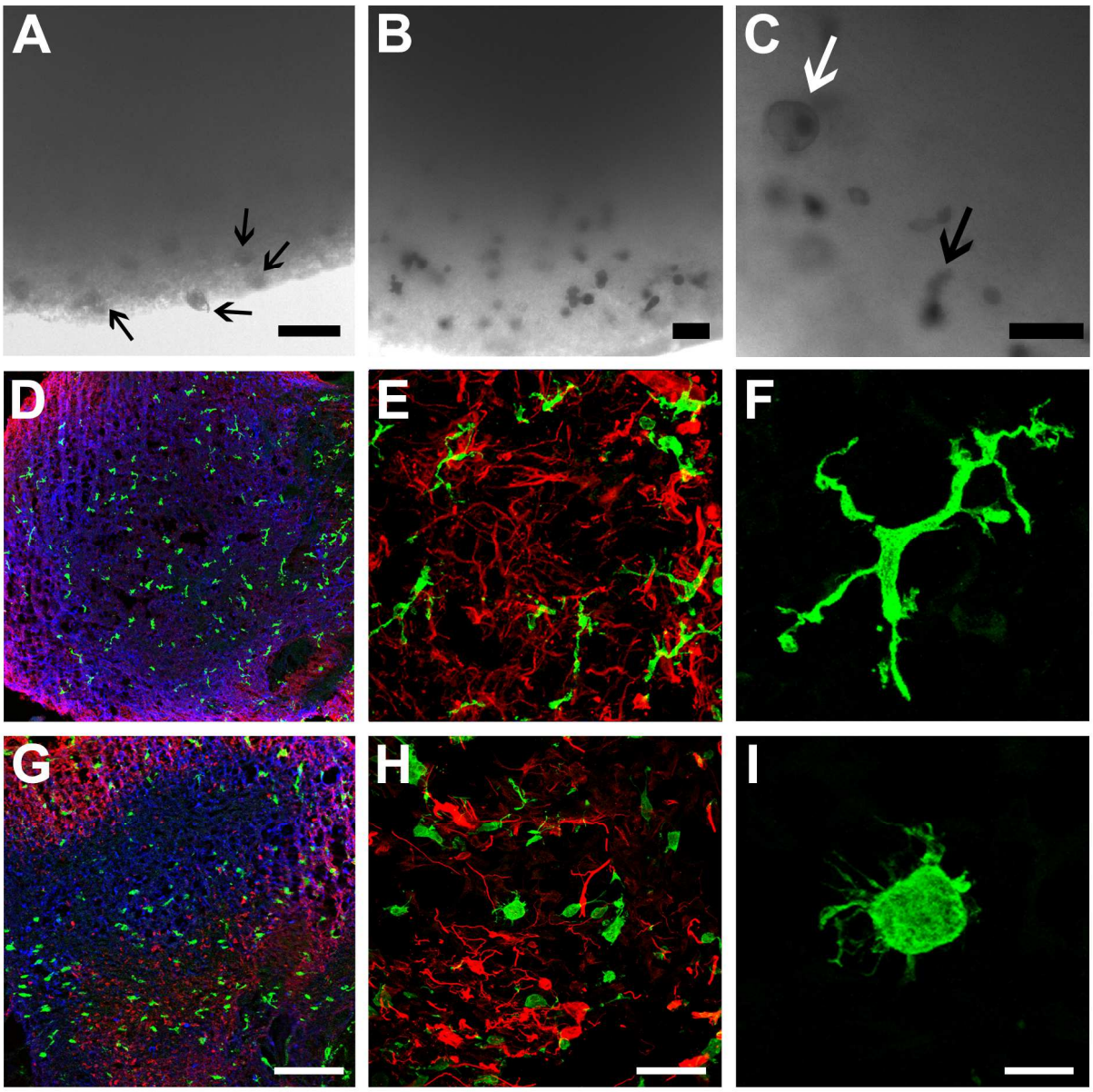

Next, we sought to examine iMGLs within the context of a CNS environment *in vivo*. To this end, iMGLs (day 38) were transplanted into the cortex of MITRG mice that are Rag2-deficient and IL2rγ-deficient mice and also express the human forms of four cytokines knocked-in (M-CSF^{h};IL-3/GM-CSF^{h};TPO^{h}), allowing for xenotransplantation and survival of myeloid and other leukocytes (Rongvaux et al., 2014). Two months after transplantation, the homeostatic state and identity of transplanted microglia were assessed with P2ry12 and the human-specific Tmem119 antibodies, respectively (Bennett et al., 2016; Butovsky et al., 2014; Haynes et al., 2006)(**Figure 1.10**). Human

Figure 1.9: iMGLs respond to the neuronal environment in 3D brain organoid co-cultures (BORGS). iMGLs (5 x10^5 cells) were added to media containing a single BORG for 7 days. **(A)** Representative bright-field image of iMGLs detected in and near BORG after 3 days. iMGLs were found in and attached to the BORG-media interface (arrows), but not free floating in the media, suggesting complete chemotaxis of iMGLs. **(B)** Representative image of iMGLs in outer and inner radius of BORG. **(C)** Embedded iMGLs exhibit macrophage-like morphology (white arrow) and extend processes (arrow) signifying ECM remodeling and surveillance respectively. Simultaneous assessment of embedded iMGL morphology in uninjured **(D-F**) and injured **(G-I)** BORGs. **(D)** Immunohistochemical analysis of BORGs reveals iMGLs begin tiling evenly throughout the BORG and project ramified processes for surveillance of the environment. BORGs are representative of developing brains *in vitro* and contain neurons (β3-tubulin, blue) and astrocytes (GFAP, red), which self-organize into a cortical-like distribution, but lack microglia. iMGLs (IBA1, green). (**E-F**) Representative immunofluorescent images of iMGLs with extended processes within the 3D CNS environment at higher magnification. **(G-I)** Representative images of iMGL morphology observed in injured BORG. **(H-I)** Round-bodied iMGLs reminiscent of amoeboid microglia are distributed in injured BORGs and closely resemble activated microglia, demonstrating that iMGLs respond appropriately to neuronal injury. Scale Bar (**A-C**) =50 μm in A-C, (**D,G**)= 200 μm (**E-H**)= 80 μm and (**F,I**) =15 μm.

specific markers, cytoplasmic Ku80 (hNuclei) and SC121 (hCyto) distinguished iMGLs from endogenous microglia. Transplanted human iMGLs co-expressing both ku80 and P2ry12 were abundant within MITRG brains suggesting long-term engraftment potential (**Figure 1.10A-D**). At higher magnification, P2ry12 is expressed in highly ramified iMGLs resembling quiescent cortical microglia; the membrane distribution accentuates the finer extended processes (**Figure 1.10B-D**)(Baron et al., 2014). Tmem119 and Iba1 were also expressed in both $hCyto^+$ soma and in highly arborized iMGL processes (**Figure 1.01E-L**). At higher magnification, Tmem119 is predominately membrane-bound and in agreement with previous studies (Bennett et al., 2016). Together, these findings demonstrate engraftment and long-term survival of iMGLs that result in highly branched microglia-like cells expressing Iba1, P2ry12 and Tmem119 (**Figure 1.10I-L**), in which iMGLs resemble quiescent mouse and human microglia (**Figure 1.10M-P**). Finally, the morphology and high P2ry12 expression suggest that transplanted iMGLs are actively surveying their neuronal environment that translates to their potential use in studying human microglia function in mouse CNS-disease models.

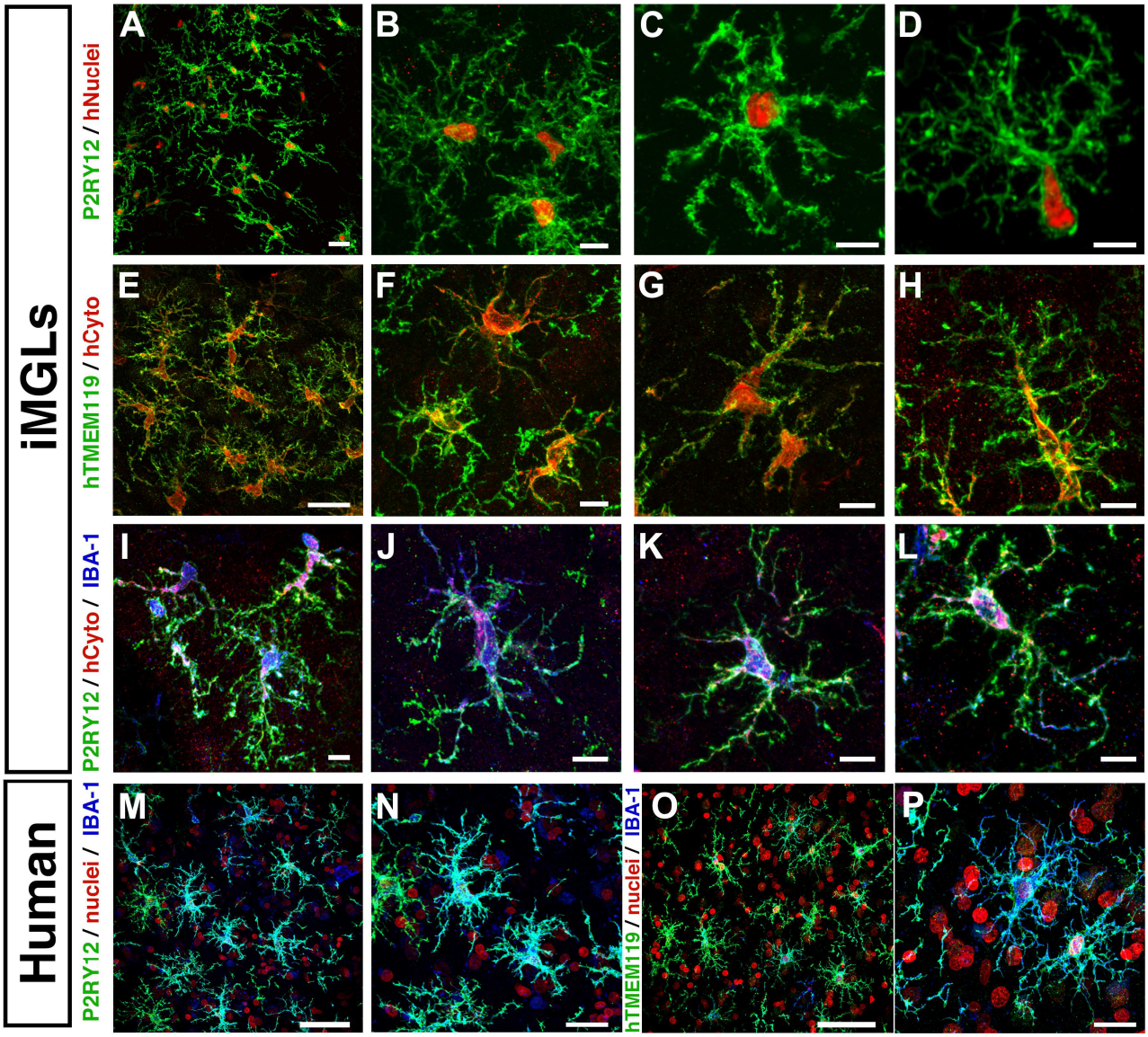

DISCUSSION

Here, we show that human microglia-like cells can be generated from iPSCs following a fully-defined and highly efficient protocol, which enables high purity (>97%) and robust scalability. Importantly, iMGLs are highly similar to cultured human adult and fetal microglia by both transcriptomic and functional analyses. Our whole-transcriptome PCA also highlights the

Figure 1.10: iMGLs transplanted into the brains of wild-type transplant competent mice are like brain microglia. Within the brains of xenotransplantation compatible mice, transplanted iMGLs are ramified and interact with the neuronal environment. (**A-L**) After two months *in vivo,* iMGLs transplanted into mice display long-term viability with highly arborized processes resembling endogenous microglia found in the brain. (**A**) Transplanted iMGLs, labeled with P2ry12 (green; HPA HPA014518, Sigma) and human nuclei (ku80, red), exhibit long-term viability in mice. (**B-D**) At higher magnification, P2ry12 is highly expressed in iMGL arborized processes, both suggestive of homeostatic microglia surveying the brain environment. (**E-H**) Ramified iMGLs also express microglia-enriched Tmem119 recognized by a human-specific Tmem119 antibody (green; ab185333, Abcam, identified and validated in [Bennet et al, PNAS 2016], and human cytoplasm maker SC121 (hCyto, red). (**I-L**) At higher magnification, representative iMGLs express P2ry12 (green), hCyto (red), and Iba1 (blue; ab5076, Abcam). (**M-P**) Human cortical tissue stained with P2ry12, hTmem119, and Iba1. Scale bars; (**A,E,N**) = 30 μm, (**P**) = 20 μm, (**B-D, F-H, I-L,**) = 10 μm, (**M,O**) = 60 μm. n=3 animals per study.

differentiation trajectory of iPSCs toward iHPCs, and then iMGLs. Moreover, our series of microglial functional assays, only possible with a high yield and pure protocol, further strengthens how iMGLs can be used to investigate microglia genes implicated in disease and understand physiological function both *in vitro* and *in vivo.*

We also demonstrate the use of iMGLs to investigate human microglial function as a therapeutic target in human disease. A recent study implicated complement and increased microglia-mediated pruning of synapses early in AD (Hong et al., 2016a; Hong et al., 2016b). Here, we found that blocking CR3, via anti-CD11b, in iMGLs reduces phagocytosis of human synaptosomes. Our findings provide one of the first examples, to our knowledge, of quantitative evidence showing human microglia engulfing human synaptosomes predominately via the CR3 axis, as implicated by transgenic mouse studies (Hong et al., 2016a). Moreover, we highlight the utility of iMGLs to examine microglia-targeted AD therapies, such as anti-CD11b, in phagocytic assays and to potentially examine or validate other complement-targeted therapies in development.

Microglia mediate neuroinflammation through surveillance of their environment and by cell surface receptor activation. Therefore, we tested iMGL response to extracellular stimuli observed in AD, such as nucleotides leaked from degenerating neurons. Microglia sense ADP release via purinergic receptors and we likewise find that iMGLs robustly express functional P2ry12 and migrate and exhibit calcium influx via an ADP-P2ry12 receptor mechanism. Also, iMGLs secrete a variety of cytokines in response to IFNγ, IL-1β, and LPS stimulation. Many of

these cytokines are known to be highly elevated in neurological diseases and/or involved in the recruitment of peripheral immune cells into the CNS under pathological conditions (Chan et al., 2007; Prinz et al., 2011; Rezaie and Male, 1999; Stalder et al., 2005). Microglial-mediated cytokine secretion can further influence the inflammatory milieu in the CNS and thus represents an excellent therapeutic target for restoring CNS homeostatic balance. Together, migration, calcium imaging, and cytokine secretion assays not only validate iMGLs to be highly similar to brain-derived microglia but provide important functional assays to assess the role of microglia in neuroinflammation. Our data highlights the potential utility of iMGLs to identify therapeutic compounds via high throughput assessment of microglia physiology.

We also highlight how neuronal co-culture can further modulate microglial gene expression and how interactions with the neuronal glycocalyx increase Siglec expression. Interestingly, iMGLs not cultured with neurons differentially expressed early microglia genes including FFAR2 (Erny et al., 2015; Matcovitch-Natan et al., 2016) suggesting that other factors are needed to further educate microglia as tissue-resident macrophages of the brain. In accordance with this notion, iMGLs cultured in 3D brain cultures actively migrate, tile and encompass the volume of the BORGs, extending processes reminiscent of early microglia development. We also show that iMGLs transplanted in mice, engraft, survive, and display characteristic ramified processes that have increased branch order complexity, closely resembling quiescent microglia (Andreasson et al., 2016). We also note that transplanted, highly ramified iMGLs were morphological heterogeneous within the brain (**Figure 1.10I-L**). This morphological diversity is indicative of microglia responding to distinct cortical layers/brain-regions and potentially reflect microglia subtypes found within the brain(Grabert et al., 2016).

Overall, these results underscore the potential of iMGLs as a renewable source of patient-derived microglial-like cells for studying the role of microglia in neurodegenerative diseases. While our comparisons were limited to cultured microglia, we showed that our cells were highly similar to primary cells and our studies have highlighted potential new ways to culture microglia within BORGs or mouse brains. This platform will allow for the identification of potential novel microglial-based translational therapies, as recently discussed (Biber et al., 2016). Finally, while technical challenges exist for isolating microglia from both human brain and BORGS for study, the development of future tools will likely make it feasible to compare microglia isolated from

BORGs with freshly isolated microglia to determine whether 3D organoid systems fully recapitulate the *in vivo* microglia signature. In summary, we demonstrate a methodology to generate human microglial-like cells, in large quantities, from renewable iPSCs that can be used as primary microglia surrogates.

Our study is one of the first to describe a fully-defined, serum-free protocol for generating microglial cells from induced pluripotent stem cells with the exception of a recently published resource from Muffat and colleagues (Muffat et al., 2016). However, their approach uses hematopoietic cells derived from EB as microglia precursors. One challenge with the use of an EB-based method and selection by cell adhesion (Muffat et al protocol) is the potential contamination by other cell types that spontaneously arise from EBs i.e. neuroectoderm including astrocytes. More recently, a protocol described the production of microglia-like cells reliant on astrocyte co-cultures and a serum-based media formulation. This protocol produces cell quantities comparable to *Muffat et al.*, that exhibit amoeboid-like morphology in *vitro* and in *vivo* (Pandya et al., 2017). Thus, some questions remain in terms of yield, scalability, and purity of homeostatic microglia using these other methods and whether the resulting cells can be used to interrogate microglial function in quantitative assays that require large numbers of pure microglia-like cells.

In summary, we have developed a highly reproducible protocol to generate iPSC-derived hematopoietic progenitor cells and microglia-like cells in high yield that can be used in functional assays to interrogate microglia function. We have also identified a commercial HPC source that can be readily differentiated to iMGLs with our protocol to study microglia biology. We demonstrate that iMGLs phagocytose, secrete cytokines, and respond to ADP-via P2ry12, similar to human primary microglia. We demonstrated that iMGLs can be studied in context with neurons and glia by examining how both rodent and human neuronal cells influence microglia phenotype and function, both *in vitro* and *in vivo*. As expected, iMGLs gene profiles shift toward a neuronal-centric phenotype and respond appropriately to injury in 3D cell culture. Together, our fully-defined protocol yields highly-pure microglia-like cells that provide a platform to investigate human microglia function for a broad range of CNS development, homeostatic function, and neurological diseases applications. While the validation of iMGLs as microglia surrogates raised several new and exciting questions related to microglia biology in development, health and disease, this new renewable resource will allow for those questions to be further addressed by the field.

CHAPTER TWO

EXAMINING ALZHEIMER'S DISEASE GENETICS USING HUMAN INDUCED PLURIPOTENT STEM CELL DERIVED MICROGLIA-LIKE CELLS

INTRODUCTION

AD is characterized by the build-up of toxic protein aggregates, Aβ and tau, coupled with CNS neuroinflammation leading to the loss of synapses and neurons. In AD, microglia cluster around Aβ plaques highlighting their inability to clear beta-amyloid (Hickman et al., 2008; Liu et al., 2010). As the innate immune cell of the CNS, microglia play important roles as the cells that mediate and respond to Aβ and tau, dying neurons, and secreted inflammatory molecules. Microglia are also implicated in the neuroinflammatory component of AD etiology, including cytokine/chemokine secretion, which exacerbate disease pathology (Guillot-Sestier and Town, 2013). In AD brains, endocytic (e.g. TREM2, ABCA7, etc.) and cytokine (e.g. TNFα, IL-1β etc.) expression are highly correlated with AD plaque pathology and suggests that increased or decreased expression of these genes are influenced via stimulation of PRRs (e.g. TLR4, etc) by Aβ (Bradshaw et al., 2013; Combs et al., 2001; Khemka et al., 2014; Villegas-Llerena et al., 2015; Walter et al., 2007; Wang et al., 2015a)

Recently, genome wide association studies (GWAS) have identified several genes expressed by microglia that are associated with the risk of developing late-onset AD (LOAD), such as TREM2 and CD33. Many of these genes are richly expressed in microglia compared to other CNS cell., Thus, microglia expressed AD GWAS genes, such as TREM2 and CD33, likely play a role in AD progression. The role of these genes in microglial function and AD are just beginning to be examined in mouse models, but the generation of human microglia-like cells would allow for the interrogation of human-specific genes that cannot be modeled in mice. Thus, there is a pressing need to further our understanding of human microglia and the influence of both pathology and disease-associated genes on microglial function. Because microglia play an increasing critical role in AD etiology, there is a need to improve our understanding of their function in both health and disease. Having established a robust method for producing large number microglial-like cells (Chapter 1), I aimed to study of fibrillary Aβ and soluble ex-vivo tau, BDTO, influence microglia physiological function and gene expression profiles.

MATERIALS AND METHODS

Chemical Reagents

All cell culture flasks, reagents, supplements, cytokines, and general reagents were purchased from Thermo Fisher Scientific, unless otherwise noted

Cell Culture

Maintenance and Culture of Human Pluripotent Stem Cells (hPSCs)

All stem cell work was performed with approval from UC Irvine Human Stem Cell Research Oversight (hSCRO) and IBC committees. The use of human fibroblast and PBMC samples for iPSC reprogramming and differentiation was approved by the University of California, Irvine Institutional Review Board (IRB Protocol #2013-9561) and informed consent was obtained from all subjects. Human iPSC cell lines ADRC 2 (Male), 4 (Male), 5 (Female), 12 (Male), 14 (Male), 20 (Female), 22 (Female), 76 (Male), 85 (Female), and 86 (Female) were generated by the UCI Alzheimer's Disease Research Center (ADRC) Induced Pluripotent Stem Cell Core using non-integrating Sendai virus (Cytotune) and are available to other researchers via http://stemcells.mind.uci.edu/. iPSCs were confirmed to be sterile and karyotypically normal via G-banding (WiCell.org). Pluripotency of all lines was confirmed via (http://pluritest.org) and further confirmed using the Human Pluripotent Stem Cell Functional Identification Kit (R&D Systems), per manufacturer's instructions.

iPSCs were maintained in 6-well plates (Corning) in feeder-free conditions using growth factor-reduced Matrigel (MTG, BD Bioscience) in complete TeSR-E8 medium (StemCell Technologies) in a humidified incubator (5% CO_2, 37^{o}C). iPSCs were fed fresh media daily and passaged every 7-8 days.

Differentiation of iPSCs to Hematopoietic Progenitor Cells (iHPCs)

Human iPSC-derived hematopoietic progenitors were generated using defined conditions with several modifications to previously published protocols (Kennedy et al., 2007; Sturgeon et al., 2014).

iHPC Differentiation Base Medium Formulation: IMDM (50%), F12 (50%), insulin (0.02 mg/ml), holo-transferrin (0.011 mg/ml), sodium selenite (13.4 µg/ml), ethanolamine (4 µg/ml)(can use ITSG-X, 2% v/v, Thermo Fisher Scientific), L-ascorbic acid 2-Phosphate magnesium (64 µg/ml; Sigma), monothioglycerol (400 µM), PVA (10 ng/ml; Sigma), Glutamax (1X), chemically-defined lipid concentrate (1X), non-essential amino acids (NEAA; 1X), Penicillin/Streptomycin (P/S;1%). Use 0.22 µm filter.

Day (-1): iPSCs were washed with room temperature 1X DPBS (minus Ca^{2+} and Mg^{2+}) once. Wash was aspirated to waste and TrypLE Select (1X; 37ºC; 1 ml per 6-well) and placed in incubator (5% CO_2, 37ºC). After 3-5 minutes, cell plate was placed in cell culture hood and the side of the plate was lightly tapped to dislodge loosely adherent iPSCs for 30 seconds. After lightly tapping the plate, 1 ml of room temperature 1X DPBS (minus Ca^{2+} and Mg^{2+}) was added to each 6 well plate. Cells were collected in to a 15-ml conical tube (Corning) using a 10-ml Stripette® (Corning). Cells were centrifuged at 200 x *g* for 5 minutes at room temperature. After centrifugation, supernatant was aspirated to waste and cells were suspended in E8 medium + Y-27632 ROCK Inhibitor (RI,10 µM; R&D Systems), and gently triturated to generate a single-cell suspension, counted, and cell density adjusted to seed at 5 x 10^5 cells/cm^2 in tissue-culture treated 6-well plates. Final volume was adjusted to 1.5 ml of E8+ RI. Cells were cultured for 24 hours under normoxic conditions (20% O_2, 37ºC).

Day (0): Cells were gently collected in to 50 ml conical tube (Corning) using 10-ml Stripette® and centrifuged at 300 x *g* for 6 minutes at room temperature (all media changes will require this step using these parameters.). Media was aspirated to waste, and media was changed to basal medium complete with FGF2 (50 ng/ml), BMP4 (50 ng/ml), Activin-A (12.5 ng/ml), RI (1 µm) and LiCl (2mM) at 2 ml per well in a 6-well plate, Cells were then placed in humidified tri-gas incubator under hypoxic cell culture conditions (5%O_2, 5%CO_2, 37ºC).

Day (2): Cells were quickly and gently collected in to 50 ml conical using 10 ml Stripette® and centrifuged. Supernatant was aspirated to waste and media was changed to pre-equilibrated (at 5%O_2, 5%CO_2, 37ºC for 1 hour) base media supplemented with FGF2 (50 ng/ml) and VEGF (50 ng/ml) and placed back in hypoxia incubator.

Day (4): Media was changed to 2 ml per well with basal media containing FGF2 (50 ng/ml), VEGF (50 ng/ml), TPO (50 ng/ml), SCF (10 ng/ml), IL-6 (50 ng/ml), and IL-3 (10 ng/ml) and placed at normoxia incubator.

Days (6 and 8): Cells were supplemented with 1ml per well of Day 4 medium.

Day (10): Cells were collected and prepped for FACS (see Method Details) and $CD43^+$ cells were isolated by FACS for iMGL differentiation. Additionally, iPSC-derived HPCs (Cellular Dynamics International) were identified as a commercial source of $CD43^+$ progenitors.

Differentiation of iHPCs to iMGLs

iMGL Differentiation Base Medium: Differentiation media consists a base media: phenol-free DMEM/F12 (1:1), insulin (0.2 mg/ml), holo-transferrin (0.011 mg/ml), sodium selenite (13.4 μg/ml) (can use ITS-G, 2%v/v,Thermo Fisher Scientific), B27 (2% v/v), N2 (0.5%, v/v), monothioglycerol (200 μM), Glutamax (1X), NEAA (1X), and additional insulin (5 μg/ml; Sigma). Use 0.22 μm filter.

Day (0; or day 10 from iPSC): Isolated $CD43^+$ iHPCs were washed using iMGL base differentiation medium and centrifuged at 300 x *g* for 6 minutes at room temperature. After centrifugation, supernatant was aspirated to waste and iHPCs were gently suspended in complete differentiation medium: M-CSF (25 ng/ml), IL-34 (100 ng/ml; Peprotech), and TGF□-1 (50 ng/ml; Militenyi) added fresh each time. Cell density was adjusted to seed at density of 1-2 $x10^5$ cells in 2 ml of complete medium per well in growth factor-reduced Matrigel-coated 6-well plates.

Every two days: Complete differentiation media was supplemented with 1 ml per well.

Day (12; or day 22 from iPSC), early iMGLs were collected (300x *g* for 6 mins at room temperature) and a 50% media change was performed.

Every two days: Complete differentiation media was supplemented with 1 ml per well.

After 25 days of microglial differentiation (35 days from iPSC), iMGLs were cultured in complete differentiation media supplemented with CD200 (100 ng/ml, Novoprotein) and CX3CL1 (100 ng/ml; Peprotech) for an additional three days before use in studies.

Generation of Microglia-like Cells from iHPCs

$CD43^+$ iHPCs were plated in Matrigel-coated 6-well plates (BD Biosciences) with serum-free complete differentiation media at a density of 1-2 $x10^5$ cells per well. Differentiation media consists a base media: phenol-free DMEM/F12 (1:1), insulin (0.2 mg/ml), holo-transferrin (0.011 mg/ml), sodium selenite (13.4 μg/ml), B27 (2% v/v), N2 (0.5%, v/v), monothioglycerol (200 μM), Glutamax (1X), NEAA (1X), and additional insulin (4 μg/ml; Sigma). Complete differentiation media includes M-CSF (25 ng/ml), IL-34 (100 ng/ml; Peprotech), and TGF□-1 (50 ng/ml; Militenyi) added just before feeding cells. Cells were supplemented with complete differentiation media every two days. At day 12, early iMGLs were collected (300x *g* for 5 mins at 25ºC) and a 50% media change was performed. After 25 days of microglial differentiation (35 days from iPSC), iMGLs were cultured in complete differentiation media supplemented with CD200 (100 ng/ml, Novoprotein) and CX3CL1 (100 ng/ml; Peprotech) for an additional three days before use in studies.

RNA-sequence library construction

Cells were harvested and washed three times with DPBS and stored in RNAlater, RNA preservation solution. RNA was extracted from all cell types using RNeasy Mini Kit (Qiagen) following manufacturer's guidelines. RNA integrity (RIN) was measured for all samples using the Bioanalzyer Agilent 2100 series. All sequencing libraries analyzed were generated from RNA samples measuring a RIN score ≥ 9. The Illumina TruSeq mRNA stranded protocol was used to obtain poly-A mRNA from all samples. 200 ng of isolated mRNA was used to construct RNA-seq libraries. Libraries were quantified and normalized using the Library Quantification Kit from Kapa Biosystems and sequenced as paired-end 100 bp reads on the Illumina HiSeq 2500 platform.

FACS and Flow Cytometer Analysis

iHPCs were collected using cold (4ºC) sterile filtered and degassed FACS buffer (1X DPBS, 2% BSA, and 0.05mM EDTA) spiked with human SCF (5 ng/ml). Cells were then filtered through 70 μm mesh to remove large clumps, washed with spiked FACS buffer (300 x *g* for 5 min 18ºC), then stained (1:200) using spiked FACS buffer on ice for 1 hour in the dark using the following antibodies: anti CD34-FITC clone 561, anti CD41-PE clone HiP8, anti CD43-APC

clone CD43-10G7, anti CD45-APC/Cy7 clone HI30 (Tonbo), anti CD235a-PE/Cy7 clone HI264, and ZombieViolet™ live/dead stain, all from Biolegend unless noted. After staining, iHPCs were washed once with spiked FACS buffer and suspended using spiked FACS buffer (500-700 µl) and sorted utilizing the BD FACSARIA Fusion (BD Biosceinces). Sorted cells were collected in cold basal iHPC differentiation medium spiked with SCF (10 ng/ml). Collected CD43+ iHPCs were thenplated for iMGL differentiation as mentioned above. iMGLs were suspended in FACS buffer and incubated with human Fc block (BD Bioscience) for 15 min at 4ºC. For detection of microglial surface markers, cells were stained with anti CD11b-FITC clone ICRF44, anti CD45-APC/Cy7 clone HI30 (Tonbo), anti CX3CR1-APC clone 2A9-1, anti CD115-PE clone 9-4D, and anti CD117-PerCP-Cy5.5 clone 104D2, ZombieViolet™ live/dead stain, all from Biolegend (San Diego, CA). Cells were sorted on a FACS Aria II, FACS Aria Fusion (BD Biosciences) and data analyzed with FlowJo software (FlowJo).

RNA Isolation and qPCR Analysis

Cells were stored in RNAlater stabilizing reagent and RNA was isolated using Qiagen RNeasy Mini Kit (Valencia, CA) following manufacturer's guidelines. qPCR analysis was performed using a ViiA™ 7 Real-Time PCR System and using Taqman qPCR primers. Analysis of AD-GWAS genes utilized a custom Taqman Low Density Array card using the primers described below.

iMGL Transplantation in Rag-5xfAD Mouse Brains

All animal procedures were performed in accordance with NIH and University of California guidelines approved IAUC protocols (IAUC #2011-3004). Rag5xfAD mice were generated in this lab and previously characterized (Marsh et al., 2016). Rag5xfAD mice display robust beta-amyloid pathology and allow for xenotransplantation of human cells. iMGLs were harvested at day 38 and suspended in injection buffer: 1X HBSS with M-CSF (10 ng/ml), IL-34 (50 ng/ml), and TGFβ-1 (25 ng/ml). iMGLs were delivered using stereotactic surgery as previously described (Blurton-Jones, et al, 2009). iMGLs were transplanted into the hippocampi of Rag-5xfADusing the following coordinates; AP: -2.06, ML: ± 1.75, DV: -1.95. After transplantation mice were killed and brains collected using previously established protocol. Briefly, mice were anesthetized using sodium-barbiturate and perfused through the left-ventricle with cold 1X HBSS

for 4 min. Perfused mice were decapitated and brain extracted and dropped-fixed in PFA (4% w/v) for 48 hours at 4ºC. Brains were then washed 3 times with PBS and sunk in sucrose (30% w/v) solution for 48 hours before coronal sectioning (40 μm) using a microtome (Leica). Free-floating sections were stored in PBS sodium azide (0.05%) solution at 4ºC until IHC was performed.

Human Adult Brain Tissue

Human adult brain tissue was provided by the UCI MIND Tissue Repository through request. Cognitively normal tissue was provided in sodium azide solution (0.05% in 1X PBS) at room temperature. Brain tissue was placed in sucrose solution (30% in 1X PBS) for 48 hours. After sinking, 40 μm thick sections were generated from tissue using a microtome and free-floating sections were stored in azide solution or processed for immunoflouresnce.

Immunocytochemistry and Immunohistochemistry

For ICC, cells were washed three times with DPBS (1X) and fixed with cold PFA (4% w/v) for 20 min at room temperature followed by three washes with PBS (1X). Cells were blocked with blocking solution (1X PBS, 5% goat or donkey serum, 0.2% Triton X-100) for 1 h at room temperature. ICC primary antibodies were added at respective dilutions (see below) in blocking solution and placed at 4ºC overnight. The next day, cells were washed 3 times with PBS for 5 min and stained with Alexa Fluor® conjugated secondary antibodies at 1:400 for 1 h at room temperature in the dark. After secondary staining, cells were washed 3 times with PBS and coverslipped with DAPI-counterstain mounting media (Fluoromount, southern Biotech). For mouse brain IHC, brains were collected, fixed, and processed as mentioned above. For AD mouse brain staining of amyloid plaques, floating sections were placed in 1X Amylo-Glo ® RTD™ (Biosensis) staining solution for 10 min at room temperature without shaking prior to block. After staining, sections were washed in PBS 3 times for 5 minutes each and briefly rinsed in MiliQ DI water before being placed back in to PBS followed by blocking. For human, Heat-mediated antigen retrieval was performed by using Citrate Buffer (10mM Citrate, 0.05% Tween 20, pH=6.0) at 97ºC for 20 min and then allowed to cool to room temperature. After antigen retrieval, sections were washed three times with PBS before proceeding with staining. uFree-floating sections were then blocked in blocking solution (1X PBS, 0.2% Triton X-100, and 10% goat serum) for 1 h at room temperature with gentle shaking. Primary antibodies were added to staining solution (1X PBS,

0.2% Triton X-100, and 1% goat serum) at appropriate dilutions (see below) and incubated overnight at 4ºC with slight shaking. The next day, sections were washed 3 times with PBS and stained with Alexa Fluor® conjugated secondary antibodies at 1:400 for 1 h at room temperature with slight shaking in the dark. After secondary staining, sections were washed in PBS 3 times for 5 min and mounted on glass slides. After mounting, slides were cover slipped with DAPI-counterstain mounting media (Fluoromount, southern Biotech). Primary antibodies:

mouse anti-β3Tubulin (1:500; Biolegend, 801201)

mouse anti-human Cytoplasm (SC121,1:100; Takara Bio Inc., Y40410),

mouse anti-human Nuclei (ku80, 1:100; Abcam, ab79220)

chicken anti-GFAP (1:500; Abcam, ab4674)

rabbit anti-Iba1 (1:500; Wako; 019-19741)

goat anti-Iba1 (1:100; Abcam ab5076) * recommend use with Alexa Fluor 488 or 555 secondary antibody only.

rabbit anti-Amyloid Fibrils (OC) (1:1,000, EMD Millipore, AB2286)

rabbit anti-Amyloid Oligomeric (A11) (1:1,000, EMD Millipore, AB9234)

mouse anti-Amyloid 1-16aa (6e10) (1:1,000, Biolegend, 803001)

Phagocytosis Assays

iMGLs were incubated with fAβ -555 or pHrodo-red BDTOs for 24 hours. The next day, cells were collected in FACS buffer, washed and prepped for flow cytometry staining. iMGls were incubated with mouse anti CD16/32 Fc-receptor block (2 mg/ml; BD Biosciences) for 15 minutes at 4ºC. Cells were then stained with anti CD45-APC clone HI30 (Tonbo Biosciences; San Diego, CA) at 1:200 in flow cytometer buffer. Samples were then analyzed using Amnis Imagestreamer®^{x} Mark II Imaging Flow Cytometer (Millipore). fAβ, and BDTO phagocytosis was analyzed using the IDEAS software onboard Internalization Wizard algorithm.

Fibrillar Aβ Preparation.

Fibrillar fluorescent amyloid-beta ($fA\beta_{1-42}$) was generated as described previously (Koenigsknecht-Talboo and Landreth, 2005). Fluorescently labeled Aβ peptide (Anaspec;

Fremont, CA) was first dissolved in NH_4OH (0.1%) to 1 mg/ml, then further diluted to 100 μg/ml using sterile endotoxin-free water, vortexed thoroughly, and incubated at 37ºC for 7 days. fAβ was thoroughly mixed prior to cell exposure.

BDTO Preparation

Brain-derived tau oligomers were purified by immunoprecipitation as described previously (Lasagna-Reeves et al., 2012). Tau oligomers were isolated by immunoprecipitation with the T22 antibody using PBS-soluble fractions of homogenates prepared from AD brain. These were then purified by fast protein liquid chromatography (FPLC) using PBS (pH 7.4). Additional analyses include Western blots to detect contamination with monomeric tau or large tau aggregates (tau-5, normally appear on top of the stacking gel) and using a mouse anti-IgG to identify non-specific bands. BDTOs were subsequently conjugated to pHrodo-red per manufacturer's protocol.

AD-GWAS qPCR Primers

The following validated and available Taqman primers were used: APOE Hs00171168_m1, CR1 Hs00559342_m1, CD33 Hs01076281_m1, ABCA7 Hs01105117_m1, TREM2 Hs00219132_m1, TREML2 Hs01077557_m1, TYROBP (DAP12) Hs00182426_m1, PICALM Hs00200318_m1, CLU Hs00156548_m1, MS4A6A Hs01556747_m1, BIN1 Hs00184913_m1, CD2AP Hs00961451_m1, CASS4 Hs00220503_m1, MEF2C Hs00231149_m1, DSG2 Hs00170071_m1, MS4A4A Hs01106863_m1, ZCWPW1 Hs00215881_m1, INPP5D Hs00183290_m1, and PTK2B Hs00169444_m1.

Quantification and Statistical Analysis

RNA-seq analysis

RNA-seq reads were mapped to the hg38 reference genome using STAR (Dobin et al., 2013) aligner and mapped to Gencode version 24 gene annotations using RSEM(Li and Dewey, 2011). Genes with expression (< 1 FPKM) across all samples were filtered from all subsequent analysis. Differential gene expression analysis was performed on TMM normalized counts with EdgeR (Robinson et al., 2010). Multiple biological replicates were used for all comparative analysis. A p-value ≤ 0.001 and a 2-fold change in expression were used in determining significant

differentially expressed genes for respective comparisons. PCA analysis was performed using the R package "rgl" and plotted using "plot3d". Clustering was performed using R "hclust2" and visualized using Java Tree View 3.0 (http://bonsai.hgc.jp/~mdehoon/software/cluster/software.htm). Differential gene analysis between groups was performed using the R package "limma" and significant genes (adjusted $p < 0.01$) were used for Gene ontology and pathway analysis. Gene ontology and pathway analysis was performed using Enrichr data base (http://amp.pharm.mssm.edu/Enrichr/) (Chen et al., 2013; Kuleshov et al., 2016).

Statistical Analysis

Statistical analysis was performed using Graphpad Prism 7 software. Comparisons involving more than two groups utilized one-way ANOVA followed by Tukey's *post hoc* test and corrected p-values for multiple comparisons were reported. Comparison's with more than two groups and comparing to a control or vehicle group utilized one-way ANOVA followed by Dunnett's *post hoc* test with corrected p-values for multiple comparisons reported. Two-Way ANOVA were followed by Sidak's multiple-comparison *post-hoc* test Comparisons of two groups utilized two-tailed Students t-test. All differences were considered significantly different when $p<0.05$. Statistical analysis for RNA-sequencing is detailed above and all further statistical analysis details are reported in the figure legends.

Data and Software Availability

Raw and normalized RNA-sequence data can be obtained at NCBI. The GEO Accession Super Series ID number for the data reported in this paper is GEO: GSE89189.

RESULTS

Utility of iMGLs to study Alzheimer's disease *in vitro*

Impaired microglia clearance of beta-amyloid (Aβ) is implicated in the pathophysiology of AD and strategies to enhance clearance of AD pathology are being actively pursued by biopharma. Therefore, we examined whether iMGLs can phagocytose Aβ or tau, two hallmark AD pathologies. Like primary microglia, iMGLs internalize fluorescently labeled fibrillar Aβ (**Figure**

2.1B). iMGLs also recognize and internalize pHrodo-labled brain–derived tau oligomers (BDTOs) (**Figure 2.1B**). Fluorescence emitted indicates trafficking of pHrodo-conjugated BDTOs to the acidic lysosomal compartment showing that iMGLs can actively ingest extracellular tau that may be released during neuronal cell death (Villegas-Llerena et al., 2015) and support recent findings that microglia may play a role in tau propagation in AD and other tauopathies (Asai et al., 2015). Together, these findings suggest that iMGLs could be utilized to identify compounds in high-throughput drug-screening assays that enhance Aβ degradation or block exosome-mediated tau release.

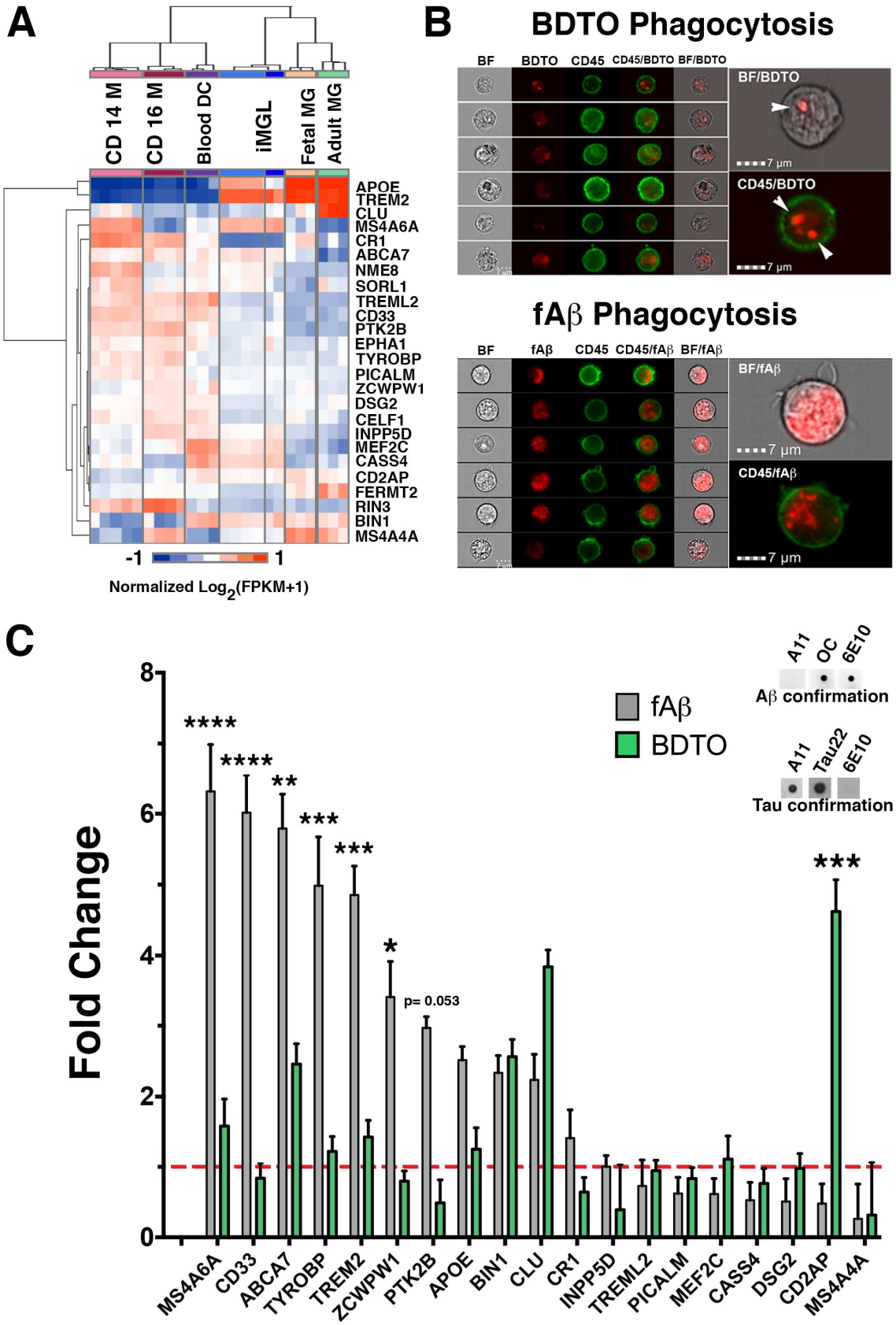
A
CD 14 M
CD 16 M
Blood DC
iMGL
Fetal MG
Adult MG
APOE
TREM2
CLU
MS4A6A
CR1
ABCA7
NME8
SORL1
TREML2
CD33
PTK2B
EPHA1
TYROBP
PICALM
ZCWPW1
DSG2
CELF1
INPP5D
MEF2C
CASS4
CD2AP
FERMT2
RIN3
BIN1
MS4A4A
-1
1
Normalized Log2(FPKM+1)
B
BDTO Phagocytosis
BF
BDTO
CD45
CD45/BDTO
BF/BDTO
7 µm
fAβ Phagocytosis
fAβ
CD45/fAβ
BF/fAβ
C
Fold Change
fAβ
BDTO
A11
OC
6E10
Aβ confirmation
Tau22
Tau confirmation
p= 0.053
MS4A6A
CD33
ABCA7
TYROBP
TREM2
ZCWPW1
PTK2B
APOE
BIN1
CLU
CR1
INPP5D
TREML2
PICALM
MEF2C
CASS4
DSG2
CD2AP
MS4A4A

Figure 2.1. Alzheimer Disease risk factor GWAS genes can be investigated using iMGLs and high throughput genomic and functional assays**.** (**A**). Heatmap of 25 immune genes with variants associated with *LOAD* reveals that major risk factors APOE and TREM2 are highly expressed in iMGLs, Adult MG, and Fetal MG. (**B**) iMGLs internalize fluorescent-labeled fAβ and pHrodo-dye BDTO. Representative images captured on Amnis Image StreamX Mark II. (**C**) iMGLs were exposed to unlabeled fAβ (5 μg-ml^{-1}) and BDTOs (5 μg/ml) for 24 h and mRNA expression of 19 GWAS genes was assessed via qPCR array. fAβ treatment elevated the expression of 10 genes above 2-fold compared to vehicle, including MS4A6A (6.3 fold), CD33 (6.1 fold), ABCA7 (5.8 fold), TYROBP (4.98) and TREM2 (4.85 fold). Whereas, BDTO exposure elevated the expression of 4 genes above two-fold compared to vehicle. Six genes were differentially expressed in fAβ compared to BDTO. Both fAβ and BDTO preparations were confirmed via dot-blot analysis with conformation structural specific antibodies for oligomers (A11), fibrils (OC) and non-structural-specific antibodies for human Aβ (6E10) and tau oligomers (Tau22). Target genes were normalized to GAPDH and compared to vehicle expression by ΔΔCt. Bars show expression fold mean ± SEM. Red hash bar is ΔΔCt = 1. Two-Way ANOVA, followed by Sidak's multiple-comparison *post-hoc* test, ***p<0.0001, **p<0.001, *p<0.05; n=6 wells/group. Data represented as mean ± SEM.

Microglia genes are implicated in late onset AD, yet how they modify disease risk remains largely unknown. Thus, iMGLs were utilized to begin investigating how these genes might influence microglia function and AD risk. Hierarchical clustering using just these 25 AD-GWAS genes also demonstrates that iMGLs resemble microglia and not peripheral myeloid cells (**Figure 2.1A**). In their investigated basal state, iMGLs and microglia express many AD-GWAS-related genes including those without murine orthologs i.e. CD33, MS4A4A, CR1. Thus, iMGLs can be used to study how altered expression of these genes influence microglia phenotype in a way that cannot be recapitulated in transgenic mice. Therefore , iMGLs were used to investigate the influence of fAβ or BDTOs on AD-GWAS gene expression in microglia (Villegas-Llerena et al., 2015). Following fAβ exposure, iMGLs increased expression of 10 genes (**Table 2.1**) including ABCA7 (5.79 ± 0.44), CD33 (6.02 ± 0.41), TREM2 (4.86 ± 0.50, and APOE (2.52 ± 0.19), genes implicated in Aβ clearance/degradation. BDTOs increased expression of 4 genes including CD2AP (4.62 ± 0.45), previously implicated in tau-mediated toxicity (Shulman et al., 2014). In addition, 6 genes were differentially elevated in fAβ compared to BDTOs (**Table 2.1**). Interestingly, CD33, TYROBP, and PICALM, genes more enriched in other myeloid cells at baseline, were upregulated by fAβ and BDTOs suggesting that proteinopathies may alter microglia phenotype to resemble invading peripheral myeloid cells (Chan et al., 2007; Prinz et al., 2011;

Stalder et al., 2005). In addition to AD GWAS genes, iMGLs express other CNS disease-related genes including APP, PSEN1/2, HTT, GRN, TARDBP, LRRK2, C9orf72, SOD1, VCP, and FUS and therefore, can likely be used to study other neurological diseases such as ALS, HD, FTD, and DLB in which microglia may play a prominent role (Bachstetter et al., 2015; Crotti et al., 2014; Lui et al., 2016; O'Rourke et al., 2016)(**Figure 2.2C**).

iMGL homeostasis and response to AD pathology is modulated by TGFβ-1, CX3CL1 and CD200

Neurons, astrocytes, and endothelial cells in the brain interact with microglia to influence gene expression and function. Our differentiation protocol attempted to recapitulate CNS cues present in the brain by including signals derived from these other cell types including CX3CL1, CD200, and TGFβ. Whole transcriptome RNA-seq analysis confirmed the importance of these factors for establishing microglia *in vitro* (**Figures 2.2**). TGFβ, a glia-derived cytokine, is needed for murine microglia development *in vivo* and in maintaining the microglial-specific transcriptome signature (Abutbul et al., 2012; Butovsky et al., 2014; Schilling et al., 2001). Differential gene expression analysis confirmed TGFβ's role in maintaining the human microglia transcriptome signature; 1262 genes were differentially expressed in iMGLs with TGFβ, whereas 1517 genes were differentially expressed in iMGLs after TGFβ removal (24 hours). Many of the differentially expressed genes are identified as core microglial signature targets including P2RY12, TGFβR1, and CD33, and transcription factors EGR1 and ETV5, and APOE (**Figure 2.2A-C**). Examination of gene ontology highlight neurodegenerative disease pathways including AD, Parkinson's, and Huntington's diseases that are TGFβ dependent (**Figure 2.2D**). Furthermore, removal of TGFβ led to significant changes in many of the human microglia homeostatic targets also identified as AD GWAS loci genes including TREM2, APOE, ABCA7, SPI1 (CELF1 locus), PILRA (ZCWPW1 locus), and the HLA-DR and MS4A gene clusters (Karch et al., 2016), suggesting many identified AD GWAS genes function in the maintenance of microglia homeostasis (**Figure 2.2E**) and underscoring the utility of iMGLs to interrogate AD GWAS gene function.

CX3CL1 and CD200 are both neuronal- and endothelial-derived cues that can further educate iMGLs toward an endogenous microglia phenotype (reviewed in (Kierdorf and Prinz, 2013). To test this hypothesis, we examined how inclusion or exclusion of these factors modulates iMGL phenotype. The addition of CD200 and CX3CL1 to iMGLs increased the expression of select genes like COMT (Bennett et al., 2016)(**Figure 2.2B**), CD52, a cell surface receptor that binds Siglec-10 and interacts with DAP12 as part of the microglia sensome (Hickman et al., 2013) and HLADRB5, a member of the MHC II complex implicated in AD, while maintaining similar expression levels of core-microglial genes (e.g. P2RY12, TYROBP, OLFML3) and AD-risk genes (**Figure 2.3A**).

Table 2.1. QPCR results of iMGLs stimulated with fAβ or BDTO.

Treatments[1]						
fAβ		**BDTO**		**fAβ vs. BDTO**		
GENES	**Fold Change (over vehicle)**	**Genes**	**Fold Change (over vehicle)**	**Genes**	**Fold difference**	**p-value**
	mean ± SE		**mean ± SE**		**mean**	
MS4A6A	6.32 ± 0.32	**CD2AP**	4.62 ± 0.45	**MS4A6A**	4.731	< 0.0001
CD33	6.02 ± 0.41	**CLU**	3.84 ± 0.67	**CD33**	5.178	< 0.0001
ABCA7	5.79 ± 0.44	**BIN1**	2.56 ± 0.66	**ABCA7**	3.333	0.0014
TYROBP	4.99 ± 0.31	**ABCA7**	2.46 ± 0.70	**TYROBP**	3.756	0.0002
TREM2	4.86 ± 0.50			**TREM2**	3.426	0.0009
ZCWPW1	3.41 ± 0.42			**ZCWPW1**	2.610	0.0323
PTK2B	2.97 ± 0.16			**PTK2B**	2.483	0.0525
APOE	2.52 ± 0.19					
BIN1	2.34 ± 0.69			**CD2AP**	-4.144	< 0.0001
CLU	2.24 ± 0. 78					

[1]Treatments: fAβ (5 μg/ml) or BDTO (5 μg/ml) 24 h.

Table 2.1. **Related to Figure 2.1**. QPCR results of iMGLs stimulated with fAβ or BDTO. Results represent genes with fold change greater than 2. Results presented as mean ± standard error. n=6 per group. Two-way ANOVA followed by Sidak's *post-hoc* test. Adjusted *p*-values for multiple comparisons. * p<0.05, **p<0.001, ***p<0.0001**.**

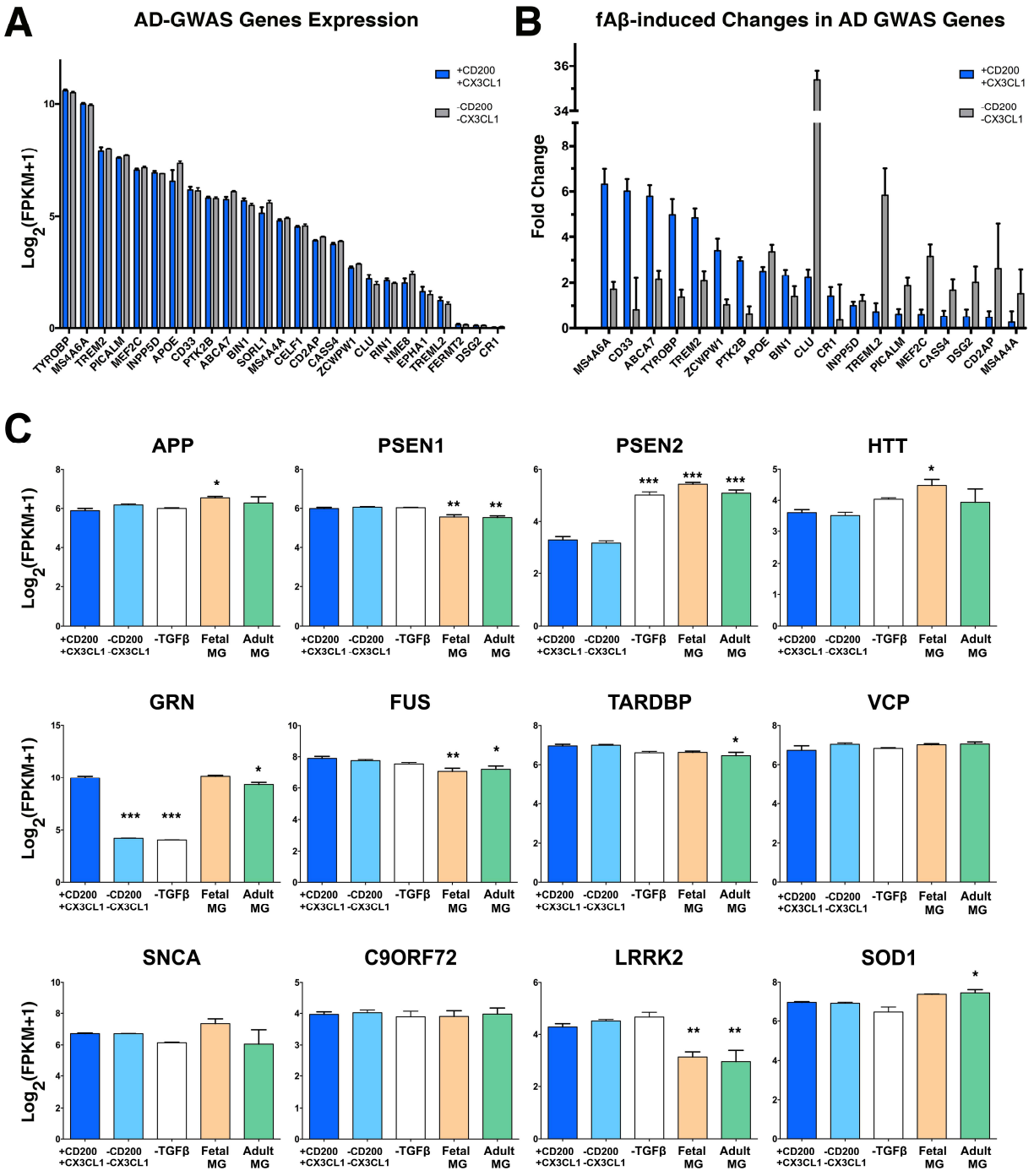
A
AD-GWAS Genes Expression
Log2(FPKM+1)
+CD200 +CX3CL1
-CD200 -CX3CL1
TYROBP MS4A6A TREM2 PICALM MEF2C INPP5D APOE CD33 PTK2B ABCA7 BIN1 SORL1 MS4A4A CELF1 CD2AP CASS4 ZCWPW1 CLU RIN1 NME8 EPHA1 TREML2 FERMT2 DSG2 CR1
B
fAβ-induced Changes in AD GWAS Genes
Fold Change
+CD200 +CX3CL1
-CD200 -CX3CL1
MS4A6A CD33 ABCA7 TYROBP TREM2 ZCWPW1 PTK2B APOE BIN1 CLU CR1 INPP5D TREML2 PICALM MEF2C CASS4 DSG2 CD2AP MS4A4A
C
APP
PSEN1
PSEN2
HTT
GRN
FUS
TARDBP
VCP
SNCA
C9ORF72
LRRK2
SOD1
Log2(FPKM+1)
+CD200 +CX3CL1
-CD200 -CX3CL1
-TGFβ
Fetal MG
Adult MG

Figure 2.2. Microglia AD-GWAS and other CNS-disease related genes can be studied using iMGLs. (**A-B**) iMGL AD-related GWAS genes respond to fAβ differentially if primed with or without CD200 and CX3CL1. iMGL exposure to CNS factors, CD200 and CX3CL1, "primes" their response to fAβ by increasing expression of genes with functions implicated to modulate microglia inflammation and function in AD, like CD33, ABCA7, TYROBP, and TREM2. Stimulation with fAβ of iMGLs not exposed to CD200 or CX3CL1 results in increase expression of AD GWAS-related genes CLU and APOE, genes involved in response to misfolded proteins as well as survival and homeostasis. (**C**) Major neurodegenerative related genes, APP (AD), SCNA (PD) and HTT (HD), are expressed in iMGLs and primary microglia. iMGLs also express genes linked to Amylotrophic Lateral Sclerosis (ALS), Frontal-temporal Dementia (FTD), and Dementia with Lewy Bodies (DLB) and support previous studies implicating microglia dysfunction**.** Bar graphs of genes implicated in neurodegenerative diseases that are detected in iMGL similarly to Fetal and Adult MG, and expressed as Log_2 (FPKM +1) and presented as mean ± SEM. Like isolated human primary microglia, iMGLs express Valosin Containing Protein (VCP), FUS binding protein (FUS), proganulin (GRN), TDP-43 (TARDBP), LRRK2, and Superoxide Dismutase (SOD). Recent literature implicates microglia dysfunction related to mutations or loss of function of these genes playing a role in the pathogenesis of ALS (SOD1, TARDBP, FUS), FTD (VCP, GRN, TARDBP), PD (LRRK2, SNCA), and DLB (SNCA), suggesting the utility of iMGLs in studying the underlying mechanism of these genes in these neurological diseases. Statistics reflect one-way ANOVA followed by Turkey's multiple-comparison *post-hoc* test. * $p<0.05$, ** $p<0.001$, *** $p<0.0001$.

Importantly, we found that CD200 and CX3CL1 modulated iMGL response to CNS stimuli, such as fAβ. In the absence of CD200 and CX3CL1, fAβ stimulated the expression of AD-GWAS genes implicated in interacting with misfolded folded protein, surface receptors, or anti-apoptotic events such as CLU (APOJ) (Yeh et al., 2016). Whereas cells exposed to these two factors responded differentially to fAβ, increasing expression of genes involved in neuronal cell surface motif recognition, or phagocytosis of CNS substrates, including MS4A genes, TREM2, TYROBP, CD33, and ABCA7 (Bradshaw et al., 2013; Fu et al., 2016; Greer et al., 2016)(**Figure 2.3B**). These studies further support the notion that CD200-CD200R1 and/or CX3CL1-CX3CR1 axis can prime microglia to respond to neurodegenerative conditions (Prinz and Priller, 2014). Thus, exposure to soluble CNS factors, like CD200 and CX3CL1, may allow for access to microglial-specific transcriptional regulator elements (enhancers and promoters) (Gosselin et al., 2014; Lavin et al., 2014), although future studies are required to fully translate these observations.

iMGLs migrate and respond to Aβ in AD transgenic mice

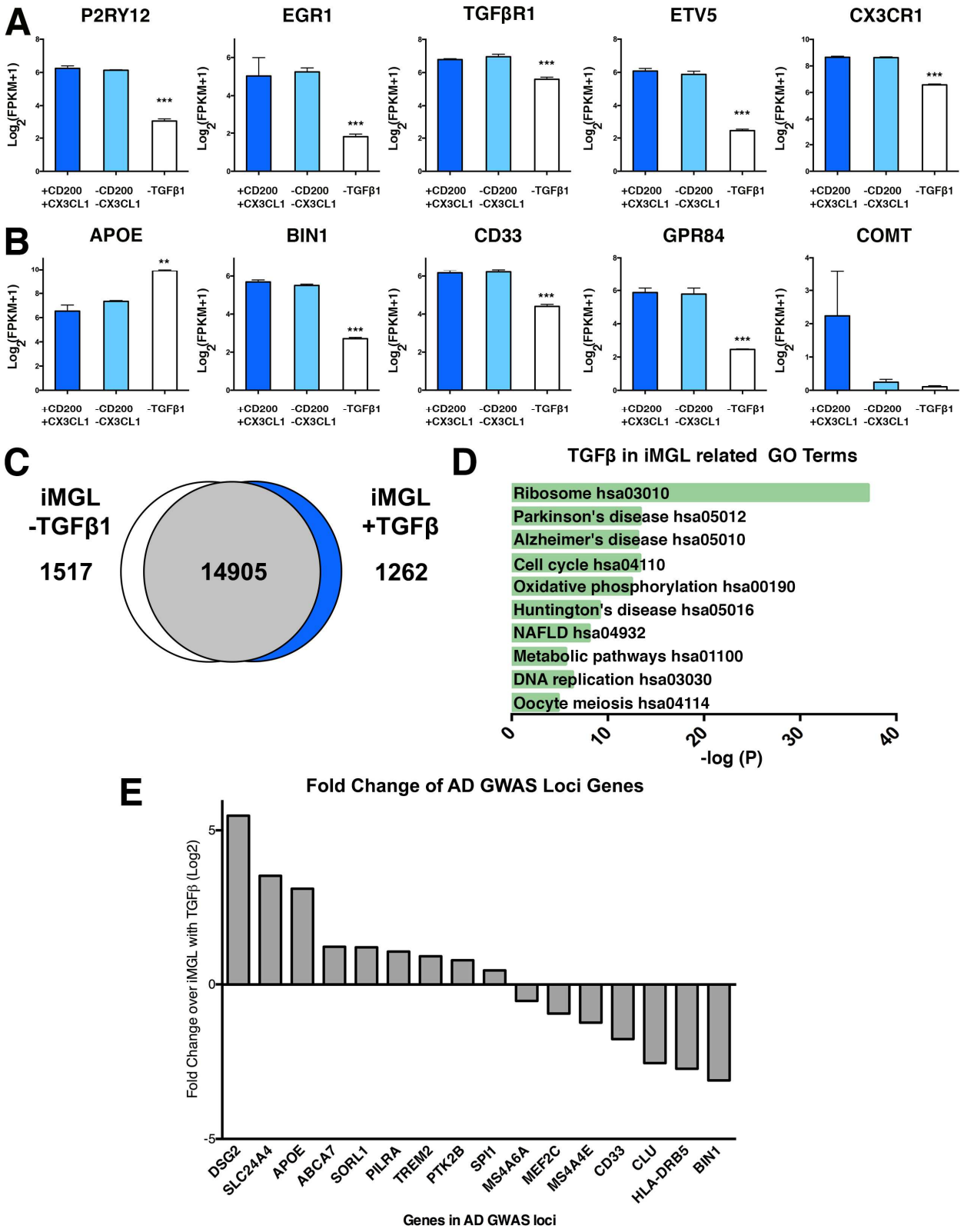

iMGLs were transplanted into the hippocampi of xenotransplantation-compatible AD mice, previously generated and characterized in our lab (Marsh et al., 2016), to examine how

iMGLs interact with AD neuropathology *in vivo* (**Figures 2.4**). Transplanted iMGLs engraft and migrate along white matter tracts, similar to microglia in development (**Figure 2.4A**). In many instances, iMGLs migrated and extended processes towards Aβ plaques to begin walling them off (**Figure 2.4 E, F**) Several iMGLs also began to phagocytose fibrillar Aβ (**Figures 2.4 D-H**).

Figure 2.3. TGFβ-1, CX3CL1, CD200 and their impact on key microglial genes are associated with modulating neuronal function and environment**.** (**A-B**) TGFβ1 maintains core microglial genes. Withdrawal of TGFβ1 for 24 h (white bars) strongly influences microglial transcriptome. In agreement with mouse studies *in vivo* (Butovsky, et al, 2014), TGFβ removal reduces expression of key microglia genes including surface receptors P2RY12, TGFβR1, and CX3CR1, while also reducing expression of microglia transcription factors EGR1 and ETV5. AD-associated pathway genes such as BIN1, CD33, and APOE are also influenced by the lack of TGFβ. Removal of CX3CL1 and CD200, does not change core microglia identity, but impacts state by influencing homeostatic gene expression such as, COMT, and APOE (*B*). (**C**) Differential gene expression analysis reveals that presence of TGFβ increases expression of 1262 genes in iMGLs, while lack of TGFβ reduces expression of 1517 genes, further supporting previous work highlighting the role of TGFB in microglia development, gene signature, and function. (**D**) KEGG pathway analysis highlights that microglial-core genes, elevated with TGFβ, modulate pathways in CNS disease including Alzheimer's, Parkinson's, and Huntington's disease. Statistics reflect one-way ANOVA followed by Dunnett's multiple-comparison post-*hoc* test. * p<0.05, **p<0.001, ***p<0.0001.

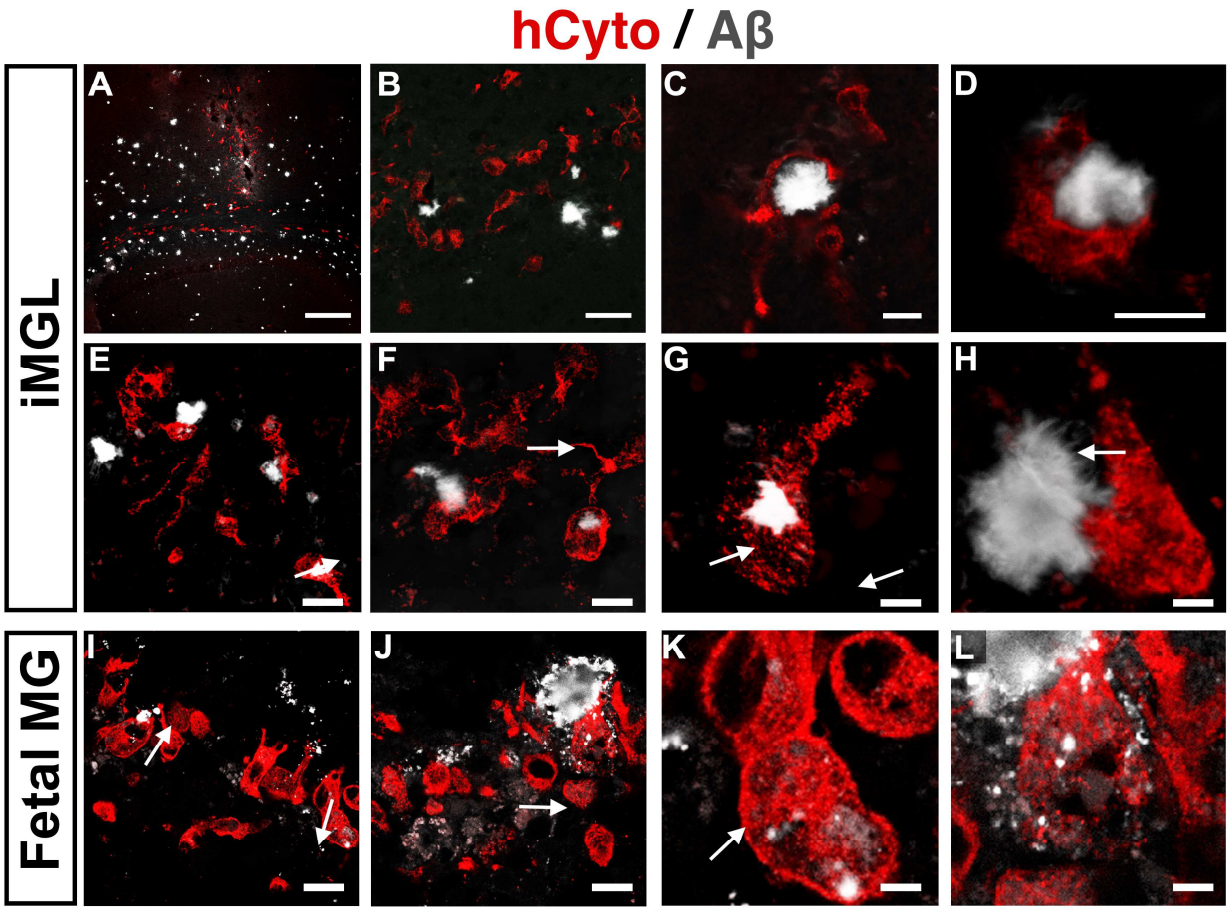

Figure 2.4 iPSC-derived microglial cells engraft and phagocytose Aβ like human fetal microglia**.** Human iMGLs and fetal microglia (hCyto, red) were transplanted into immune deficient AD mouse model, Rag5xfAD, (Marsh et al., 2016), and respond to beta-amyloid plaques. Transplanted iMGLs extend projections and migrate to plaques. iMGLs fully encompass amyloid plaques (**C**) and begin to phagocytose amyloid (**D.**) (**I-L**). Fetal microglia are observed surrounding plaques (**C**), and phagocytosing Aβ. Scale bars (B) = 30 μm, (C,D) = 10 μm, (**A**) = 300 μm. n=3 animals per study. Scale bars (I, J, E, F) = 20 μm, (G, H, K, L) 5 μm.

Similarly, human fetal microglia migrated towards Aβ, extended processes, and phagocytosed Aβ when transplanted in the same AD transgenic model (**Figure 2.4 I-L**).

DISCUSSION

The robust generation of human iPSC-microglia has allowed for the opportunity to begin investigating how microglia physiology is impacted in response the AD brain environment. As discussed in Chapter 1, our reproducible protocol yields large numbers of normal iMGLs, which can be used to study how cytokines and toxic proteins, Aβ and Tau aggregates, impact microglial gene expression and function. Since the discovery of SNPs in immune genes as AD-risk factors, microglia have been further highlighted in human neurological health and disease. Several of these AD-GWAS genes, including CD33 and CR1, lack functionally-similar murine orthologs, making iMGLs the appropriate model for studying the function of these and other human-only genes.

Here, we utilized iMGLs to investigate changes in mRNA expression of AD-GWAS genes. By RNA-sequencing and heatmap analyses, we confirmed that iMGL AD-GWAS transcriptome profile was highly similar to primary microglia, again showing that iMGLs can serve as surrogates for primary microglia. By qPCR we found that Aβ fibrils upregulated (> 2-fold) the expression of 10 genes, with MS4A6A gene expression increased the greatest (>6-fold). While the role of the MS4A gene cluster in microglia function and AD risk is still unknown, our data suggests a MS4a genes playing a potential role in modulating Aβ interactions. APOE, TREM2, CD33, and APOJ, genes previously implicated in modulating Aβ phagocytosis and clearance, as well as microglial survival (Bradshaw et al., 2013; Yeh et al., 2016) were also upregulated by beta-amyloid. Interestingly, the functions of APOJ, APOE and TREM2 have been shown to be shared, including binding to Aβ and mediating cell survival signals in immune cells (Bates et al., 2009; Hammad et al., 1997; Kontargiris et al., 2004; Merino-Zamorano et al., 2016; Poliani et al., 2015; Theendakara

et al., 2016; Trougakos et al., 2009; Wang et al., 2015b). Furthermore, APOE and J have been shown to be TREM2 ligands, suggesting a common mechanism in which these three risk-associated genes can facilitate Aβ uptake by microglia.(Bailey et al., 2015; Yeh et al., 2016).

Using the same AD-GWAS qPCR assay, we also investigated how tau oligomers, BDTOs, influenced iMGL gene expression. BDTOs increased the expression of 5 genes (>2 fold) in iMGLs after 24 hours. Again, MS4a6a expression was increased (>2 fold), as well as APOJ and BIN1. BDTOs exhibited their greatest effects on CD2AP, which in the dendrites of neurons has been shown to cooperate with BIN1 in the endocytic recycling of surface proteins such as APP and BACE1. The proper recycling of APP and BACE prevents their physical interaction in the cell membrane and thus, reduce APP processing to Aβ, suggesting that loss-of-function SNPs found in CD2AP and BIN can lead to increase Aβ production (Ubelmann et al., 2017). However, BIN1 protein levels have been previously reported to correlate stronger with neurofibrillary tangles (NFTs; hyper-phosphorylated tau) (Holler et al., 2014) thus, suggesting conflicting results or implicating a diverse role of BIN1 possible by indirectly modifying Aβ production or directly misprocessing tau. While both studies focused on neurons, the expression of CD2AP and BIN1 in microglia may suggest a role of dysfunctional CD2AP/BIN1 related endocytic and exocytic pathways involved in tauopathies. As an example, microglia have recently been implicated to be involved in the propagation of tau via secreted exosomes, again suggesting a strong role of endocytic genes, like PICALM, CD2AP, and BIN1, in microglia-mediated modulation of AD pathology (Asai et al., 2015).

While fAβ and BDTOs elevated the expression of myeloid/microglia-enriched AD-GWAS genes after 24 hours, other microglia genes involved in the modulation of inflammation or pathology were not studied. Whole-transcriptome studies would greatly expand upon our existing qPCR data and would allow for the discovery of affected microglial biological pathways. Additionally, exposure to Aβ, BDTOs, or Aβ and BDTO for longer periods of time could better model chronic inflammation, a one major characteristic of AD disease-progression observed in humans. Finally, there is growing evidence that diverse multimeric Aβ species exist early in, at the onset of, and late in AD, and these species can differentially influence microglia gene expression and function through microglia PRRs (Hatami et al., 2017; Kreutzer et al., 2017; Lesne et al., 2006). Similar to the reports of diverse Aβ species existing *in vivo*, a recent study has identified

18 new prion tau strains generated from a monoclonal cell line that stably expresses repeat domains in one species of pathological tau, 2N4R. Inoculation of PS19 (Tau P301S) transgenic mice with these 18 prion tau strains produced diverse pathological tau species that were expressed in different patterns in the hippocampi thus, accounting for the diversity of tauopathies found in humans (Kaufman et al., 2016).

Microglia respond to toxic proteins in the environment, yet they do so under varying and dynamic 'states', which are dictated by the presence or lack of apoptotic or necrotic cells, foreign or endogenous debris, and pro- and anti-inflammatory cytokines. To this end, we investigated how CNS-derived factors, TGFβ1, CD200, CX3CL1, influence microglia transcriptome. CNS-derived ligands, such as CD200 and CX3CL1, have been shown to influence microglia function and their effects are usually uncovered after microglial stimulation or environmental challenge (*reviewed in*(Kierdorf and Prinz, 2013). While iMGL core microglial transcriptome signature was not impacted by the lack of CD200 and CX3CL1 exposure, we found that CD200 and CX3CL1 were important CNS cues that modified iMGL response to fAβ. While fAβ increased the expression of 10 genes in iMGLs pre-exposed to CD200 and CX3CL1, the lack of these factors followed by fAβ exposure increased (>2 fold) the expression of 7 genes, including APOE, APOJ, and TREM2, genes that were also increased in iMGLs exposed to CD200 and CX3CL1. Interestingly, increased APOE, APOJ, and TREM2 combined with reduced expression of CD33 in iMGLs not exposed to CD200 and CX3CL1 may suggest that these iMGLs are still primed for phagocytosis but potentially coupled with inflammatory cytokine secretion (Bradshaw et al., 2013; Chan et al., 2015; Griciuc et al., 2013; Lajaunias et al., 2005). As a corollary, our findings that iMGLs exposed to CNS ligands followed by Aβ stimulate leads to increased expression phagocytic related genes (e.g. TREM2, APOJ, etc.) as well as CD33, and therefore suggest that CNS ligands like CD200 and CX3CL1 may stimulate phagocytosis with reduced or repressed inflammatory cytokine secretion. However, this hypothesis has yet to be tested fully using direct comparison studies that include potential reversal-attempt studies (i.e. repeat stimulation of non-exposed cells newly exposed to CD200 and CX3CL1).

These data implicate these factors play roles in antagonizing cell surface signals, such as ITAM vs ITIM phosphorylation events and/or modulating promoter/enhancer regions that enables appropriate responses to stimuli, as previously observed in macrophages (Gosselin et al., 2014;

Lavin et al., 2014)(further reviewed in (Glass and Natoli, 2016). Lastly, a TGFβ-dependent homeostatic microglia signature was identified that paralleled murine studies and highlight that AD GWAS genes function in microglia homeostasis. Withdrawal of TGFβ1 after 24 hours dramatically altered the microglial-genes expression in iMGLs. Differentially gene and gene ontology analyses showed that many microglial genes maintained by TGFβ1 treatment have been implicated in playing a role in many neurological disease, such as Huntington's, Alzheimer's and Parkinson's disease. These findings are in in agreement with previous studies showing that microglia require TGFβ1 to maintain homeostasis in the CNS(Abutbul et al., 2012; Butovsky et al., 2014; De Simone et al., 2010; Moore et al., 2015; Town et al., 2008). Taken together, our studies emphasize the importance of microglia in AD risk and the utility of iMGLs to interrogate genotype-phenotype relationships of recent AD GWAS single nucleotide polymorphisms.

Finally, we show again that iMGLs can populate an immune deficient mouse brain capable of human cell engraftment. Interestingly, iMGLs transplanted in the hippocampi of AD mice utilize white-tract pathways to move medial-laterally in the hippocampus. Not only do iMGLs engraft in Rag-5xfAD mice, but are observed to migrate towards Aβ. iMGLs also are observed to encircle plaques and compacting Aβ similar to microglia observed in transgenic mice and human brain tissue. Like fetal microglia transplanted in the brains of Rag-5xfAD mice, iMGLs were amoeboid and were also observed internalizing beta-amyloid. iMGL integration and interaction with pathology in transgenic mice may prove to be a useable platform for studying how microglial genes function in a complete brain environment. For example, our lab has begun to generate iMGLs from human patient lines harboring TREM2 SNPs with associated AD risk, such as R47H. R47H iMGL phenotype and interaction with beta-amyloid can be studied using Rag-5xfAD mice in similar fashion to previous studies that have suggested that TREM2 plays a role in the compaction of Aβ plaques (Yuan et al., 2016). Novel transplantation experiments with patient lines, such as R47H TREM2 lines, include live-imaging using 2-photon microscopy and isolation of iMGLs from transgenic mouse brains for subsequent whole transcriptome analysis. Thus, iMGL transplanted in xenotransplantation compatible transgenic mouse models create a new platform in which human microglial gene function can be investigated in a complete CNS environment. Finally, iMGLs can be used to generate the first humanized/chimeric transgenic mouse brain that can be utilized to study human microglia in development and disease. The remarkable similarity

of iMGLs to microglia *in vitro* and *in vivo* highlights their profound utility in studying innate immunity in the CNS.

DISSERTATION CONCLUDING REMARKS

Alzheimer disease (AD) is the leading cause of age-related dementia that impairs memory and causes cognitive and psychiatric deficits. AD afflicts over 35 million people worldwide, including 5.3 million in the USA alone. By 2050, the incidence of AD in the USA is projected to almost quadruple and will cost an estimated $1.1 trillion (Alzheimer's, 2016). Although the median survival for those diagnosed with AD is between 5-10 years, AD patients may live up to 20 years after the initial diagnosis, placing a tremendous burden on caregivers and their families (Brookmeyer et al., 2002; Helzner et al., 2008). AD remains a clinical, social, and economic liability for our society with no approved therapies to halt the underlying disease process. While AD has been known to the field of medicine for over 100 years, effective AD therapies have remained elusive in part because of the complex nature of AD neuropathology.

AD is characterized by the accumulation of β-amyloid (Aβ) and neurofibrillary tangles (NFTs), and widespread neuronal and synaptic loss. The identification of genes that cause familial AD has increased our understanding of APP biology and provided support for the Amyloid Cascade Hypothesis, which posits that amyloid is the initiating event that triggers downstream events (Bates et al., 2009). Therapies that decrease Aβ by targeting the enzymes responsible for APP proteolysis and Aβ production have entered clinical trials and failed to demonstrate efficacy, possibly due to off-target effects or poor experimental design due to understudied components of AD, like immunity and inflammation. Despite the early promise of Aβ-based immunotherapy, the scientific community must continue in the pursuit of new therapies. There is a great need for viable therapeutics if we are to alleviate the tremendous burden that AD will have on our society and our healthcare system in the near future. The development of novel targets must be grounded in, multi-dimensional fundamental scientific discovery that will increase our understanding of the molecular pathways of AD pathology and as history has demonstrated, is usually the best course if we are to find a cure. Therefore, elucidating the specific molecular mechanisms underlying AD is of great importance.

Recently, GWA studies in AD patients identified many genes implicated in the most prevalent form of AD, late-onset sporadic AD. These new studies igniting a new wave of interest in AD biologist looking to understand how new risk factors, like p.R47H TREM2, contribute to

the either the establishment or progression of AD. TREM2 was of great interest for a few reasons. TREM2 SNP conferred a 2-4 fold increased risk in developing AD, the first significant risk factor associated to AD besides APOE. The SNP associated with risk is encoded in exon2 of all isoforms reported of TREM2. TREM2 is known to be exposed in myeloid cells, which in the brain is microglia. TREM2 in microglia had been shown to increase phagocytosis. The associated neurological disease, Nasu-Hakola Disease, is caused by loss of function of TREM2 or its adaptor protein, TYROBP (Guerreiro et al., 2013; Jonsson et al., 2013). Since the report of TREM2, other innate-immune related genes were subsequently reported (Cruchaga et al., 2013; Karch et al., 2016; Seshadri et al., 2010; Villegas-Llerena et al., 2015).

The role of these genes and how they modify AD risk remain unknown, but many are expressed by microglia (Karch et al., 2016; Villegas-Llerena et al., 2015). Microglia are the innate immune cells of the CNS and play important roles in synaptic plasticity, neurogenesis, and homeostatic functions in immune surveillance. Because many of the identified AD risk genes lack murine homologs, human microglia must be used to investigate their role in AD. Studying human microglia in health or in neurological diseases is challenging because of the rarity and difficulty in acquiring primary cells from human fetal or adult CNS tissue. To date, most human microglia-related studies utilized fetal tissue from elective abortions or adult tissue from epileptic patients. These sources of glia are inconsistent; they vary in age, maturation, and disease-phenotype. For example, microgliosis is a recognized component of epilepsy (Blanc et al., 2011), yet the predominant source of adult microglia is from patients undergoing epileptic foci resection. As highlighted recently, microglia appear to be highly reactive to neuronal brain activity, further highlighting the limited use of primary adult microglia derived from epileptic tissue (Devinsky et al., 2013; Iaccarino et al., 2016; Turrin and Rivest, 2004; Vezzani et al., 2011)..

Prior to the start of my dissertation studies, only one protocol existed for generating microglia-like cells from mouse embryonic stem cells, ESdMs. Initially, ESdMs showed promise in that they were positive for microglial genes like CX3CR1, CD11b, IBA1, and TREM2 (Beutner et al., 2010; Napoli et al., 2009). Unfortunately, these genes are also expressed by other myeloid cells, like macrophages and dendritic cells, and cannot be used to separate microglia from other myeloid cells like CNS or peripheral derived macrophages. In addition, other mouse microglial markers, like Fcrls and F4.80 (EMR1), are not expressed by human microglia thus, liming the tool-

box available for isolating human microglia from macrophages. More worrisome is that gene-expression analysis of ESdMs revealed that they resemble immortalized microglial cell lines like BV2s and RAW 264.7 macrophages. Furthermore, ESdMs did not resemble cultured or *ex vivo* microglia (Butovsky et al., 2014) by transcriptome analyses. The challenges in generating microglia from human pluripotent stem cells are due to their unique origin during embryonic development. Microglia are derived from primitive yolk sac erythromyeloid (EMP) cells generated during primitive hematopoiesis (Chan et al., 2007; Ginhoux et al., 2013; Hoeffel et al., 2015; Kierdorf et al., 2013; Schulz et al., 2012). EMPs further develop to CD45+/CX3CR1- (A1) and migrate in to the developing neural tube as CD45+/CX3CR1+ (A2) progenitors (Kierdorf et al., 2013)(also reviewed in (Prinz and Priller, 2014). In the brain, microglial progenitors develop into ramified cells with high expression of CX3CR1, P2RY12, GPR34, and TMEM119 (Butovsky et al., 2014; De Simone et al., 2010; Haynes et al., 2006; Michaelis et al., 2015; Mildner et al., 2017; Moore et al., 2015) (Bennett et al., 2016; Cardona et al., 2006; Limatola and Ransohoff, 2014).

Recently, murine knockout models have identified key cytokines, cell receptors, and transcription factors required for the development and survival of microglia *in vivo*. Microglial cytokine factors include interleukin-34 (IL-34) and transforming growth factor beta-1 (TGF-β1) (Greter et al., 2012; Wang et al., 2012; Yamasaki et al., 2014). Many established protocols have outlined hematopoietic progenitor cell production from hPSCs and are likely candidates for microglia generation (Choi et al., 2011; Kennedy et al., 2007; Sturgeon et al., 2014; Uenishi et al., 2014; Vodyanik et al., 2005). Therefore, there existed a potential for guiding iHPCs to generate human microglia *in vitro* by providing an environment that mimics the cues that iHPCs are normally exposed during development. Furthermore, microglia precursors continue to be exposed to microglia-differentiation factors duringmigration into the developing neural tube.

The main goal of my dissertation studies was to generate human microglia from iPSCs to study human microglia function in AD. To accomplish this, I synthesized from the literature a two-step protocol for generating microglia under fully defined conditions. From microglia gene ontogeny studies, it was clear that the bottle-neck for generating microglia was the generation of a primitive hematopoietic progenitors (HPCs) that was faithful to microglia development origins. HPCs that were $CD43^{+}/235a^{+}/41a^{+}$ were the candidate populations as these makers have been associated to be exclusive in primitive HPCs (de Jong and Zon, 2005; Ginhoux et al., 2010;

Kennedy et al., 2012; Kennedy et al., 2007; Kierdorf et al., 2013; Sturgeon et al., 2014). The use of fully-defined conditions, serum-free and cytokine-based medium, was necessary to control for all experimental variants that would be used to generate a primitive HPC form iPSCs. I accomplished generating a protocol that produced high yields of primitive iHPCs that are $CD43^{+}/235a^{+}/41a^{+}$ by flow cytometry (**Figure 1.1**). In this endeavor alone, I confirmed that key cytokine signals play important roles in recapitulating developmental, such as Activin-A increasing primitive $CD235a^{+}$ cells (Sturgeon et al., 2014). Furthermore, the iHPC yield utilizing my protocol appear to be greater than currently reported protocols (data not shown). I also identified a commercial source of HPCs that can be used to fast track the generation of iMGLs across labs. Next, I used my iHPCs and commercial HPCs go develop a serum-free fully defined protocol that produced large quantities of microglial-like cells, iMGLs. While two recent studies have reported two different protocols on making microglia-like cells, these studies protocols' differ from out studies in terms of yield, transcriptomic profiling, functional validation, and novel diseased-related discoveries (Muffat et al., 2016; Pandya et al., 2017).

In contrast to the two studies, my protocol yields on average, 40 $x10^{6}$ microglia per every $1x10^{6}$ iPSCs. iMGLs are highly similar to primary cultured fetal and adult microglia by whole-transcriptome analysis and by functional studies. RNA-sequence analysis showed that iMGLs robustly expressed core microglial genes, such as P2RY12, OLFML3, C1Q, TREM2, and GPR34, at similar levels to primary microglia. By functional analyses, we showed that iMGL phagocytose E.*coli* beads less than macrophages and internalized fAβ, as expected. Our novel functional assays included showing that iMGLs have an increased preference for phagocytosing human synaptosomes and it is in part mediated via CR3-dependent pathway, in agreement with previous studies (Hong et al., 2016a; Linnartz et al., 2012; Linnartz-Gerlach et al., 2016). My studies also showed the iMGLs express functional P2ry12 using ADP-mediated migration assays and calcium transients. Preserved P2ry12 function has been rarely reported in primary microglia and not at all in microglial-like cell models (De Simone et al., 2010; Haynes et al., 2006{Moore, 2015 #57; Honda et al., 2001; Moore et al., 2015). Thus, our approach will allow for the studying of P2ry12-mediated physiological changes in microglia, as ATP/ADP has been shown to be leaked from degenerating neurons or used as a neuronal-derived signaling molecule under homeostasis (Fields and Stevens, 2000; Neary et al., 1999; Neary et al., 2006; Stevens et al., 2004). Our studies are the first to show that human microglia-like cells can populate mouse brains, opening a new method

for studying human microglia in a physiological relevant 3D environment. We showed the iMGLs integrate in to the brains of immune-deficient mice expressing human myeloid cytokines, M-CSF, IL-3, GM-CSF, and THPO. This mouse, MITRG strain, allowed for the engraftment and survival of iMGLs. After two months, iMGL morphology is extremely similar to endogenous mouse microglia and human microglia from post-mortem tissue immunofluorescence analysis. iMGLs were highly branched and positive for P2ry12 and human-specific Tmem119. These protein markers co-localized greater to the fine processes of iMGLs with similar staining observed in endogenous microglia.

Understanding how Aβ influences AD-GWAS gene expression in microglia is of great need in the field of neuroimmunology and AD pathology. Using iMGLs, my studies have shown that Aβ and tau differentially influence mRNA expression of genes like Ms4a6a, TREM2, CD33, APOE, BIN1, and CD2AP. Endocytic genes like BIN1 and CD2AP have been implicated in preventing BACE1 and APP1 processing thus, influencing subsequent fAβ production. We also found that iMGLs not exposed to CNS ques CX3CL1 and CD200 followed by fAβ stimulation predominately increased the expression of molecules that possess dual roles in binding to beta-amyloid and mediating microglia survival signals. Thus, these studies highlighted the utility of iMGLs to investigate human microglia involvement in AD. As a proof-in-principle, we transplanted iMGLs in the brains of immune-deficient AD transgenic mouse (Rag-5xfAD) previously generated in our lab and characterized to have robust plaque deposition (Marsh et al., 2016). iMGLs engrafted in Rag-5xfAD mouse brains and migrated towards beta-amyloid plaques. Confocal Z-series image analysis showed the iMGLs encircle plaques and cells are observed to have phagocytosed Aβ. As a comparison, human fetal microglia were also transplanted in Rag-5xfAD and were observed to have exact morphology and response to beta-amyloid as iMGLs, once again, showing that iMGLs can serve as proper replacement for primary microglia.

In conclusion, my dissertation studies and results have provided one of the first sets of findings implicating how human microglia may function in AD. My robust and pure microglia differentiation protocol allowed for the generation of rich RNA-transcriptome data that was utilized to confirm the identity of iMGLs as microglial-like cells as well as investigate how CNS cytokines contribute to changes in microglia RNA expression. While we didn't test how these cytokines influenced chromatin accessibility or priming (via ATAC-Seq), we showed that

microglia not interacting with the CNS ques have differential response to CNS proteins like Aβ. Finally, my dissertation studies highlight a new platform in which to study human microglia in a CNS microenvironment by showing the iMGLs populate immune deficient mouse brains and exhibit complex ramified morphology resembling microglia seen in the brain. iMGLs transplanted in AD transgenic mice were observed to encircle and internalized beta-amyloid plaques. These transplantation studies suggest that the possibility of using human-mouse chimeric brains populated by all human CNS types now that microglia can be generating using my protocol. Taken together, my dissertation studies highlight that microglia are important in neurological function in health and disease, and even suggests that microglia may be a major causative cell of CNS diseases, like Alzheimer's disease.

REFERENCES

Abbas, N., Bednar, I., Mix, E., Marie, S., Paterson, D., Ljungberg, A., Morris, C., Winblad, B., Nordberg, A., and Zhu, J. (2002). Up-regulation of the inflammatory cytokines IFN-gamma and IL-12 and down-regulation of IL-4 in cerebral cortex regions of APP(SWE) transgenic mice. J Neuroimmunol *126*, 50-57.

Abdollahi, A., Lord, K.A., Hoffman-Liebermann, B., and Liebermann, D.A. (1991). Interferon regulatory factor 1 is a myeloid differentiation primary response gene induced by interleukin 6 and leukemia inhibitory factor: role in growth inhibition. Cell Growth Differ *2*, 401-407.

Abutbul, S., Shapiro, J., Szaingurten-Solodkin, I., Levy, N., Carmy, Y., Baron, R., Jung, S., and Monsonego, A. (2012). TGF-beta signaling through SMAD2/3 induces the quiescent microglial phenotype within the CNS environment. Glia *60*, 1160-1171.

Aguzzi, A., Barres, B.A., and Bennett, M.L. (2013). Microglia: scapegoat, saboteur, or something else? Science *339*, 156-161.

Aikawa, Y., Katsumoto, T., Zhang, P., Shima, H., Shino, M., Terui, K., Ito, E., Ohno, H., Stanley, E.R., Singh, H.*, et al.* (2010). PU.1-mediated upregulation of CSF1R is crucial for leukemia stem cell potential induced by MOZ-TIF2. Nat Med *16*, 580-585, 581p following 585.

Ajami, B., Bennett, J.L., Krieger, C., McNagny, K.M., and Rossi, F.M. (2011). Infiltrating monocytes trigger EAE progression, but do not contribute to the resident microglia pool. Nat Neurosci *14*, 1142-1149.

Alzheimer's, A. (2016). 2016 Alzheimer's disease facts and figures. Alzheimers Dement *12*, 459-509.

Amanzada, A., Moriconi, F., Mansuroglu, T., Cameron, S., Ramadori, G., and Malik, I.A. (2014). Induction of chemokines and cytokines before neutrophils and macrophage recruitment in different regions of rat liver after TAA administration. Lab Invest *94*, 235-247.

Andjelkovic, A.V., Nikolic, B., Pachter, J.S., and Zecevic, N. (1998). Macrophages/microglial cells in human central nervous system during development: an immunohistochemical study. Brain Res *814*, 13-25.

Andreasson, K.I., Bachstetter, A.D., Colonna, M., Ginhoux, F., Holmes, C., Lamb, B., Landreth, G., Lee, D.C., Low, D., Lynch, M.A.*, et al.* (2016). Targeting innate immunity for neurodegenerative disorders of the central nervous system. J Neurochem *138*, 653-693.

Arinobu, Y., Mizuno, S., Chong, Y., Shigematsu, H., Iino, T., Iwasaki, H., Graf, T., Mayfield, R., Chan, S., Kastner, P.*, et al.* (2007). Reciprocal activation of GATA-1 and PU.1 marks initial specification of hematopoietic stem cells into myeloerythroid and myelolymphoid lineages. Cell Stem Cell *1*, 416-427.

Asai, H., Ikezu, S., Tsunoda, S., Medalla, M., Luebke, J., Haydar, T., Wolozin, B., Butovsky, O., Kugler, S., and Ikezu, T. (2015). Depletion of microglia and inhibition of exosome synthesis halt tau propagation. Nat Neurosci *18*, 1584-1593.

Bachstetter, A.D., Van Eldik, L.J., Schmitt, F.A., Neltner, J.H., Ighodaro, E.T., Webster, S.J., Patel, E., Abner, E.L., Kryscio, R.J., and Nelson, P.T. (2015). Disease-related microglia heterogeneity in the hippocampus of Alzheimer's disease, dementia with Lewy bodies, and hippocampal sclerosis of aging. Acta Neuropathol Commun *3*, 32.

Bailey, C.C., DeVaux, L.B., and Farzan, M. (2015). The Triggering Receptor Expressed on Myeloid Cells 2 Binds Apolipoprotein E. J Biol Chem *290*, 26033-26042.

Barnes, D.E., Beiser, A.S., Lee, A., Langa, K.M., Koyama, A., Preis, S.R., Neuhaus, J., McCammon, R.J., Yaffe, K., Seshadri, S.*, et al.* (2014). Development and validation of a brief dementia screening indicator for primary care. Alzheimers Dement *10*, 656-665 e651.

Baron, R., Babcock, A.A., Nemirovsky, A., Finsen, B., and Monsonego, A. (2014). Accelerated microglial pathology is associated with Abeta plaques in mouse models of Alzheimer's disease. Aging Cell *13*, 584-595.

Bates, K.A., Verdile, G., Li, Q.X., Ames, D., Hudson, P., Masters, C.L., and Martins, R.N. (2009). Clearance mechanisms of Alzheimer's amyloid-beta peptide: implications for therapeutic design and diagnostic tests. Mol Psychiatry *14*, 469-486.

Beecham, G.W., Hamilton, K., Naj, A.C., Martin, E.R., Huentelman, M., Myers, A.J., Corneveaux, J.J., Hardy, J., Vonsattel, J.P., Younkin, S.G.*, et al.* (2014). Genome-wide association meta-analysis of neuropathologic features of Alzheimer's disease and related dementias. PLoS Genet *10*, e1004606.

Bennett, M.L., Bennett, F.C., Liddelow, S.A., Ajami, B., Zamanian, J.L., Fernhoff, N.B., Mulinyawe, S.B., Bohlen, C.J., Adil, A., Tucker, A.*, et al.* (2016). New tools for studying microglia in the mouse and human CNS. Proc Natl Acad Sci U S A *113*, E1738-1746.

Beutner, C., Linnartz-Gerlach, B., Schmidt, S.V., Beyer, M., Mallmann, M.R., Staratschek-Jox, A., Schultze, J.L., and Neumann, H. (2013). Unique transcriptome signature of mouse microglia. Glia *61*, 1429-1442.

Beutner, C., Roy, K., Linnartz, B., Napoli, I., and Neumann, H. (2010). Generation of microglial cells from mouse embryonic stem cells. Nat Protoc *5*, 1481-1494.

Bianchin, M.M., Capella, H.M., Chaves, D.L., Steindel, M., Grisard, E.C., Ganev, G.G., da Silva Junior, J.P., Neto Evaldo, S., Poffo, M.A., Walz, R.*, et al.* (2004). Nasu-Hakola disease (polycystic lipomembranous osteodysplasia with sclerosing leukoencephalopathy--PLOSL): a dementia associated with bone cystic lesions. From clinical to genetic and molecular aspects. Cell Mol Neurobiol *24*, 1-24.

Biber, K. (2017). Reestablishing microglia function: good news for Alzheimer's therapy? EMBO J *36*, 565-567.

Biber, K., Moller, T., Boddeke, E., and Prinz, M. (2016). Central nervous system myeloid cells as drug targets: current status and translational challenges. Nat Rev Drug Discov *15*, 110-124.

Biber, K., Neumann, H., Inoue, K., and Boddeke, H.W. (2007). Neuronal 'On' and 'Off' signals control microglia. Trends Neurosci *30*, 596-602.

Blanc, F., Martinian, L., Liagkouras, I., Catarino, C., Sisodiya, S.M., and Thom, M. (2011). Investigation of widespread neocortical pathology associated with hippocampal sclerosis in epilepsy: a postmortem study. Epilepsia *52*, 10-21.

Blum-Degen, D., Muller, T., Kuhn, W., Gerlach, M., Przuntek, H., and Riederer, P. (1995). Interleukin-1 beta and interleukin-6 are elevated in the cerebrospinal fluid of Alzheimer's and de novo Parkinson's disease patients. Neurosci Lett *202*, 17-20.

Bradshaw, E.M., Chibnik, L.B., Keenan, B.T., Ottoboni, L., Raj, T., Tang, A., Rosenkrantz, L.L., Imboywa, S., Lee, M., Von Korff, A.*, et al.* (2013). CD33 Alzheimer's disease locus: altered monocyte function and amyloid biology. Nat Neurosci *16*, 848-850.

Brookmeyer, R., Corrada, M.M., Curriero, F.C., and Kawas, C. (2002). Survival following a diagnosis of Alzheimer disease. Arch Neurol *59*, 1764-1767.

Bruttger, J., Karram, K., Wortge, S., Regen, T., Marini, F., Hoppmann, N., Klein, M., Blank, T., Yona, S., Wolf, Y.*, et al.* (2015). Genetic Cell Ablation Reveals Clusters of Local Self-Renewing Microglia in the Mammalian Central Nervous System. Immunity *43*, 92-106.

Butovsky, O., Jedrychowski, M.P., Moore, C.S., Cialic, R., Lanser, A.J., Gabriely, G., Koeglsperger, T., Dake, B., Wu, P.M., Doykan, C.E.*, et al.* (2014). Identification of a unique TGF-beta-dependent molecular and functional signature in microglia. Nat Neurosci *17*, 131-143.

Butovsky, O., Siddiqui, S., Gabriely, G., Lanser, A.J., Dake, B., Murugaiyan, G., Doykan, C.E., Wu, P.M., Gali, R.R., Iyer, L.K.*, et al.* (2012). Modulating inflammatory monocytes with a unique microRNA gene signature ameliorates murine ALS. J Clin Invest *122*, 3063-3087.

Caldeira, C., Oliveira, A.F., Cunha, C., Vaz, A.R., Falcao, A.S., Fernandes, A., and Brites, D. (2014). Microglia change from a reactive to an age-like phenotype with the time in culture. Front Cell Neurosci *8*, 152.

Cardona, A.E., Pioro, E.P., Sasse, M.E., Kostenko, V., Cardona, S.M., Dijkstra, I.M., Huang, D., Kidd, G., Dombrowski, S., Dutta, R.*, et al.* (2006). Control of microglial neurotoxicity by the fractalkine receptor. Nat Neurosci *9*, 917-924.

Carson, M.J., Reilly, C.R., Sutcliffe, J.G., and Lo, D. (1998). Mature microglia resemble immature antigen-presenting cells. Glia *22*, 72-85.

Chan, G., White, C.C., Winn, P.A., Cimpean, M., Replogle, J.M., Glick, L.R., Cuerdon, N.E., Ryan, K.J., Johnson, K.A., Schneider, J.A.*, et al.* (2015). CD33 modulates TREM2: convergence of Alzheimer loci. Nat Neurosci *18*, 1556-1558.

Chan, W.Y., Kohsaka, S., and Rezaie, P. (2007). The origin and cell lineage of microglia: new concepts. Brain Res Rev *53*, 344-354.

Chen, E.Y., Tan, C.M., Kou, Y., Duan, Q., Wang, Z., Meirelles, G.V., Clark, N.R., and Ma'ayan, A. (2013). Enrichr: interactive and collaborative HTML5 gene list enrichment analysis tool. BMC Bioinformatics *14*, 128.

Choi, K.D., Vodyanik, M., and Slukvin, II (2011). Hematopoietic differentiation and production of mature myeloid cells from human pluripotent stem cells. Nat Protoc *6*, 296-313.

Chung, W.S., Clarke, L.E., Wang, G.X., Stafford, B.K., Sher, A., Chakraborty, C., Joung, J., Foo, L.C., Thompson, A., Chen, C.*, et al.* (2013). Astrocytes mediate synapse elimination through MEGF10 and MERTK pathways. Nature *504*, 394-400.

Colonna, M., and Butovsky, O. (2017). Microglia Function in the Central Nervous System During Health and Neurodegeneration. Annu Rev Immunol.

Combs, C.K., Karlo, J.C., Kao, S.C., and Landreth, G.E. (2001). beta-Amyloid stimulation of microglia and monocytes results in TNFalpha-dependent expression of inducible nitric oxide synthase and neuronal apoptosis. J Neurosci *21*, 1179-1188.

Crotti, A., Benner, C., Kerman, B.E., Gosselin, D., Lagier-Tourenne, C., Zuccato, C., Cattaneo, E., Gage, F.H., Cleveland, D.W., and Glass, C.K. (2014). Mutant Huntingtin promotes autonomous microglia activation via myeloid lineage-determining factors. Nat Neurosci *17*, 513-521.

Cruchaga, C., Kauwe, J.S., Harari, O., Jin, S.C., Cai, Y., Karch, C.M., Benitez, B.A., Jeng, A.T., Skorupa, T., Carrell, D.*, et al.* (2013). GWAS of cerebrospinal fluid tau levels identifies risk variants for Alzheimer's disease. Neuron *78*, 256-268.

Cummings, J.L., Morstorf, T., and Zhong, K. (2014). Alzheimer's disease drug-development pipeline: few candidates, frequent failures. Alzheimers Res Ther *6*, 37.

de Jong, J.L., and Zon, L.I. (2005). Use of the zebrafish system to study primitive and definitive hematopoiesis. Annu Rev Genet *39*, 481-501.

De Lucia, C., Rinchon, A., Olmos-Alonso, A., Riecken, K., Fehse, B., Boche, D., Perry, V.H., and Gomez-Nicola, D. (2016). Microglia regulate hippocampal neurogenesis during chronic neurodegeneration. Brain Behav Immun *55*, 179-190.

De Simone, R., Niturad, C.E., De Nuccio, C., Ajmone-Cat, M.A., Visentin, S., and Minghetti, L. (2010). TGF-beta and LPS modulate ADP-induced migration of microglial cells through P2Y1 and P2Y12 receptor expression. J Neurochem *115*, 450-459.

DeKoter, R.P., Lee, H.J., and Singh, H. (2002). PU.1 regulates expression of the interleukin-7 receptor in lymphoid progenitors. Immunity *16*, 297-309.

Devinsky, O., Vezzani, A., Najjar, S., De Lanerolle, N.C., and Rogawski, M.A. (2013). Glia and epilepsy: excitability and inflammation. Trends Neurosci *36*, 174-184.

Ditadi, A., Sturgeon, C.M., Tober, J., Awong, G., Kennedy, M., Yzaguirre, A.D., Azzola, L., Ng, E.S., Stanley, E.G., French, D.L.*, et al.* (2015). Human definitive haemogenic endothelium and arterial vascular endothelium represent distinct lineages. Nat Cell Biol *17*, 580-591.

Dobin, A., Davis, C.A., Schlesinger, F., Drenkow, J., Zaleski, C., Jha, S., Batut, P., Chaisson, M., and Gingeras, T.R. (2013). STAR: ultrafast universal RNA-seq aligner. Bioinformatics *29*, 15-21.

Doody, R.S., Raman, R., Farlow, M., Iwatsubo, T., Vellas, B., Joffe, S., Kieburtz, K., He, F., Sun, X., Thomas, R.G.*, et al.* (2013). A phase 3 trial of semagacestat for treatment of Alzheimer's disease. N Engl J Med *369*, 341-350.

Droin, N., and Solary, E. (2010). Editorial: CSF1R, CSF-1, and IL-34, a "menage a trois" conserved across vertebrates. J Leukoc Biol *87*, 745-747.

El Khoury, J.B., Moore, K.J., Means, T.K., Leung, J., Terada, K., Toft, M., Freeman, M.W., and Luster, A.D. (2003). CD36 mediates the innate host response to beta-amyloid. J Exp Med *197*, 1657-1666.

Elmore, M.R., Lee, R.J., West, B.L., and Green, K.N. (2015). Characterizing newly repopulated microglia in the adult mouse: impacts on animal behavior, cell morphology, and neuroinflammation. PLoS One *10*, e0122912.

Elmore, M.R., Najafi, A.R., Koike, M.A., Dagher, N.N., Spangenberg, E.E., Rice, R.A., Kitazawa, M., Matusow, B., Nguyen, H., West, B.L.*, et al.* (2014). Colony-stimulating factor 1 receptor signaling is necessary for microglia viability, unmasking a microglia progenitor cell in the adult brain. Neuron *82*, 380-397.

Erny, D., Hrabe de Angelis, A.L., Jaitin, D., Wieghofer, P., Staszewski, O., David, E., Keren-Shaul, H., Mahlakoiv, T., Jakobshagen, K., Buch, T.*, et al.* (2015). Host microbiota constantly control maturation and function of microglia in the CNS. Nat Neurosci *18*, 965-977.

Falsig, J., van Beek, J., Hermann, C., and Leist, M. (2008). Molecular basis for detection of invading pathogens in the brain. J Neurosci Res *86*, 1434-1447.

Fields, R.D., and Stevens, B. (2000). ATP: an extracellular signaling molecule between neurons and glia. Trends Neurosci *23*, 625-633.

Ford, A.L., Goodsall, A.L., Hickey, W.F., and Sedgwick, J.D. (1995). Normal adult ramified microglia separated from other central nervous system macrophages by flow cytometric sorting. Phenotypic differences defined and direct ex vivo antigen presentation to myelin basic protein-reactive CD4+ T cells compared. J Immunol *154*, 4309-4321.

Fu, Y., Hsiao, J.H., Paxinos, G., Halliday, G.M., and Kim, W.S. (2016). ABCA7 Mediates Phagocytic Clearance of Amyloid-beta in the Brain. J Alzheimers Dis *54*, 569-584.

Gemma, C., and Bachstetter, A.D. (2013). The role of microglia in adult hippocampal neurogenesis. Front Cell Neurosci *7*, 229.

Ginhoux, F., Greter, M., Leboeuf, M., Nandi, S., See, P., Gokhan, S., Mehler, M.F., Conway, S.J., Ng, L.G., Stanley, E.R.*, et al.* (2010). Fate mapping analysis reveals that adult microglia derive from primitive macrophages. Science *330*, 841-845.

Ginhoux, F., Lim, S., Hoeffel, G., Low, D., and Huber, T. (2013). Origin and differentiation of microglia. Front Cell Neurosci *7*, 45.

Gispert, J.D., Suarez-Calvet, M., Monte, G.C., Tucholka, A., Falcon, C., Rojas, S., Rami, L., Sanchez-Valle, R., Llado, A., Kleinberger, G.*, et al.* (2016). Cerebrospinal fluid sTREM2 levels are associated with gray matter volume increases and reduced diffusivity in early Alzheimer's disease. Alzheimers Dement *12*, 1259-1272.

Glass, C.K., and Natoli, G. (2016). Molecular control of activation and priming in macrophages. Nat Immunol *17*, 26-33.

Glenner, G.G., and Wong, C.W. (1984). Alzheimer's disease: initial report of the purification and characterization of a novel cerebrovascular amyloid protein. Biochem Biophys Res Commun *120*, 885-890.

Golde, T.E., Schneider, L.S., and Koo, E.H. (2011). Anti-abeta therapeutics in Alzheimer's disease: the need for a paradigm shift. Neuron *69*, 203-213.

Goldmann, T., Wieghofer, P., Muller, P.F., Wolf, Y., Varol, D., Yona, S., Brendecke, S.M., Kierdorf, K., Staszewski, O., Datta, M.*, et al.* (2013). A new type of microglia gene targeting shows TAK1 to be pivotal in CNS autoimmune inflammation. Nat Neurosci *16*, 1618-1626.

Gomez-Nicola, D., and Perry, V.H. (2015). Microglial dynamics and role in the healthy and diseased brain: a paradigm of functional plasticity. Neuroscientist *21*, 169-184.

Gorczyca, W., Sun, Z.Y., Cronin, W., Li, X., Mau, S., and Tugulea, S. (2011). Immunophenotypic pattern of myeloid populations by flow cytometry analysis. Methods Cell Biol *103*, 221-266.

Gosselin, D., Link, V.M., Romanoski, C.E., Fonseca, G.J., Eichenfield, D.Z., Spann, N.J., Stender, J.D., Chun, H.B., Garner, H., Geissmann, F.*, et al.* (2014). Environment drives selection and

function of enhancers controlling tissue-specific macrophage identities. Cell *159*, 1327-1340.

Grabert, K., Michoel, T., Karavolos, M.H., Clohisey, S., Baillie, J.K., Stevens, M.P., Freeman, T.C., Summers, K.M., and McColl, B.W. (2016). Microglial brain region-dependent diversity and selective regional sensitivities to aging. Nat Neurosci *19*, 504-516.

Greer, P.L., Bear, D.M., Lassance, J.M., Bloom, M.L., Tsukahara, T., Pashkovski, S.L., Masuda, F.K., Nowlan, A.C., Kirchner, R., Hoekstra, H.E.*, et al.* (2016). A Family of non-GPCR Chemosensors Defines an Alternative Logic for Mammalian Olfaction. Cell *165*, 1734-1748.

Greter, M., Lelios, I., Pelczar, P., Hoeffel, G., Price, J., Leboeuf, M., Kundig, T.M., Frei, K., Ginhoux, F., Merad, M.*, et al.* (2012). Stroma-derived interleukin-34 controls the development and maintenance of langerhans cells and the maintenance of microglia. Immunity *37*, 1050-1060.

Griciuc, A., Serrano-Pozo, A., Parrado, A.R., Lesinski, A.N., Asselin, C.N., Mullin, K., Hooli, B., Choi, S.H., Hyman, B.T., and Tanzi, R.E. (2013). Alzheimer's disease risk gene CD33 inhibits microglial uptake of amyloid beta. Neuron *78*, 631-643.

Guerreiro, R., and Hardy, J. (2014). Genetics of Alzheimer's disease. Neurotherapeutics *11*, 732-737.

Guerreiro, R., Wojtas, A., Bras, J., Carrasquillo, M., Rogaeva, E., Majounie, E., Cruchaga, C., Sassi, C., Kauwe, J.S., Younkin, S.*, et al.* (2013). TREM2 variants in Alzheimer's disease. N Engl J Med *368*, 117-127.

Guillot-Sestier, M.V., Doty, K.R., and Town, T. (2015). Innate Immunity Fights Alzheimer's Disease. Trends Neurosci *38*, 674-681.

Guillot-Sestier, M.V., and Town, T. (2013). Innate immunity in Alzheimer's disease: a complex affair. CNS Neurol Disord Drug Targets *12*, 593-607.

Gylys, K.H., Fein, J.A., and Cole, G.M. (2000). Quantitative characterization of crude synaptosomal fraction (P-2) components by flow cytometry. J Neurosci Res *61*, 186-192.

Hamerman, J.A., Jarjoura, J.R., Humphrey, M.B., Nakamura, M.C., Seaman, W.E., and Lanier, L.L. (2006). Cutting edge: inhibition of TLR and FcR responses in macrophages by triggering receptor expressed on myeloid cells (TREM)-2 and DAP12. J Immunol *177*, 2051-2055.

Hammad, S.M., Ranganathan, S., Loukinova, E., Twal, W.O., and Argraves, W.S. (1997). Interaction of apolipoprotein J-amyloid beta-peptide complex with low density lipoprotein receptor-related protein-2/megalin. A mechanism to prevent pathological accumulation of amyloid beta-peptide. J Biol Chem *272*, 18644-18649.

Hanisch, U.K. (2013). Functional diversity of microglia - how heterogeneous are they to begin with? Front Cell Neurosci *7*, 65.

Hanna, R.N., Carlin, L.M., Hubbeling, H.G., Nackiewicz, D., Green, A.M., Punt, J.A., Geissmann, F., and Hedrick, C.C. (2011). The transcription factor NR4A1 (Nur77) controls bone marrow differentiation and the survival of Ly6C- monocytes. Nat Immunol *12*, 778-785.

Hatami, A., Monjazeb, S., Milton, S., and Glabe, C.G. (2017). Familial Alzheimer's Disease Mutations within the Amyloid Precursor Protein Alter the Aggregation and Conformation of the Amyloid-beta Peptide. J Biol Chem *292*, 3172-3185.

Haynes, S.E., Hollopeter, G., Yang, G., Kurpius, D., Dailey, M.E., Gan, W.B., and Julius, D. (2006). The P2Y12 receptor regulates microglial activation by extracellular nucleotides. Nat Neurosci *9*, 1512-1519.

Helzner, E.P., Scarmeas, N., Cosentino, S., Tang, M.X., Schupf, N., and Stern, Y. (2008). Survival in Alzheimer disease: a multiethnic, population-based study of incident cases. Neurology *71*, 1489-1495.

Heneka, M.T., Kummer, M.P., and Latz, E. (2014). Innate immune activation in neurodegenerative disease. Nat Rev Immunol *14*, 463-477.

Heppner, F.L., Ransohoff, R.M., and Becher, B. (2015). Immune attack: the role of inflammation in Alzheimer disease. Nat Rev Neurosci *16*, 358-372.

Hickman, S.E., Allison, E.K., and El Khoury, J. (2008). Microglial dysfunction and defective beta-amyloid clearance pathways in aging Alzheimer's disease mice. J Neurosci *28*, 8354-8360.

Hickman, S.E., Kingery, N.D., Ohsumi, T.K., Borowsky, M.L., Wang, L.C., Means, T.K., and El Khoury, J. (2013). The microglial sensome revealed by direct RNA sequencing. Nat Neurosci *16*, 1896-1905.

Hoeffel, G., Chen, J., Lavin, Y., Low, D., Almeida, F.F., See, P., Beaudin, A.E., Lum, J., Low, I., Forsberg, E.C.*, et al.* (2015). C-Myb(+) erythro-myeloid progenitor-derived fetal monocytes give rise to adult tissue-resident macrophages. Immunity *42*, 665-678.

Hohsfield, L.A., and Humpel, C. (2015). Migration of blood cells to beta-amyloid plaques in Alzheimer's disease. Exp Gerontol *65*, 8-15.

Holler, C.J., Davis, P.R., Beckett, T.L., Platt, T.L., Webb, R.L., Head, E., and Murphy, M.P. (2014). Bridging integrator 1 (BIN1) protein expression increases in the Alzheimer's disease brain and correlates with neurofibrillary tangle pathology. J Alzheimers Dis *42*, 1221-1227.

Hollingworth, P., Harold, D., Sims, R., Gerrish, A., Lambert, J.C., Carrasquillo, M.M., Abraham, R., Hamshere, M.L., Pahwa, J.S., Moskvina, V.*, et al.* (2011). Common variants at ABCA7,

MS4A6A/MS4A4E, EPHA1, CD33 and CD2AP are associated with Alzheimer's disease. Nat Genet *43*, 429-435.

Honda, S., Sasaki, Y., Ohsawa, K., Imai, Y., Nakamura, Y., Inoue, K., and Kohsaka, S. (2001). Extracellular ATP or ADP induce chemotaxis of cultured microglia through Gi/o-coupled P2Y receptors. J Neurosci *21*, 1975-1982.

Hong, S., Beja-Glasser, V.F., Nfonoyim, B.M., Frouin, A., Li, S., Ramakrishnan, S., Merry, K.M., Shi, Q., Rosenthal, A., Barres, B.A.*, et al.* (2016a). Complement and microglia mediate early synapse loss in Alzheimer mouse models. Science *352*, 712-716.

Hong, S., Dissing-Olesen, L., and Stevens, B. (2016b). New insights on the role of microglia in synaptic pruning in health and disease. Curr Opin Neurobiol *36*, 128-134.

Huang, G., Zhang, P., Hirai, H., Elf, S., Yan, X., Chen, Z., Koschmieder, S., Okuno, Y., Dayaram, T., Growney, J.D.*, et al.* (2008). PU.1 is a major downstream target of AML1 (RUNX1) in adult mouse hematopoiesis. Nat Genet *40*, 51-60.

Iaccarino, H.F., Singer, A.C., Martorell, A.J., Rudenko, A., Gao, F., Gillingham, T.Z., Mathys, H., Seo, J., Kritskiy, O., Abdurrob, F.*, et al.* (2016). Gamma frequency entrainment attenuates amyloid load and modifies microglia. Nature *540*, 230-235.

Ito, D., Imai, Y., Ohsawa, K., Nakajima, K., Fukuuchi, Y., and Kohsaka, S. (1998). Microglia-specific localisation of a novel calcium binding protein, Iba1. Brain Res Mol Brain Res *57*, 1-9.

Ito, H., and Hamerman, J.A. (2012). TREM-2, triggering receptor expressed on myeloid cell-2, negatively regulates TLR responses in dendritic cells. Eur J Immunol *42*, 176-185.

Jack, C.R., Jr., Knopman, D.S., Jagust, W.J., Petersen, R.C., Weiner, M.W., Aisen, P.S., Shaw, L.M., Vemuri, P., Wiste, H.J., Weigand, S.D.*, et al.* (2013). Tracking pathophysiological processes in Alzheimer's disease: an updated hypothetical model of dynamic biomarkers. Lancet Neurol *12*, 207-216.

Jagannathan-Bogdan, M., and Zon, L.I. (2013). Hematopoiesis. Development *140*, 2463-2467.

Jay, T.R., Hirsch, A.M., Broihier, M.L., Miller, C.M., Neilson, L.E., Ransohoff, R.M., Lamb, B.T., and Landreth, G.E. (2017). Disease Progression-Dependent Effects of TREM2 Deficiency in a Mouse Model of Alzheimer's Disease. J Neurosci *37*, 637-647.

Jay, T.R., Miller, C.M., Cheng, P.J., Graham, L.C., Bemiller, S., Broihier, M.L., Xu, G., Margevicius, D., Karlo, J.C., Sousa, G.L.*, et al.* (2015). TREM2 deficiency eliminates TREM2+ inflammatory macrophages and ameliorates pathology in Alzheimer's disease mouse models. J Exp Med *212*, 287-295.

Jonsson, T., Stefansson, H., Steinberg, S., Jonsdottir, I., Jonsson, P.V., Snaedal, J., Bjornsson, S., Huttenlocher, J., Levey, A.I., Lah, J.J.*, et al.* (2013). Variant of TREM2 associated with the risk of Alzheimer's disease. N Engl J Med *368*, 107-116.

Karch, C.M., Ezerskiy, L.A., Bertelsen, S., Alzheimer's Disease Genetics, C., and Goate, A.M. (2016). Alzheimer's Disease Risk Polymorphisms Regulate Gene Expression in the ZCWPW1 and the CELF1 Loci. PLoS One *11*, e0148717.

Karperien, A., Ahammer, H., and Jelinek, H.F. (2013). Quantitating the subtleties of microglial morphology with fractal analysis. Front Cell Neurosci *7*, 3.

Kaufman, S.K., Sanders, D.W., Thomas, T.L., Ruchinskas, A.J., Vaquer-Alicea, J., Sharma, A.M., Miller, T.M., and Diamond, M.I. (2016). Tau Prion Strains Dictate Patterns of Cell Pathology, Progression Rate, and Regional Vulnerability In Vivo. Neuron *92*, 796-812.

Kennedy, M., Awong, G., Sturgeon, C.M., Ditadi, A., LaMotte-Mohs, R., Zuniga-Pflucker, J.C., and Keller, G. (2012). T lymphocyte potential marks the emergence of definitive hematopoietic progenitors in human pluripotent stem cell differentiation cultures. Cell Rep *2*, 1722-1735.

Kennedy, M., D'Souza, S.L., Lynch-Kattman, M., Schwantz, S., and Keller, G. (2007). Development of the hemangioblast defines the onset of hematopoiesis in human ES cell differentiation cultures. Blood *109*, 2679-2687.

Kettenmann, H., Hanisch, U.K., Noda, M., and Verkhratsky, A. (2011). Physiology of microglia. Physiol Rev *91*, 461-553.

Khemka, V.K., Ganguly, A., Bagchi, D., Ghosh, A., Bir, A., Biswas, A., Chattopadhyay, S., and Chakrabarti, S. (2014). Raised serum proinflammatory cytokines in Alzheimer's disease with depression. Aging Dis *5*, 170-176.

Kierdorf, K., Erny, D., Goldmann, T., Sander, V., Schulz, C., Perdiguero, E.G., Wieghofer, P., Heinrich, A., Riemke, P., Holscher, C.*, et al.* (2013). Microglia emerge from erythromyeloid precursors via Pu.1- and Irf8-dependent pathways. Nat Neurosci *16*, 273-280.

Kierdorf, K., and Prinz, M. (2013). Factors regulating microglia activation. Front Cell Neurosci *7*, 44.

Kleinberger, G., Yamanishi, Y., Suarez-Calvet, M., Czirr, E., Lohmann, E., Cuyvers, E., Struyfs, H., Pettkus, N., Wenninger-Weinzierl, A., Mazaheri, F.*, et al.* (2014). TREM2 mutations implicated in neurodegeneration impair cell surface transport and phagocytosis. Sci Transl Med *6*, 243ra286.

Koenigsknecht-Talboo, J., and Landreth, G.E. (2005). Microglial phagocytosis induced by fibrillar beta-amyloid and IgGs are differentially regulated by proinflammatory cytokines. J Neurosci *25*, 8240-8249.

Kontargiris, E., Kolettas, E., Vadalouca, A., Trougakos, I.P., Gonos, E.S., and Kalfakakou, V. (2004). Ectopic expression of clusterin/apolipoprotein J or Bcl-2 decreases the sensitivity of HaCaT cells to toxic effects of ropivacaine. Cell Res *14*, 415-422.

Kreutzer, A.G., Yoo, S., Spencer, R.K., and Nowick, J.S. (2017). Stabilization, Assembly, and Toxicity of Trimers Derived from Abeta. J Am Chem Soc *139*, 966-975.

Kuleshov, M.V., Jones, M.R., Rouillard, A.D., Fernandez, N.F., Duan, Q., Wang, Z., Koplev, S., Jenkins, S.L., Jagodnik, K.M., Lachmann, A.*, et al.* (2016). Enrichr: a comprehensive gene set enrichment analysis web server 2016 update. Nucleic Acids Res *44*, W90-97.

Lajaunias, F., Dayer, J.M., and Chizzolini, C. (2005). Constitutive repressor activity of CD33 on human monocytes requires sialic acid recognition and phosphoinositide 3-kinase-mediated intracellular signaling. Eur J Immunol *35*, 243-251.

Lancaster, M.A., Renner, M., Martin, C.A., Wenzel, D., Bicknell, L.S., Hurles, M.E., Homfray, T., Penninger, J.M., Jackson, A.P., and Knoblich, J.A. (2013). Cerebral organoids model human brain development and microcephaly. Nature *501*, 373-379.

Lasagna-Reeves, C.A., Castillo-Carranza, D.L., Sengupta, U., Sarmiento, J., Troncoso, J., Jackson, G.R., and Kayed, R. (2012). Identification of oligomers at early stages of tau aggregation in Alzheimer's disease. FASEB J *26*, 1946-1959.

Lavin, Y., Winter, D., Blecher-Gonen, R., David, E., Keren-Shaul, H., Merad, M., Jung, S., and Amit, I. (2014). Tissue-resident macrophage enhancer landscapes are shaped by the local microenvironment. Cell *159*, 1312-1326.

Leone, C., Le Pavec, G., Meme, W., Porcheray, F., Samah, B., Dormont, D., and Gras, G. (2006). Characterization of human monocyte-derived microglia-like cells. Glia *54*, 183-192.

Lesne, S., Koh, M.T., Kotilinek, L., Kayed, R., Glabe, C.G., Yang, A., Gallagher, M., and Ashe, K.H. (2006). A specific amyloid-beta protein assembly in the brain impairs memory. Nature *440*, 352-357.

Li, B., and Dewey, C.N. (2011). RSEM: accurate transcript quantification from RNA-Seq data with or without a reference genome. BMC Bioinformatics *12*, 323.

Liakhovitskaia, A., Lana-Elola, E., Stamateris, E., Rice, D.P., van 't Hof, R.J., and Medvinsky, A. (2010). The essential requirement for Runx1 in the development of the sternum. Dev Biol *340*, 539-546.

Limatola, C., and Ransohoff, R.M. (2014). Modulating neurotoxicity through CX3CL1/CX3CR1 signaling. Front Cell Neurosci *8*, 229.

Linnartz, B., Kopatz, J., Tenner, A.J., and Neumann, H. (2012). Sialic acid on the neuronal glycocalyx prevents complement C1 binding and complement receptor-3-mediated removal by microglia. J Neurosci *32*, 946-952.

Linnartz-Gerlach, B., Mathews, M., and Neumann, H. (2014). Sensing the neuronal glycocalyx by glial sialic acid binding immunoglobulin-like lectins. Neuroscience *275*, 113-124.

Linnartz-Gerlach, B., Schuy, C., Shahraz, A., Tenner, A.J., and Neumann, H. (2016). Sialylation of neurites inhibits complement-mediated macrophage removal in a human macrophage-neuron Co-Culture System. Glia *64*, 35-47.

Liu, S., Liu, Y., Hao, W., Wolf, L., Kiliaan, A.J., Penke, B., Rube, C.E., Walter, J., Heneka, M.T., Hartmann, T.*, et al.* (2012). TLR2 is a primary receptor for Alzheimer's amyloid beta peptide to trigger neuroinflammatory activation. J Immunol *188*, 1098-1107.

Liu, Z., Condello, C., Schain, A., Harb, R., and Grutzendler, J. (2010). CX3CR1 in microglia regulates brain amyloid deposition through selective protofibrillar amyloid-beta phagocytosis. J Neurosci *30*, 17091-17101.

Loo, D.T., Copani, A., Pike, C.J., Whittemore, E.R., Walencewicz, A.J., and Cotman, C.W. (1993). Apoptosis is induced by beta-amyloid in cultured central nervous system neurons. Proc Natl Acad Sci U S A *90*, 7951-7955.

Lui, H., Zhang, J., Makinson, S.R., Cahill, M.K., Kelley, K.W., Huang, H.Y., Shang, Y., Oldham, M.C., Martens, L.H., Gao, F.*, et al.* (2016). Progranulin Deficiency Promotes Circuit-Specific Synaptic Pruning by Microglia via Complement Activation. Cell *165*, 921-935.

Luo, J., Elwood, F., Britschgi, M., Villeda, S., Zhang, H., Ding, Z., Zhu, L., Alabsi, H., Getachew, R., Narasimhan, R.*, et al.* (2013). Colony-stimulating factor 1 receptor (CSF1R) signaling in injured neurons facilitates protection and survival. J Exp Med *210*, 157-172.

Malik, M., Parikh, I., Vasquez, J.B., Smith, C., Tai, L., Bu, G., LaDu, M.J., Fardo, D.W., Rebeck, G.W., and Estus, S. (2015). Genetics ignite focus on microglial inflammation in Alzheimer's disease. Mol Neurodegener *10*, 52.

Marsh, S.E., Abud, E.M., Lakatos, A., Karimzadeh, A., Yeung, S.T., Davtyan, H., Fote, G.M., Lau, L., Weinger, J.G., Lane, T.E.*, et al.* (2016). The adaptive immune system restrains Alzheimer's disease pathogenesis by modulating microglial function. Proc Natl Acad Sci U S A *113*, E1316-1325.

Matcovitch-Natan, O., Winter, D.R., Giladi, A., Vargas Aguilar, S., Spinrad, A., Sarrazin, S., Ben-Yehuda, H., David, E., Zelada Gonzalez, F., Perrin, P.*, et al.* (2016). Microglia development follows a stepwise program to regulate brain homeostasis. Science *353*, aad8670.

Mawuenyega, K.G., Sigurdson, W., Ovod, V., Munsell, L., Kasten, T., Morris, J.C., Yarasheski, K.E., and Bateman, R.J. (2010). Decreased clearance of CNS beta-amyloid in Alzheimer's disease. Science *330*, 1774.

McKercher, S.R., Torbett, B.E., Anderson, K.L., Henkel, G.W., Vestal, D.J., Baribault, H., Klemsz, M., Feeney, A.J., Wu, G.E., Paige, C.J.*, et al.* (1996). Targeted disruption of the PU.1 gene results in multiple hematopoietic abnormalities. EMBO J *15*, 5647-5658.

Melchior, B., Garcia, A.E., Hsiung, B.K., Lo, K.M., Doose, J.M., Thrash, J.C., Stalder, A.K., Staufenbiel, M., Neumann, H., and Carson, M.J. (2010). Dual induction of TREM2 and tolerance-related transcript, Tmem176b, in amyloid transgenic mice: implications for vaccine-based therapies for Alzheimer's disease. ASN Neuro *2*, e00037.

Merino-Zamorano, C., Fernandez-de Retana, S., Montanola, A., Batlle, A., Saint-Pol, J., Mysiorek, C., Gosselet, F., Montaner, J., and Hernandez-Guillamon, M. (2016). Modulation of Amyloid-beta1-40 Transport by ApoA1 and ApoJ Across an in vitro Model of the Blood-Brain Barrier. J Alzheimers Dis *53*, 677-691.

Michaelis, M., Nieswandt, B., Stegner, D., Eilers, J., and Kraft, R. (2015). STIM1, STIM2, and Orai1 regulate store-operated calcium entry and purinergic activation of microglia. Glia *63*, 652-663.

Mildner, A., Huang, H., Radke, J., Stenzel, W., and Priller, J. (2017). P2Y12 receptor is expressed on human microglia under physiological conditions throughout development and is sensitive to neuroinflammatory diseases. Glia *65*, 375-387.

Moore, C.S., Ase, A.R., Kinsara, A., Rao, V.T., Michell-Robinson, M., Leong, S.Y., Butovsky, O., Ludwin, S.K., Seguela, P., Bar-Or, A.*, et al.* (2015). P2Y12 expression and function in alternatively activated human microglia. Neurol Neuroimmunol Neuroinflamm *2*, e80.

Moynagh, P.N. (2005). The interleukin-1 signalling pathway in astrocytes: a key contributor to inflammation in the brain. J Anat *207*, 265-269.

Muffat, J., Li, Y., Yuan, B., Mitalipova, M., Omer, A., Corcoran, S., Bakiasi, G., Tsai, L.H., Aubourg, P., Ransohoff, R.M.*, et al.* (2016). Efficient derivation of microglia-like cells from human pluripotent stem cells. Nat Med.

Naj, A.C., Jun, G., Beecham, G.W., Wang, L.S., Vardarajan, B.N., Buros, J., Gallins, P.J., Buxbaum, J.D., Jarvik, G.P., Crane, P.K.*, et al.* (2011). Common variants at MS4A4/MS4A6E, CD2AP, CD33 and EPHA1 are associated with late-onset Alzheimer's disease. Nat Genet *43*, 436-441.

Nandi, S., Gokhan, S., Dai, X.M., Wei, S., Enikolopov, G., Lin, H., Mehler, M.F., and Stanley, E.R. (2012). The CSF-1 receptor ligands IL-34 and CSF-1 exhibit distinct developmental brain expression patterns and regulate neural progenitor cell maintenance and maturation. Dev Biol *367*, 100-113.

Napoli, I., Kierdorf, K., and Neumann, H. (2009). Microglial precursors derived from mouse embryonic stem cells. Glia *57*, 1660-1671.

Nazem, A., Sankowski, R., Bacher, M., and Al-Abed, Y. (2015). Rodent models of neuroinflammation for Alzheimer's disease. J Neuroinflammation *12*, 74.

Neary, J.T., Kang, Y., Bu, Y., Yu, E., Akong, K., and Peters, C.M. (1999). Mitogenic signaling by ATP/P2Y purinergic receptors in astrocytes: involvement of a calcium-independent protein kinase C, extracellular signal-regulated protein kinase pathway distinct from the phosphatidylinositol-specific phospholipase C/calcium pathway. J Neurosci *19*, 4211-4220.

Neary, J.T., Kang, Y., Shi, Y.F., Tran, M.D., and Wanner, I.B. (2006). P2 receptor signalling, proliferation of astrocytes, and expression of molecules involved in cell-cell interactions. Novartis Found Symp *276*, 131-143; discussion 143-137, 233-137, 275-181.

Noto, D., Sakuma, H., Takahashi, K., Saika, R., Saga, R., Yamada, M., Yamamura, T., and Miyake, S. (2014). Development of a culture system to induce microglia-like cells from haematopoietic cells. Neuropathol Appl Neurobiol *40*, 697-713.

Nutt, S.L., Metcalf, D., D'Amico, A., Polli, M., and Wu, L. (2005). Dynamic regulation of PU.1 expression in multipotent hematopoietic progenitors. J Exp Med *201*, 221-231.

O'Rourke, J.G., Bogdanik, L., Yanez, A., Lall, D., Wolf, A.J., Muhammad, A.K., Ho, R., Carmona, S., Vit, J.P., Zarrow, J.*, et al.* (2016). C9orf72 is required for proper macrophage and microglial function in mice. Science *351*, 1324-1329.

Ohgidani, M., Kato, T.A., Setoyama, D., Sagata, N., Hashimoto, R., Shigenobu, K., Yoshida, T., Hayakawa, K., Shimokawa, N., Miura, D.*, et al.* (2014). Direct induction of ramified microglia-like cells from human monocytes: dynamic microglial dysfunction in Nasu-Hakola disease. Sci Rep *4*, 4957.

Paloneva, J., Kestila, M., Wu, J., Salminen, A., Bohling, T., Ruotsalainen, V., Hakola, P., Bakker, A.B., Phillips, J.H., Pekkarinen, P.*, et al.* (2000). Loss-of-function mutations in TYROBP (DAP12) result in a presenile dementia with bone cysts. Nat Genet *25*, 357-361.

Paloneva, J., Manninen, T., Christman, G., Hovanes, K., Mandelin, J., Adolfsson, R., Bianchin, M., Bird, T., Miranda, R., Salmaggi, A.*, et al.* (2002). Mutations in two genes encoding different subunits of a receptor signaling complex result in an identical disease phenotype. Am J Hum Genet *71*, 656-662.

Pandya, H., Shen, M.J., Ichikawa, D.M., Sedlock, A.B., Choi, Y., Johnson, K.R., Kim, G., Brown, M.A., Elkahloun, A.G., Maric, D.*, et al.* (2017). Differentiation of human and murine induced pluripotent stem cells to microglia-like cells. Nat Neurosci.

Paolicelli, R.C., Bolasco, G., Pagani, F., Maggi, L., Scianni, M., Panzanelli, P., Giustetto, M., Ferreira, T.A., Guiducci, E., Dumas, L.*, et al.* (2011). Synaptic pruning by microglia is necessary for normal brain development. Science *333*, 1456-1458.

Parkhurst, C.N., Yang, G., Ninan, I., Savas, J.N., Yates, J.R., 3rd, Lafaille, J.J., Hempstead, B.L., Littman, D.R., and Gan, W.B. (2013). Microglia promote learning-dependent synapse formation through brain-derived neurotrophic factor. Cell *155*, 1596-1609.

Patel, N.S., Paris, D., Mathura, V., Quadros, A.N., Crawford, F.C., and Mullan, M.J. (2005). Inflammatory cytokine levels correlate with amyloid load in transgenic mouse models of Alzheimer's disease. J Neuroinflammation *2*, 9.

Poliani, P.L., Wang, Y., Fontana, E., Robinette, M.L., Yamanishi, Y., Gilfillan, S., and Colonna, M. (2015). TREM2 sustains microglial expansion during aging and response to demyelination. J Clin Invest *125*, 2161-2170.

Pont-Lezica, L., Bechade, C., Belarif-Cantaut, Y., Pascual, O., and Bessis, A. (2011). Physiological roles of microglia during development. J Neurochem *119*, 901-908.

Prinz, M., and Priller, J. (2014). Microglia and brain macrophages in the molecular age: from origin to neuropsychiatric disease. Nat Rev Neurosci *15*, 300-312.

Prinz, M., Priller, J., Sisodia, S.S., and Ransohoff, R.M. (2011). Heterogeneity of CNS myeloid cells and their roles in neurodegeneration. Nat Neurosci *14*, 1227-1235.

Ran, D., Shia, W.J., Lo, M.C., Fan, J.B., Knorr, D.A., Ferrell, P.I., Ye, Z., Yan, M., Cheng, L., Kaufman, D.S.*, et al.* (2013). RUNX1a enhances hematopoietic lineage commitment from human embryonic stem cells and inducible pluripotent stem cells. Blood *121*, 2882-2890.

Ransohoff, R.M. (2011). Microglia and monocytes: 'tis plain the twain meet in the brain. Nat Neurosci *14*, 1098-1100.

Ransohoff, R.M., and Cardona, A.E. (2010). The myeloid cells of the central nervous system parenchyma. Nature *468*, 253-262.

Rapsinski, G.J., Wynosky-Dolfi, M.A., Oppong, G.O., Tursi, S.A., Wilson, R.P., Brodsky, I.E., and Tukel, C. (2015). Toll-like receptor 2 and NLRP3 cooperate to recognize a functional bacterial amyloid, curli. Infect Immun *83*, 693-701.

Redecke, V., Wu, R., Zhou, J., Finkelstein, D., Chaturvedi, V., High, A.A., and Hacker, H. (2013). Hematopoietic progenitor cell lines with myeloid and lymphoid potential. Nat Methods *10*, 795-803.

Remington, L.T., Babcock, A.A., Zehntner, S.P., and Owens, T. (2007). Microglial recruitment, activation, and proliferation in response to primary demyelination. Am J Pathol *170*, 1713-1724.

Rezaie, P., and Male, D. (1999). Colonisation of the developing human brain and spinal cord by microglia: a review. Microsc Res Tech *45*, 359-382.

Robinson, M.D., McCarthy, D.J., and Smyth, G.K. (2010). edgeR: a Bioconductor package for differential expression analysis of digital gene expression data. Bioinformatics *26*, 139-140.

Rongvaux, A., Willinger, T., Martinek, J., Strowig, T., Gearty, S.V., Teichmann, L.L., Saito, Y., Marches, F., Halene, S., Palucka, A.K.*, et al.* (2014). Development and function of human innate immune cells in a humanized mouse model. Nat Biotechnol *32*, 364-372.

Rothwell, N. (2003). Interleukin-1 and neuronal injury: mechanisms, modification, and therapeutic potential. Brain Behav Immun *17*, 152-157.

Roy, K. (2012). Establishment of microglial precursors derived from human induced pluripotent stem cells to model SOD1-mediated amyotrophic lateral sclerosis. In Faculty of Mathematics and Natural Sciences (Bonn, Germany: Rheinische-Friedrich-Wilhelms University of Bon).

Rustenhoven, J., Park, T.I., Schweder, P., Scotter, J., Correia, J., Smith, A.M., Gibbons, H.M., Oldfield, R.L., Bergin, P.S., Mee, E.W.*, et al.* (2016). Isolation of highly enriched primary human microglia for functional studies. Sci Rep *6*, 19371.

Saijo, K., and Glass, C.K. (2011). Microglial cell origin and phenotypes in health and disease. Nat Rev Immunol *11*, 775-787.

Salvagiotto, G., Burton, S., Daigh, C.A., Rajesh, D., Slukvin, II, and Seay, N.J. (2011). A defined, feeder-free, serum-free system to generate in vitro hematopoietic progenitors and differentiated blood cells from hESCs and hiPSCs. PLoS One *6*, e17829.

Samokhvalov, I.M., Samokhvalova, N.I., and Nishikawa, S. (2007). Cell tracing shows the contribution of the yolk sac to adult haematopoiesis. Nature *446*, 1056-1061.

Sasaki, A., Kakita, A., Yoshida, K., Konno, T., Ikeuchi, T., Hayashi, S., Matsuo, H., and Shioda, K. (2015). Variable expression of microglial DAP12 and TREM2 genes in Nasu-Hakola disease. Neurogenetics *16*, 265-276.

Savage, J.C., Jay, T., Goduni, E., Quigley, C., Mariani, M.M., Malm, T., Ransohoff, R.M., Lamb, B.T., and Landreth, G.E. (2015). Nuclear receptors license phagocytosis by trem2+ myeloid cells in mouse models of Alzheimer's disease. J Neurosci *35*, 6532-6543.

Schilling, T., Nitsch, R., Heinemann, U., Haas, D., and Eder, C. (2001). Astrocyte-released cytokines induce ramification and outward K+ channel expression in microglia via distinct signalling pathways. Eur J Neurosci *14*, 463-473.

Schmid, C.D., Sautkulis, L.N., Danielson, P.E., Cooper, J., Hasel, K.W., Hilbush, B.S., Sutcliffe, J.G., and Carson, M.J. (2002). Heterogeneous expression of the triggering receptor expressed on myeloid cells-2 on adult murine microglia. J Neurochem *83*, 1309-1320.

Schulz, C., Gomez Perdiguero, E., Chorro, L., Szabo-Rogers, H., Cagnard, N., Kierdorf, K., Prinz, M., Wu, B., Jacobsen, S.E., Pollard, J.W.*, et al.* (2012). A lineage of myeloid cells independent of Myb and hematopoietic stem cells. Science *336*, 86-90.

Scott, E.W., Simon, M.C., Anastasi, J., and Singh, H. (1994). Requirement of transcription factor PU.1 in the development of multiple hematopoietic lineages. Science *265*, 1573-1577.

Seok, J., Warren, H.S., Cuenca, A.G., Mindrinos, M.N., Baker, H.V., Xu, W., Richards, D.R., McDonald-Smith, G.P., Gao, H., Hennessy, L.*, et al.* (2013). Genomic responses in mouse models poorly mimic human inflammatory diseases. Proc Natl Acad Sci U S A *110*, 3507-3512.

Seshadri, S., Fitzpatrick, A.L., Ikram, M.A., DeStefano, A.L., Gudnason, V., Boada, M., Bis, J.C., Smith, A.V., Carassquillo, M.M., Lambert, J.C.*, et al.* (2010). Genome-wide analysis of genetic loci associated with Alzheimer disease. JAMA *303*, 1832-1840.

Sheedy, F.J., Grebe, A., Rayner, K.J., Kalantari, P., Ramkhelawon, B., Carpenter, S.B., Becker, C.E., Ediriweera, H.N., Mullick, A.E., Golenbock, D.T.*, et al.* (2013). CD36 coordinates NLRP3 inflammasome activation by facilitating intracellular nucleation of soluble ligands into particulate ligands in sterile inflammation. Nat Immunol *14*, 812-820.

Shigemoto-Mogami, Y., Hoshikawa, K., Goldman, J.E., Sekino, Y., and Sato, K. (2014). Microglia enhance neurogenesis and oligodendrogenesis in the early postnatal subventricular zone. J Neurosci *34*, 2231-2243.

Shulman, J.M., Imboywa, S., Giagtzoglou, N., Powers, M.P., Hu, Y., Devenport, D., Chipendo, P., Chibnik, L.B., Diamond, A., Perrimon, N.*, et al.* (2014). Functional screening in Drosophila identifies Alzheimer's disease susceptibility genes and implicates Tau-mediated mechanisms. Hum Mol Genet *23*, 870-877.

Siemers, E.R., Quinn, J.F., Kaye, J., Farlow, M.R., Porsteinsson, A., Tariot, P., Zoulnouni, P., Galvin, J.E., Holtzman, D.M., Knopman, D.S.*, et al.* (2006). Effects of a gamma-secretase inhibitor in a randomized study of patients with Alzheimer disease. Neurology *66*, 602-604.

Sierra, A., Encinas, J.M., Deudero, J.J., Chancey, J.H., Enikolopov, G., Overstreet-Wadiche, L.S., Tsirka, S.E., and Maletic-Savatic, M. (2010). Microglia shape adult hippocampal neurogenesis through apoptosis-coupled phagocytosis. Cell Stem Cell *7*, 483-495.

Sirkis, D.W., Bonham, L.W., Aparicio, R.E., Geier, E.G., Ramos, E.M., Wang, Q., Karydas, A., Miller, Z.A., Miller, B.L., Coppola, G.*, et al.* (2016). Rare TREM2 variants associated with Alzheimer's disease display reduced cell surface expression. Acta Neuropathol Commun *4*, 98.

Stalder, A.K., Ermini, F., Bondolfi, L., Krenger, W., Burbach, G.J., Deller, T., Coomaraswamy, J., Staufenbiel, M., Landmann, R., and Jucker, M. (2005). Invasion of hematopoietic cells into the brain of amyloid precursor protein transgenic mice. J Neurosci *25*, 11125-11132.

Stephan, A.H., Barres, B.A., and Stevens, B. (2012). The complement system: an unexpected role in synaptic pruning during development and disease. Annu Rev Neurosci *35*, 369-389.

Stevens, B., Ishibashi, T., Chen, J.F., and Fields, R.D. (2004). Adenosine: an activity-dependent axonal signal regulating MAP kinase and proliferation in developing Schwann cells. Neuron Glia Biol *1*, 23-34.

Strobel, S., Grunblatt, E., Riederer, P., Heinsen, H., Arzberger, T., Al-Sarraj, S., Troakes, C., Ferrer, I., and Monoranu, C.M. (2015). Changes in the expression of genes related to neuroinflammation over the course of sporadic Alzheimer's disease progression: CX3CL1, TREM2, and PPARgamma. J Neural Transm (Vienna) *122*, 1069-1076.

Sturgeon, C.M., Ditadi, A., Awong, G., Kennedy, M., and Keller, G. (2014). Wnt signaling controls the specification of definitive and primitive hematopoiesis from human pluripotent stem cells. Nat Biotechnol *32*, 554-561.

Sturgeon, C.M., Ditadi, A., Clarke, R.L., and Keller, G. (2013). Defining the path to hematopoietic stem cells. Nat Biotechnol *31*, 416-418.

Suarez-Calvet, M., Araque Caballero, M.A., Kleinberger, G., Bateman, R.J., Fagan, A.M., Morris, J.C., Levin, J., Danek, A., Ewers, M., Haass, C.*, et al.* (2016a). Early changes in CSF sTREM2 in dominantly inherited Alzheimer's disease occur after amyloid deposition and neuronal injury. Sci Transl Med *8*, 369ra178.

Suarez-Calvet, M., Kleinberger, G., Araque Caballero, M.A., Brendel, M., Rominger, A., Alcolea, D., Fortea, J., Lleo, A., Blesa, R., Gispert, J.D.*, et al.* (2016b). sTREM2 cerebrospinal fluid levels are a potential biomarker for microglia activity in early-stage Alzheimer's disease and associate with neuronal injury markers. EMBO Mol Med *8*, 466-476.

Takahashi, K., Rochford, C.D., and Neumann, H. (2005). Clearance of apoptotic neurons without inflammation by microglial triggering receptor expressed on myeloid cells-2. J Exp Med *201*, 647-657.

Terme, M., Tomasello, E., Maruyama, K., Crepineau, F., Chaput, N., Flament, C., Marolleau, J.P., Angevin, E., Wagner, E.F., Salomon, B.*, et al.* (2004). IL-4 confers NK stimulatory capacity to murine dendritic cells: a signaling pathway involving KARAP/DAP12-triggering receptor expressed on myeloid cell 2 molecules. J Immunol *172*, 5957-5966.

Theendakara, V., Peters-Libeu, C.A., Spilman, P., Poksay, K.S., Bredesen, D.E., and Rao, R.V. (2016). Direct Transcriptional Effects of Apolipoprotein E. J Neurosci *36*, 685-700.

Thrash, J.C., Torbett, B.E., and Carson, M.J. (2009). Developmental regulation of TREM2 and DAP12 expression in the murine CNS: implications for Nasu-Hakola disease. Neurochem Res *34*, 38-45.

Town, T., Laouar, Y., Pittenger, C., Mori, T., Szekely, C.A., Tan, J., Duman, R.S., and Flavell, R.A. (2008). Blocking TGF-beta-Smad2/3 innate immune signaling mitigates Alzheimer-like pathology. Nat Med *14*, 681-687.

Trougakos, I.P., Lourda, M., Antonelou, M.H., Kletsas, D., Gorgoulis, V.G., Papassideri, I.S., Zou, Y., Margaritis, L.H., Boothman, D.A., and Gonos, E.S. (2009). Intracellular clusterin inhibits mitochondrial apoptosis by suppressing p53-activating stress signals and stabilizing the cytosolic Ku70-Bax protein complex. Clin Cancer Res *15*, 48-59.

Turnbull, I.R., Gilfillan, S., Cella, M., Aoshi, T., Miller, M., Piccio, L., Hernandez, M., and Colonna, M. (2006). Cutting edge: TREM-2 attenuates macrophage activation. J Immunol *177*, 3520-3524.

Turrin, N.P., and Rivest, S. (2004). Innate immune reaction in response to seizures: implications for the neuropathology associated with epilepsy. Neurobiol Dis *16*, 321-334.

Ubelmann, F., Burrinha, T., Salavessa, L., Gomes, R., Ferreira, C., Moreno, N., and Guimas Almeida, C. (2017). Bin1 and CD2AP polarise the endocytic generation of beta-amyloid. EMBO Rep *18*, 102-122.

Uenishi, G., Theisen, D., Lee, J.H., Kumar, A., Raymond, M., Vodyanik, M., Swanson, S., Stewart, R., Thomson, J., and Slukvin, I. (2014). Tenascin C promotes hematoendothelial development and T lymphoid commitment from human pluripotent stem cells in chemically defined conditions. Stem Cell Reports *3*, 1073-1084.

Varvel, N.H., Grathwohl, S.A., Degenhardt, K., Resch, C., Bosch, A., Jucker, M., and Neher, J.J. (2015). Replacement of brain-resident myeloid cells does not alter cerebral amyloid-beta deposition in mouse models of Alzheimer's disease. J Exp Med *212*, 1803-1809.

Veerhuis, R., Nielsen, H.M., and Tenner, A.J. (2011). Complement in the brain. Mol Immunol *48*, 1592-1603.

Vezzani, A., French, J., Bartfai, T., and Baram, T.Z. (2011). The role of inflammation in epilepsy. Nat Rev Neurol *7*, 31-40.

Villegas-Llerena, C., Phillips, A., Garcia-Reitboeck, P., Hardy, J., and Pocock, J.M. (2015). Microglial genes regulating neuroinflammation in the progression of Alzheimer's disease. Curr Opin Neurobiol *36*, 74-81.

Vodyanik, M.A., Bork, J.A., Thomson, J.A., and Slukvin, II (2005). Human embryonic stem cell-derived CD34+ cells: efficient production in the coculture with OP9 stromal cells and analysis of lymphohematopoietic potential. Blood *105*, 617-626.

von Bernhardi, R., Tichauer, J.E., and Eugenin, J. (2010). Aging-dependent changes of microglial cells and their relevance for neurodegenerative disorders. J Neurochem *112*, 1099-1114.

Walter, S., Letiembre, M., Liu, Y., Heine, H., Penke, B., Hao, W., Bode, B., Manietta, N., Walter, J., Schulz-Schuffer, W*., et al.* (2007). Role of the toll-like receptor 4 in neuroinflammation in Alzheimer's disease. Cell Physiol Biochem *20*, 947-956.

Wang, W.Y., Tan, M.S., Yu, J.T., and Tan, L. (2015a). Role of pro-inflammatory cytokines released from microglia in Alzheimer's disease. Ann Transl Med *3*, 136.

Wang, Y., Cella, M., Mallinson, K., Ulrich, J.D., Young, K.L., Robinette, M.L., Gilfillan, S., Krishnan, G.M., Sudhakar, S., Zinselmeyer, B.H*., et al.* (2015b). TREM2 lipid sensing sustains the microglial response in an Alzheimer's disease model. Cell *160*, 1061-1071.

Wang, Y., and Neumann, H. (2010). Alleviation of neurotoxicity by microglial human Siglec-11. J Neurosci *30*, 3482-3488.

Wang, Y., Szretter, K.J., Vermi, W., Gilfillan, S., Rossini, C., Cella, M., Barrow, A.D., Diamond, M.S., and Colonna, M. (2012). IL-34 is a tissue-restricted ligand of CSF1R required for the development of Langerhans cells and microglia. Nat Immunol *13*, 753-760.

Wlodarczyk, A., Lobner, M., Cedile, O., and Owens, T. (2014). Comparison of microglia and infiltrating CD11c(+) cells as antigen presenting cells for T cell proliferation and cytokine response. J Neuroinflammation *11*, 57.

Wunderlich, P., Glebov, K., Kemmerling, N., Tien, N.T., Neumann, H., and Walter, J. (2013). Sequential proteolytic processing of the triggering receptor expressed on myeloid cells-2 (TREM2) protein by ectodomain shedding and gamma-secretase-dependent intramembranous cleavage. J Biol Chem *288*, 33027-33036.

Yamasaki, R., Lu, H., Butovsky, O., Ohno, N., Rietsch, A.M., Cialic, R., Wu, P.M., Doykan, C.E., Lin, J., Cotleur, A.C*., et al.* (2014). Differential roles of microglia and monocytes in the inflamed central nervous system. J Exp Med *211*, 1533-1549.

Yeh, F.L., Wang, Y., Tom, I., Gonzalez, L.C., and Sheng, M. (2016). TREM2 Binds to Apolipoproteins, Including APOE and CLU/APOJ, and Thereby Facilitates Uptake of Amyloid-Beta by Microglia. Neuron *91*, 328-340.

Yoshida, H., Hayashi, S., Kunisada, T., Ogawa, M., Nishikawa, S., Okamura, H., Sudo, T., Shultz, L.D., and Nishikawa, S. (1990). The murine mutation osteopetrosis is in the coding region of the macrophage colony stimulating factor gene. Nature *345*, 442-444.

Yuan, P., Condello, C., Keene, C.D., Wang, Y., Bird, T.D., Paul, S.M., Luo, W., Colonna, M., Baddeley, D., and Grutzendler, J. (2016). TREM2 Haplodeficiency in Mice and Humans Impairs the Microglia Barrier Function Leading to Decreased Amyloid Compaction and Severe Axonal Dystrophy. Neuron *90*, 724-739.

Zhang, D.E., Hohaus, S., Voso, M.T., Chen, H.M., Smith, L.T., Hetherington, C.J., and Tenen, D.G. (1996). Function of PU.1 (Spi-1), C/EBP, and AML1 in early myelopoiesis: regulation of multiple myeloid CSF receptor promoters. Curr Top Microbiol Immunol *211*, 137-147.

Zhang, M., Angata, T., Cho, J.Y., Miller, M., Broide, D.H., and Varki, A. (2007). Defining the in vivo function of Siglec-F, a CD33-related Siglec expressed on mouse eosinophils. Blood *109*, 4280-4287.

Zhang, Y., Chen, K., Sloan, S.A., Bennett, M.L., Scholze, A.R., O'Keeffe, S., Phatnani, H.P., Guarnieri, P., Caneda, C., Ruderisch, N.*, et al.* (2014). An RNA-sequencing transcriptome and splicing database of glia, neurons, and vascular cells of the cerebral cortex. J Neurosci *34*, 11929-11947.